UNIVERSITY OF OKLAHOMA

GRADUATE COLLEGE

THE ECO-PHYSIOLOGY, STRESS RESPONSE REGULATION, AND ENGINEERING OF *SHEWANELLA* SPECIES FOR INDUSTRIAL AND ENVIRONMENTAL APPLICATIONS

A DISSERTATION

SUBMITTED TO THE GRADUATE FACULTY

in partial fulfillment of the requirements for the

Degree of

DOCTOR OF PHILOSOPHY

By

MING XIE
Norman, Oklahoma
2016

THE ECO-PHYSIOLOGY, STRESS RESPONSE REGULATION, AND ENGINEERING OF *SHEWANELLA* SPECIES FOR INDUSTRIAL AND ENVIRONEMNTAL APPLICATIONS

A DISSERTATION APPROVED FOR THE
DEPARTMENT OF MICROBIOLOGY AND PLANT BIOLOGY

BY

_____
Dr. Jizhong Zhou, Chair

_____
Dr. Michael McInerney

_____
Dr. Anne Dunn

_____
Dr. Paul Lawson

_____
Dr. Michael Kaspari

Acknowledgements

This has been a long and cumbersome journey for me. As this journey is getting close to finishing, I would like to take the opportunity here to acknowledge all the people that have helped me throughout this process. It is their support and help that provided me the confidence to continue on this path.

I would like to thank my mentor, Dr. Jizhong Zhou, for his tremendous help and support through the years, especially in the past year when my family was in crisis. During the years working in his lab I was deeply influenced by his enthusiasm in research and his working ethic. I learned from him how to conduct experiments and to think critically, how to tackle problems and communicate. These have taught me what it takes to become a researcher and also influenced me as a person.

I am grateful for having a very supportive committee. I have taken courses from Dr. Michael McInerney, Dr. Anne Dunn, and Dr. Michael Kaspari. Besides, I have also worked as TA for Dr. Dunn, and Dr. Paul Lawson. I have learned a lot from them through their instructions in their class, and discussion with them about my projects. Their different styles in teaching and communication also provided me thoughts from different aspects. Besides, it is the support from Dr. McInerney and Dr. Dunn, former and current department chair made it possible for me to participate in CPT so I can work on the bioanode part of my dissertation in the University of Texas.

I would like to specifically thank Dr. David Schmidtke in the University of Texas at Dallas for providing the opportunity for me to work on the bioanode project in my thesis in his laboratory during my CPT. It was a very pleasant experience to be part of his team. He has treated me just like his students, spending countless hours to discuss

with me about experimental design, data interpretation, solving problems, and writing. Although the 7-months stay in his lab is rather short, it has been a very efficient period, when we generated lots of data for my thesis and also a manuscript.

I have worked with Dr. Dongru Qiu, former postdoc in Dr. Zhou's lab for several years over projects related to *Shewanella* and learned a lot from him. I would like to take this chance to thank him and his student, Dr. Jingcheng Dai, for all their support and everything that we have worked on together.

I'd like also to thank people in Institute for Environmental Genomics for their help over the years. Discussion with Dr. Zhili He and Dr. Aifen Zhou has helped me a lot for my experimental design and manuscript drafting. I have also received lots of help from Dr. Joy Van Nostrand, Dr. Liyou Wu, Dr. Tong Yuan, Dr. Daliang Ning, Dr. Bo Wu, and Dr. Ye Deng, for experiment and data analysis. Besides, I would like to thank all my colleague students in Dr. Zhou's lab for their support through all the years.

I would like to thank Dr. Xueduan Liu, my Masters' advisor and Dr. Huaqun Yin, whom I know long time ago in Central South University, for their extensive support after I left CSU for my Ph.D. in the States.

Lastly, I must thank my family for everything. My beloved wife, Jie Chen, and the three wonderful kids are the reason for me to strive for a better tomorrow. Jie has undertaken so many burdens on her shoulder so that I can focus on my program. My parents, parent in-laws, and grandparents have provided us with their tremendous support, including multiples trips and stays in the US to take care of my family. It is their unconditional love, optimism, and encouragement that supported me through all the years and during ups and downs.

Table of Contents

List of Tables

List of Figures

Abstract

In recent decades, there has been tremendous interest in applying environmental microbiology for waste treatment, bioremediation and sustainable energy production. As one of the most important model environmental microbes, *Shewanella* species are renowned for their flexible growth, capability of surviving and growing in a wide gradient of various environmental conditions, and excellent respiratory versatility. There is great prospect of using this organism for production of valuable chemicals, treatment of various types of contamination, and for energy generation in Microbial Fuel Cells. However, the real-life application of *Shewanella* is hindered by the relatively low level of performance. Fundamental knowledge of the physiology, ecology, stress response mechanism, as well as correct engineering, are indispensable for discovering novel properties and to boost the performance of *Shewanella*-based applications.

In an initial effort of understanding gene functions and regulations, a particularly interesting mutant of *Shewanella loihica* PV-4 that could accumulate significant amount of red pigmentation was identified via transposon mutant library screening. The mutation was then found to be on gene Shew_2229 which encodes ferrochelatase. Using analytical methods, the red pigment was verified as protoporphyrin IX (PPIX), an important chemical involved in the synthesis of hemoglobin. Quantification of the yield of PPIX in this mutant was estimated to be 11.2mg/g cell dry weight, which was at least hundreds of times higher compared to other reported bacterial strains and similar to the

level of a fully engineered strain that require multiple types of antibiotics to be supplied for its fermentation. A patent for using this PV-4 mutant strain for industrial production of PPIX was issued (US patent No. 9273334B2).

Of great interest was that, the genome of PV-4 contains two paralogues of the *hemH* gene, designated as *hemH1* (Shew_2229) and *hemH2* (Shew_1140). It was discovered that single disruption of *hemH1* resulted in PPIX accumulation, while single disruption of *hemH2* had no apparent phenotype. Therefore, it is hypothesized that there is functional redundancy among the two paralogues with *hemH1* as the dominant gene and *hemH2* playing a supplementary role. To test this hypothesis, the regulation mechanisms of *hemH1* and *hemH2* were analyzed via comparative genomics. Sequence analysis of the promoter region of the two paralogues indicated that the two genes were regulated differently. The promoter sequence of *hemH1* contains the binding box of the constitutively expressed sigma factor RpoD, while the promoter sequence of *hemH2* harbors the binding sequence of the extracellular family sigma factor RpoE2, which suggested that the expression of the two paralogues might be different. Consistently, *hemH1* was found constitutively expressed while expression of *hemH2* was minimal in presence of a non-disrupted *hemH1* but increased significantly when *hemH1* was disrupted, supporting the supplementary role of *hemH2* in PV-4. Besides, the up-regulation of *hemH2* was also observed when PV-4 was exposed to the oxidative stress, either by introduction of hydrogen peroxide or due to accumulation of the photosensitive PPIX. We found that expression of *hemH2* was significantly higher when the *hemH1* mutant was exposed to light, and accumulation of PPIX was no longer observed under such condition. All these findings suggest that *hemH2* plays a more

important role under oxidative stressed conditions although its expression is minimal under normal conditions. The apparent redundancy of the *hemH* paralogues may contribute to the survival of this strain under stress conditions.

Salt stress is one of the most commonly observed stresses for microbes in the natural environment. It is often associated with environmental pollution and can be introduced during bioremediation processes, such as neutralizing pH for sites with high acidity or alkalinity. Understanding the mechanism for salt stress response of microbes is a fundamental step toward boosting the performance of environmental microbiology applications. Although there has been ample documentation regarding the salt stress response in various microbes, knowledge about the microbial response to long term salt stress is lacking. The *Shewanella putrefaciens* CN-32 strain is an excellent candidate for bioremediation or MFCs. Using the strategy of experimental evolution, the response to salt (NaCl) stress over long term lab incubation was investigated. The changes of growth phenotype, metabolite profile, and transcriptome in evolved populations were analyzed. The mutations occurred in evolved populations were captured by sequencing population DNAs to help interpret fitness changes.

Profound differences in phenotypes were observed among the evolved populations. Populations evolved under salt stress (ES) exhibited significant advantage in growth rate and peak biomass compared with populations evolved under control conditions (EC) or ancestor (AN), indicating gain of fitness. However, the evolved populations were inferior in terms of motility compared to the ancestor, likely one of the tradeoffs during the evolutionary course. Analysis of metabolite profile via Detrended Correspondence Analysis showed that culture condition (salt stress vs. control) and the

condition of evolution are the key factors shaping the metabolite composition. Interesting patterns of metabolites were identified, such as the significant higher amount of two compatible solutes, proline and ectoine, in the ES populations, indicating that these two metabolites may play critical role for salt tolerance in this organism.

Transcriptome analysis of select populations revealed that significant up-regulation of genes involved in proline uptake and synthesis was shared across the populations, again reflected the importance of proline accumulation for salt stress protection. Whole-genome-resequencing revealed interesting mutations that may contribute to the improved salt tolerance in ES populations.

The potential application of *Shewanella* species as bioanode for electricity generation in MFCs was investigated. Redox polymer was introduced with the aim of boosting current generation. The effect of various factors was investigated, such as different *Shewanella* strains, loading of the redox polymer, and methods of bacteria incorporation. The results showed that electrode surface modification by coating of PVP-Os redox polymer led to several folds of increase in current density. Among the four strains studied, namely *Shewanella oneidensis* MR-1, *Shewanella putrefaciens* W3-18-1, *Shewanella loihica* PV-4, and *Shewanella putrefaciens* CN-32, strain W3-18-1 showed the best current density with or without redox polymer. Using W3-18-1 as the target organism, the effect of polymer loading, and methods of incorporation were further investigated. Increased amount of PVP-OS loading alone did not lead to an increase of current density, as the increased thickness might perturb efficient electron communication between the redox centers. Four different methods of bacteria incorporation with PVP-OS were compared, the suspension method, lay-over method,

mix and cast method, and layer-by-layer method using a gold electrode. The layer-by-layer method produced significantly higher current density compared with other methods, but take longer time to reach peak current density. The suspension method showed second highest current density and quickest response, while the LO and MAC methods showed significantly lower current density.

In summary, the mechanisms of PPIX accumulation and oxidative stress response in *Shewanella loihica* PV-4, the long term salt adaptation in *Shewanella putrefaciens* CN-32, and current generation in several *Shewanella* strains, were investigated via systematic analysis of mutagenesis, functional genomics, comparative genomics, and electrochemistry. Results of this study expands our current knowledge of the physiology, genetics, stress response, and evolution of the *Shewanella* genus, providing important clues for environmental applications such as bioremediation and MFC, as well as using this type of organism for industrial production of valuable chemicals such as PPIX.

Keywords: **environmental microbiology, *Shewanella*, oxidative stress, salt stress, experimental evolution, heme synthesis regulation, protoporphyrin IX, paralogous genes, in-frame deletion, metabolite profile, transcriptome, single nucleotide polymorphisms, bioanode, redox polymer, cyclic voltammetry.**

Chapter 1: Introduction

1.1 Environmental microbiology applications and current limitations

The world population is projected to reach 9.7 billion by year 2050 based on a 2015 prediction from United Nations Department of Economic and Social Affairs (http://www.un.org/en/development/desa/news/population/2015-report.html). The rapid growth of global population requires extensive energy input and products from agriculture and industry. As a result, there will be rapid increase in demand for energy, food, and products. In the meantime, since the era of industrial revolution, pollution due to energy harvesting, agricultural and industrial activities, and the resulting wastes, have caused severe pollution of air and water, which significantly deteriorated the environment and quality of life. The paradox between the increasing demand for resources and the deteriorating environmental conditions must be resolved to allow the sustainable development of human society. Therefore, how to effectively treat various types of environmental pollutions has been a central global issue in recent decades.

Environmental microbes may provide a solution for the contamination issue and partly aid the energy need. The discipline of Environmental Microbiology has a rather short definition according to Nature magazine: "Environmental Microbiology is the scientific study of microorganisms in the environment" (http://www.nature.com/subjects/environmental-microbiology). Despite this simple definition, environmental microbiology has profound influence on biological sciences and human society. One classical example is the discovery of thermal-stable DNA polymerase from thermophiles that led to rapid development of Polymerase Chain Reaction(Saiki et al., 1988), one of the most fundamental techniques for modern

molecular biology and widely used in clinical field. In recent decades, the potential applications of environmental microbiology in industry, bioremediation, and bioenergy received increasing recognition.

The major advantage of environmental microbiology applications lies in the relatively low cost, high versatility, and sustainability. For industrial applications, the extremely high diversity of environmental microorganisms provides valuable resource that can be utilized for numerous purposes. With the combination of modern molecular biology and synthetic biology, large scale production of a great variety of valuable products that originated from environmental microorganisms have been realized for various industrial needs, such as research (e.g. various types of enzymes), food, and healthcare (e.g. nutritional supplements and drugs).

In terms of contamination treatment, for virtually every type of contamination, there are microorganisms that are capable of thriving in the contaminated area. These microorganisms possess the cellular machinery to not only withstand the contamination condition that could potentially be harmful to the organism, but also reduce the level of contamination via mechanisms such as breaking down the contaminant, convert the contaminant to less toxic or benign molecules, or change the physical/chemical property of the contaminants to make them precipitate, facilitating their removal (Leahy and Colwell, 1990; Yilmaz, 2003). As a typical example, application of microorganism for domestic sewage water treatment has been in practice for centuries. However, it is not until in the 1980s people began to use microorganisms for what we now refer to as bioremediation for various types of contaminations (Bouwer and McCarty, 1983; Bouwer et al., 1981). Through means such as stimulation of natural resident

microorganisms, or introducing non-native microorganisms that are capable of degrading the particular contaminants of interest to the contaminated site, or combination of both, there has been numerous success cases of bioremediation for various type of contaminations, including heavy metals, pesticides, oil spills, etc. (Ahmad, 2013; Baba Uqab, 2016; Kumar.A, 2011; Wasi et al., 2013).

Energy generation from environmental microorganisms typically does not constitute a dominant proportion for energy supply but rather as supplementary energy sources (Mustafa Balat, 2009). However, with exhausting fossil fuels, bioenergy is playing more important roles nowadays. Fuels, such as ethanol, butanol, and even short chain alkanes, can now be generated from cellulose and lignin previously regarded as waste materials, through engineering of environmental microorganisms (Lin and Tanaka, 2006; Zverlov et al., 2006). Other types of energy such as hydrogen and methane can also be generated from microorganism (Elizabeth S. Heidrich, 2014). Electricity can be produced with microbial fuel cells (Franks and Nevin, 2010). With a thorough survey of the environmental conditions and carefully designed infrastructure, in-situ energy generation can be the sole energy source for applications, such as for powering environmental sensors that are placed in discrete area for environmental monitoring purposes, and for self-sustaining waste water treatment plants, with no need of external energy input (Sun et al., 2015).

How to increase the efficiency of environmental microbiology applications remains the key challenge for real life practice (Balan, 2014; Logan and Regan, 2006). Due to the high level of complexity and constantly changing environmental conditions, knowledge about the fundamental physiology, genetics, regulation of environmental

microorganisms, and ecology, are indispensable to boost the functionality and explore new area of applications. Investigations on model environmental organisms can provide detailed and systematic information regarding the mechanism for functions of interest, thereby providing critical clues for functional improvement. In this thesis, the physiology, adaptation, stress response regulations, and genetic engineering of an important environmental bacteria genus *Shewanella*, was investigated to provide insights into the molecular level mechanisms of these versatile bacteria, for promoting existing applications of this genus and exploring new fields of application.

1.2 Shewanella as model environmental organism

The *Shewanella* genus is named in memory of Dr. James M. Shewan for his contributions to fisheries microbiology (Macdonell and Colwell, 1985). The earliest isolates were first identified as *Achromobacter putrefaciens* in the 1930s, and then renamed to *Pseudonomas putrefaciens* in the 1940s. In 1970s, the type strain was renamed as *Altermonomas putrefaciens* before it is reclassified as a new genus, *Shewanella,* based on the 5S rRNA sequence. Nowadays, DNA: DNA hybridization and 16S rRNA sequence were used to determine taxonomy of *Shewanella*.

The genus *Shewanella* consists of a diverse group of bacterium. These microbes are facultative anaerobes frequently isolated from various aquatic environments. They are Gram negative, rod shaped bacteria with an average length of 2 to 3 μm and diameter of ~0.4 to 0.7 μm. They are motile with single polar flagella. These microorganisms are renowned for two prominent characteristics, 1)respiratory versatility, and 2) extremely flexible growth (Fredrickson et al., 2008). Because of these

unique properties, these bacteria can thrive in a wide gradient of various environmental factors, such as redox potential, temperature, salinity, and barometric pressure (Hau and Gralnick, 2007). Consistently, they were frequently isolated from diverse habitats such as fresh water, lake sediment, marine water and sediment, deep sea sediment, waste water, etc., (Gao et al., 2006; Huang et al., 2010; Reid and Gordon, 1999). In most cases these are free living microbes but some can also form symbiotic or epibiotic relationships with other organisms (Senderovich and Halpern, 2013). Most of these microorganisms are non-pathogenic but some strains can cause food spoilage or cause disease as opportunistic pathogens (Hjelm et al., 2002; Sharma and Kalawat, 2010).

The extraordinary respiration versatility of *Shewanella* is reflected in the broad spectrum of organic and inorganic final electron acceptors they can respire. The organic terminal electron acceptors include trimethylamine-N-oxide, dimethyl sulfoxide, tetrachloromethane, polychlorinated biphenyls, pentachloroethane, cyclic nitramines and nitroaromatic compounds (Luan et al., 2015; Zhao et al., 2005). Inorganic electron acceptors encompass a great variety of metal elements and non-metal compounds. The most commonly electron acceptors include Fe (III), Mn (IV), Cr (VI), while other unusual elements that can be reduced by *Shewanella* include Co, Ur, I, Tc, Np, Se, Pu, Te, and V (Boukhalfa et al., 2007; Carpentier et al., 2003; Farrenkopf et al., 1997; Klonowska et al., 2005; Lloyd et al., 2000; Wielinga et al., 2001; Wildung et al., 2000). It is worth noting that the dissmilatory metal reduction in *Shewanella* not only occurs on metals in the form of ions but also on solid metal oxides. The latter procedure requires transportation of electrons through the cell membrane to reach the surface of metal oxides in the environment, a process used to be regarded as impossible in microbes.

Metal reduction on solid metal oxides has been shown realized by multiple cytochromes that work in concert. There is only a couple of microbial genus that are capable of accomplishing this procedure. These excellent respiration properties, together with the variety of carbon sources that can be used by *Shewanealla,* made them ideal candidates for bioremediations and for microbial fuel cell.

The fact that *Shewanella* can survive in a broad range of redox potential, temperature, salinity, and pressure made them more flexible compared to other environmental microorganisms. For example, being facultative anaerobes, these bacteria show excellent growth when oxygen is the terminal electron acceptor. Meanwhile, they were well adapted to anoxic conditions when other electron acceptors are available. Most of the *Shewanellae* are psychrotolerant mesophiles with optimum growth temperature close to 30ºC, while they are still able to grow at low temperatures (0-4ºC) (Bowman et al., 1997). Some of the strains can tolerate temperature as high as 43ºC (Gao et al., 2006). *Shewanella* can also tolerate high level of salt as growth is observed for many strains with 0.5% to 8% NaCl, with optimal NaCl concentration of ~2% (Holt et al., 2005). In fact, many strains were isolated from marine sites and this genus is considered to have a marine origin (Toffin et al., 2004). This high level of flexibility is largely attributed to their complex sensing and regulatory machinery. Previous study reported that there is a predicted number of 211 one-component system and 47 two-component system genes in the type strain *Shewanella oneidensis* MR-1 (Heidelberg et al., 2002). In consistence with this, signal transduction proteins in the following three classes were significantly more abundant in MR-1 than other bacteria: chemotaxis, PAS (Period circadian protein, Aryl hydrocarbon receptor nuclear

translocator protein, and Single-minded protein) domain containing proteins, and secondary messenger cyclic nucleotide signaling modulators (Heidelberg et al., 2002). The complex sensing and regulatory network may allow the rapid response to environmental stimuli and chemotaxis toward favorable habitat.

Besides the apparent advantage of *Shewanella* in respiration and flexibility, there are several other factors that make them ideal model organisms. Firstly, these organisms are easy to culture and grow in laboratory settings, without the need for complicated growth medium or advanced culture equipment. Similar to *E.coli*, dense bacterial populations of *Shewanella* can be obtained with overnight agitated culture in Luria Broth. Secondly, *Shewanella* is relatively easy for genetic manipulation. Electroporation is highly effective for introducing foreign DNA to *Shewanella*. There are various vectors available for genetic engineering such as in-frame deletion or complementation, which are indispensable for elucidating gene function, regulation, and synthetic engineering (Dai et al., 2015; Wu et al., 2011). Thirdly, the whole genome sequence information for a number of the *Shewanella* strains is now publicly available. In the post-genomics era, such information is indispensable in that 1) it allows for bioinformatic analysis and comparative genomics analysis to generate scientific hypothesis to be tested and 2) it provides critical information for molecular cloning, making the procedure much easier.

In summary, there is great potential environmental and industrial application of *Shewanella*. The available bioinformatics and genetic manipulation platforms allow the feasibility of systematic and in-depth investigation on their physiology, regulation, and function, which makes them ideal model organisms for environmental microbes.

Knowledge from such studies can greatly enhance our capability of utilizing this organism for solving real-life problems, while providing important clues for research of other environmental microorganisms.

1.3 Potential industrial and environmental application of Shewanella

As aforementioned, the capability of flexible growth and respiration made the genus of *Shewanella* ideal candidates for bioremediation, microbial fuel cells, and for other biotechnology applications. These applications are briefly summarized in this section.

Various members of the *Shewanella* genus were reported to be able to reduce toxic compounds into less toxic molecules or leading to drastically reduced solubility, resulting precipitation of these compounds from the aquatic environment, allowing for sequestration or mineralization of toxic compounds. For example, various *Shewanella* were reported to reduce toxic elements Ur (VI) to Ur (IV), Tc (VII) to Tc (IV), Co (III) to Co (II), and Cr (VI) to Cr (III) with the oxidized form being soluble and the reduced form precipitate, facilitating removal of these contaminants from waste and ground water (Belchik et al., 2011; Sheng and Fein, 2014, Hau et al., 2008)However, it is to pertinent note that because *Shewanella* can also use other compounds that are more soluble in their reduced state, such as Hg or As, activity of *Shewanella* can actually increase their solubility, resulting in exacerbated contamination (Wiatrowski et al., 2006). Similar considerations need to be applied for treating contamination of halogenated organics, as in many cases the reduced compound is still toxic. Reduction of tetrachloromethane by *Shewanella* will produce toxic chloroform (Picardal et al.,

1993). However, chloroform can be further converted to harmless compounds if *Shewanella* is applied in a consortium of microorganisms. Therefore, careful planning is necessary when using *Shewanella* in bioremediation of such toxic compounds. Decision shall be made based on both the nature of the primary contaminant and the geochemical property of the site fully surveyed.

Microbial fuel cell technology is another important application of *Shewanella*. MFCs convert energy in organic compounds (typically waste material) into electricity. A microbe that can be applied in MFCs must be able to 1) harness high energy electrons from substrate to support their growth and metabolism, and 2) be able to shuttle electrons to the electrode. The latter part is usually the obstacle for many conventional microorganisms as they lack such machinery. To date, the microbial electron shuttling mechanisms were classified into three categories: 1) direct electron transfer (DET), in which electron is directly transported from cell to electrode via membrane proteins, typically outer-membrane cytochromes (Shi et al., 2009); 2) mediated electron transfer (MET), in which free diffusing electron shuttling molecules are produced and secreted by the bacteria that 'deliver' the electron to the electrode (Schroder, 2007); and 3) conductive pili, which are filamentous apparatus that derive from the bacterial cell to connect to the electrode for electron transfer (Gorby et al., 2006). *Shewanella* are one of the very few microbes that possess the machinery for all three mechanisms, making them ideal candidates for MFC applications. Numerous studies have been conducted to investigate the mechanism of *Shewanella* as anode or cathode organism, as well as genetically engineer for enhanced MFC performance (Bretschger et al., 2010; Fapetu et al., 2016; Jorge and Hazael, 2016).

Shewanella can also be used for production of valuable compounds. For example, production of omega-3 unsaturated fatty acids is a common trait in *Shewanella* species (Dailey et al., 2016). *Shewanella* and other marine bacteria were regarded as the primary source for production of the omega-3 fatty acids in marine fish oil. The pathway for eicosapentaenoic acid (EPA) in MR-1 is fully elucidated (Jeong et al., 2006). The gene cluster responsible for EPA synthesis in MR-1 has been cloned into *E. coli* for production of EPA (Lee et al., 2006).

1.4 Foci of this study

Understanding the fundamental physiology, metabolism, regulation, stress response, and genetics of *Shewanella* is a necessary step to improve their functionality. Incorporation of proper engineering with such knowledge provides the opportunity to fully explore their potential for environmental and industrial needs. In this thesis, studies on several important *Shewanella* strains were conducted from various approaches in an effort to screen for differing phenotypes, to investigate gene function and regulation, with the aim of understanding the stress response mechanism, improving the performance of *Shewanella* based environmental applications, and exploring for new areas of application.

In chapter 2, a unique red-pigmentation accumulating phenotype identified from transposon mutant library of *Shewanella loihica* PV-4 is described. Such phenotype is verified with in-frame deletion of *hemH1* gene, leading to the discovery of functionally redundant ferrochelatase encoding genes. We hypothesized that the red pigment accumulated is the immediate precursor of heme, PPIX. Multiple physical and chemical

tests were conducted to test this. The data obtained collectively supported the hypothesis. The yield of PPIX is also estimated to be much higher than previously reported *hemH* mutants from other bacterial species, reaching 11.2mg/g dry cell weight. This finding is patented and marks a new application of the *Shewanella* genus that could potentially be industrialized.

Chapter 3 follows on the genetic redundancy of the heme synthesis genes in PV-4, with focus on the ferrochelatase encoding genes *hemH1* and *hemH2*. It is hypothesized that the two *hemH* genes were functionally overlapping but under different expressional regulation. A series of analysis regarding the temporal expression pattern, promoter sequence, respective transcription regulator, and transcriptome were conducted to test the hypothesis. The link between heme synthesis regulation and oxidative stress response was uncovered, reflecting the fine-tune of gene regulation when experiencing different stresses. Lastly, we showed that the genetic redundancy of genes involved in heme synthesis also occurs on several other genes, which makes the level of redundancy in heme synthesis genes in *Shewanella* much higher than other bacteria. With these findings, a model depicting heme homeostasis in association with oxidative stress in *Shewanella* is proposed.

Chapter 4 focused on the effect of long term salt stress and the underlying mechanism of another important *Shewanella* strain, *Shewanella putrefaciens* CN-32, using the strategy of experimental evolution. It is hypothesized that one thousand generations of propagation under salt stress will confer higher salt stress tolerance than the ancestor and populations transferred under control condition. The improvement in phenotype can be attributed to differences occurred at various levels as a result of

adaptation during the course of evolution, such as metabolite, transcriptome and genome sequence. To test this hypothesis, the phenotypic characteristics, the metabolome, transcriptome, and population level genome sequence were investigated.

How to further increase the current generation and power density output of *Shewanella* based MFCs is a key issue perturbing real life applications. In Chapter 5, the effect of electrode modification with a redox polymer was evaluated on *Shewanella* based bioanodes. We hypothesized that 1) modifying the electrode surface with PVP-Os redox polymer can boost the electron communication between electrode and *Shewanella*, leading to significant improvement in current generation; 2) different *Shewanella* strains were reported to behave differently with unmodified electrode, similarly, different strains will also exhibit different current generation with PVP-Os redox polymer, 3) the amount of redox polymer used for coating the electrode affects the bacteria-electrode communication and therefore current generation, and 4) the bacteria/polymer incorporation have a huge impact on bioanode performance.

Chapter 2: Production of PPIX using the *hemH1* single mutant of *Shewanella loihica* PV-4

2.1 Abstract

Microorganisms have showed great potential for industrial production of valuable chemicals and drugs with fermentation. Although concurrent fermentation for industrial productions were mainly focused on model organisms such as *E. coli* and yeast, due to the nature of the particularly desired chemical and the unique physiological properties developed during the course of evolution, some environmental microbes may be more advantageous for production of certain products. In this study, a mutant with very high level of red pigment was identified in *Shewanella loihica* PV-4, an organism isolated from ocean sediment in our lab. The mutation was found in a gene encoding the ferrochelatase, Shew_2229. Since ferrochelatase catalyze the insertion of ferrous ion into the protoporphyrin IX (PPIX) to produce protoheme, we speculated that the red pigmentation is due to accumulation of PPIX. Various physical tests, including absorption spectrum, fluorescence spectrum, High Performance Liquid Chromatography tandem Mass Spectrum (HPLC-MS/MS), were performed on mutant samples and PPIX standard reagent. The result showed that the red pigmentation is indeed protoporphyrin IX (PPIX). PPIX is the immediate precursor of protoheme and is critical for heme synthesis, and in turn, the synthesis of hemoglobin. There is a great potential for industrial production of PPIX and use it as nutritional supplement, as photosensitizer or drug deliver and imaging in the field of photodynamic therapy (PDT) of cancer, for treating bacterial infections, as well as a basal compound for synthesis of various type of metalloporphyrins. The estimated yield of PPIX is 11.2mg/g dry cell weight, which is hundreds of times higher than other strains or mutants reported to accumulate PPIX, and is at the same level of a patented engineered *E. coli* strain (patent No. US20050089972). However, one major advantage of the mutant strain lies in the fact that there is no need to supply antibiotics to maintain the PPIX accumulating phenotype. In

addition, the accumulated PPIX are secreted outside of the cell, resulting in much easier procedure for separation and extraction of the PPIX. The purity of the raw product is high and can be further purified by conventional HPLC. The findings of this study have led to published patent under patent number US 9273334 (US20160002687, or WO 2014144329 A3).

Keywords: *Shewanella loihica* PV-4, transposon mutant library, in-frame deletion, ferrochelatase, protoporphyrin IX, HPLC/MSMS, HPLC-Fluorescence detection

2.2 Introduction

Application of microorganisms in human society has a very long history. The practice of fermentation can be dated back to 7000 to 6600 BC (McGovern et al., 2004), long before people realize that microorganisms were responsible for production of wine and pickled vegetable, etc. It is not until 1856 when French scientist Louis Pasteur linked yeast to the fermentation process (Manchester, 1995). During the past two centuries, the rapid development in microbiology has revolutionized the conventional concept of microorganisms. It is known that a vast majority of microorganisms with extremely high diversity are playing critical roles in almost every aspect of processes occurring on the Earth. Along with the discovery of novel microorganisms and increased understanding of their physiology, applications of microbes have expanded to fields such as probiotics, and production of valuable compounds and enzymes in large scale. Examples include *Lactococcus* that are being used for probiotics (Kimoto et al., 1999), and production of sorbose by *Acetobacter* (Joshi and Tamhane, 1974) for Vitamin C manufacturing, etc., many of which were already industrialized. In this chapter, we will focus on using bacteria for production of valuable compounds.

The explosion of molecular biology techniques in the last few decades has brought microbiology to a new depth. Similar to the invention of microscopy that allowed us to visualize these tiny life forms, the various molecular tools and methods enabled us to monitor the cellular processes at DNA, RNA, protein, or metabolite level, which greatly enhanced our understanding of the characteristics, physiology, and genetics of various microbes. In the meantime, industrial microbiology also benefited greatly from the new knowledge. Whereas in the past engineering typically refers to

efforts to seek for the optimum growth condition by adjusting factors such as nutrient, temperature, pH, oxygenation, etc., with the aid of modern molecular biology methods we can now manipulate the target microorganisms to achieve particular properties of interest, through strategies such as direct modification of genome sequence; adjusting expression level of single or multiple genes; introducing single or multiple genes originated from a different organism, or the more recently developed strategy with the mindset of metabolic engineering and synthetic biology to 'create' new metabolic pathways in microbes to allow for production of interesting compounds, etc., with the purpose of increasing the yield of a desirable product, or higher tolerance to waste accumulation and sorts.

Numerous engineered microorganisms have been reported to produce high yield of a great variety of products. Typically, these microorganisms are model organisms with better known physiology and genetics, especially the relatively abundant molecular biology tools, which made the modification of these organisms a lot easier. Some of the examples include *Pseudomonas* (Foti et al., 2013; Solaiman et al., 2001), *Actinobacteria* (Weber et al., 2015), and especially *E. coli* (Hanai et al., 2007; Thakker et al., 2013; Wen et al., 2013). The products from engineered microorganisms have expanded to biofuels such as ethanol, butyrate, and even short chain alcohols that more closely resemble the component in fossil based fuels (Wen et al., 2013); biodegradable materials such as polyhydroxyalkanoates (Solaiman et al., 2001), basal materials for various industrial applications like poly-glutamic acid (Yoon et al., 2000), medicines such as antibiotics (Weber et al., 2015), as well as proteins and enzymes for industrial or research applications, etc. More recently, incorporation of metabolic engineering

with genetic engineering has shown great potential to optimize the product yield from the molecular level, via metabolic flux analysis and well-designed pathway in which expression level of each gene can be controlled.

Another strategy of metabolic engineering with the mindset of synthetic biology eliminated the need of using live microorganisms, by engineering enzymes for higher catalytic efficiency and revised optimal condition (e.g. higher optimum temperature). The major advantages of this method include precise control and significantly enhanced predictability of yield and less undesired byproducts (Ye et al., 2012). However, the enzymes need to be replenished as they lose stability and catalytic efficiency during the fermentation process. This situation can be exacerbated when multiple enzymes are needed to turn starting material into desired product. A problem with any one enzyme in the series of biochemical reactions can lead to failure of the process. Besides, production and purification of these engineered enzymes in large scale can be very resource consuming. In contrast, this is not an issue when using live microbes as they continuously grow and produce the enzymes needed for the process.

Protoporphyrin IX (PPIX) is an intermediate metabolite involved in the biosynthesis of heme. It is highly hydrophobic and forms aggregates in water based solvents. It is a well-documented photosensitizer and produces toxic reactive oxygen species when exposed to light (Buettner and Oberley, 1979; Diez et al., 2009). In humans, precipitation of excessive PPIX onto skin can occur when the PPIX produced is not effectively converted to heme for hemoglobin production. Such deposition can lead to a disease named porphyria, in which sun exposure of patients will lead to irritation and other symptoms (Sassa, 2006). However, because of the unique physical

and chemical properties of this compound, there are numerous applications in therapeutic and imaging fields. PPIX itself, as well as the numerous types of metalloporphyrins that it can form with various metal elements such as Zinc, Copper, Magnesium, etc. were critical photosensitizers that have been widely applied in photodynamic therapy for treatment of cancer and infections (Allison et al., 2004; Hamblin and Hasan, 2004). Besides, these compounds also have great potential application in targeted drug delivery and imaging (Basoglu et al., 2016; Dong et al., 2016; Fang et al., 2016). It has also been proposed that the metalloporphyrins can be used as antibiotics for various types of pathogens (Maisch et al., 2007).

In this study, we report the identification of several transposon mutant strains of *Shewanella loihica* PV-4 that was able to produce significant amount of red pigmentation. The mutation occurs in a single gene, *hemH1*. It is hypothesized that the red pigmentation is PPIX. The hypothesis is then tested with various analytical methods with the *hemH1*in-frame deletion mutant. The results confirmed the hypothesis and the yield of PPIX is determined. While the transposon insertion mutant requires supply of kanamycin during culture and maintenance, the *hemH1* in-frame deletion strain does not. Other advantages of this mutant based PPIX production includes 1) the PPIX accumulation phenotype of the in-frame deletion strain is stable; 2) the mutant is easy to culture and no antibiotics is needed; 3) The PPIX extraction procedure is relatively easy and 4) the high purify of product from our bacterial culture. A patent based on this finding is published under patent number US 9273334B2.

2.3 Materials and Methods

2.3.1 Strains and plasmids used in this study

The strains and plasmids used in this study are listed in table 2.1.

Table 2. 1 Strains and plasmids used in this study

Strain/Plasmid	Description	Reference
Shewanella loihica PV-4	Wild-type strain isolated from the iron-rich microbial mat at a hydrothermal vent of Loihi Seamount, Pacific Ocean	(Gao et al., 2006)
Escherichia coli WM3064	*thrB1004 pro thi rpsL hsdS lacZDM15 RP4-1360 (araBAD)567 dapA1341::[erm pir(wt)]*	W. Metcalf
Shewanella loihica PV-4 parental strain	The *PstI* (Shew_0993) and *pstM* (Shew_0992) double deletion mutant of PV-4	This study
PV-4 Δ*hemH1*	*hemH1* (Shew_2229) deletion mutant derived from the PV-4 parental strain	This study
E. coli TOP10	F ¯*mcrA* Δ(*mrr-hsdRMS-mcrBC*) ϕ80d*lacZ*ΔM15 Δ*lacX74 deoR recA1 araD139*Δ (*ara-leu*)*7697 galU galK rpsL* (Str^r) *endA1 nupG*	Invitrogen
E. coli EC100D+	F ¯ *mcrA* Δ (*mrr-hsdRMS-mcrBC*) ϕ80d*lacZ*ΔM15Δ*lacX74 recA1 endA1 araD139*Δ (*ara, leu*)*7697 galU galK*λ^- *rpsL* (Str^r) *nupG pir*$^+$(DHFR)	Epicentre Technologies
pmini*Hmar* RB1	Suicide vector for building mariner transposon library	Daad Saffarini
pDS3.0	Suicide vector derived from pCDV224; Ampr Gmr *sacB*	(Wan et al., 2004)
pDS3.0-PV-hemH1ko	Suicide plasmid for deletion of *hemH1* derived from PV-4	This study
pDS3.0-PV-hemH2ko	Suicide plasmid for deletion of *hemH2* derived from PV-4	This study

2.3.2 Mutagenesis

A transposon mutant library was first constructed by introducing pmini*Hmar* RB1 vector into PV-4 wild type cells. After screening with kanamycin (Kan) resistance, large amount of Kan^R colonies were collected to provide ~20X coverage. Mutants were then screened for desired phenotypes. The red pigmented colonies were isolated and the transposon insertion site was identified via inverted PCR.

In-frame deletion was based on the suicidal vector pDS3.0 using a double crossover strategy. Briefly, the upstream and downstream DNA sequences immediately flanking the target gene were amplified, fused, and incorporated into the SacI site on pDS3.0. The constructed plasmid is introduced into $EC100D^+$ and verified with enzyme digestion and sequencing before transformed into the conjugation host WM3064 strain. After conjugation, the cells were plated on LB + Gentamycin (Gen) agar plates to screen for single crossover strains, which are gentamycin resistant. These gentamycin resistance colonies were verified with PCR and then cultured in LB medium without antibiotics overnight for resolution to occur. A small portion of the culture is then diluted and spread onto LB agar plates to obtain isolated colonies. These colonies were then 'counter selected by' transferring onto LB + sucrose plate and LB + Gen plates. Those grow on plates containing sucrose but do not grow on plates containing Gen were further verified with PCR to obtain the desired in-frame deletion mutant.

2.3.3 Culture condition and extraction of red pigment

To extract the red pigment, the Δ*hemH1* strain was revived and cultured overnight in 100 ml of Luria Broth (LB) at 30˚C with 200 rpm shaking. Significant

aggregation of the dark red substance was observed in the liquid culture. After centrifugation of the culture, the top layer containing the red pigment was carefully scraped and transferred into a 15ml Falcon tube. An acetone/ammonium 9:1 solution was used to dissolve the dark pigment. The solution was centrifuged again to remove any undissolved residuals and the resulting supernatant was used for all characterization processes.

2.3.4 Identification of the red pigmentation

The UV-vis spectrum analysis was conducted on a spectrophotometer (Biowave II WPA). High Performance Liquid Chromatography-Mass Spectrum/Mass Spectrum (HPLC-MS/MS) was conducted in University of Oklahoma Health Science center using a Michrom Bioresources Paradigm MSRB capillary HPLC and HCT Ultra ion trap (Bruker Daltonics) with the following procedure using a Magic MS C18 column (5 µm, 100 Å, 0.5 by 150 mm). Solvent A contains 0.09% formic acid, 0.01% trifluoroacetic acid (TFA), 2% CH3CN, 97.9% water. Solvent B contains 0.09% formic acid, 0.0085% TFA, 95% CH3CN, 4.9% water. Running gradient is as follows: 30% to 100% solvent B over 15 min, hold 3 min, 100% to 30% over 2 min. For standard and sample preparation, 1.3 mg of standard was dissolved in 1.3 ml of 100% methanol and diluted 10 times with the solution containing 0.1% formic acid, 50% acetonitrile, and 50% water, and 10 µl was loaded on an HPLC-UV-MS system. Two hundred microliters of sample were dried with Speed-Vac and then reconstituted with 200 µl of solution containing 0.1% formic acid, 50% acetonitrile, and 50% water. Ten microliters of samples were loaded onto a 40 µl loop into an HPLC-UV-MS system (flow rate,

20µl/min; UV wavelength 216 nm). The mass spectrometry system was a Bruker Daltonics HCT Ultra ion trap; mode, positive (target mass, m/z 500). The fluorescence spectra of the PPIX standard and samples were measured by a Nicolet Magna-760 (Fourier transform infrared spectroscopy [FTIR]) system at the Oak Ridge National Laboratory, TN.

2.3.5 PPIX yield estimation

An HPLC-Fluorescence detection method was used for purification and estimating the yield of PPIX. Multiple 10 ml samples were harvested from biological replicates 50 ml liquid cultures of PV-4 Δ*hemH1*. The 10 ml samples were then centrifuged and the supernatant removed. Then 0.5 ml of HCOOH was added to the pellet, mixed well, then 4.5ml of DMSO was added to the mixture and homogenized for 20min. The resulting solution is then centrifuged at 10,000 rpm for 10min to get rid of any undissolved residual. 20 µl of the supernatant from each sample was then taken and mixed with 180 µl of mobile phase A (100g ammonium acetate in 1.1 liter of nanopure water, 125ml acetonitrile, use glacial acetic acid to bring pH to 5.16) before loaded into HPLC. Mobile phase B is methanol: acetic acid 10:1 solution. An Agilent 1200 series HPLC station is used for analysis with an Agilent Zorbax 300extend C18 reverse phase column and an Agilent 1260 FLD Spectra instrument (Agilent, Santa Clara, CA, USA). The excitation and emission wavelengths were set to 405 nm and 630 nm, respectively. The HPLC running protocol is as follows: mobile phase B was increased from 0 to 100% in 10 min, hold for 2 min, then decrease to 0% in 2 min, hold for 2 min before next sample is taken. The yield estimation was calculated based on the peak area

of the emission and a standard curve generated using standard PPIX reagent purchased from Sigma Aldridge (St. Louis, MO, USA).

2.4 Results

2.4.1 Strain description

First reported by our lab in 2005, *Shewanella loihica* PV-4 strain was isolated from a very special site, at the deep-sea, hydrothermal Naha Vent from iron-rich microbial mats on the South Rift of Loihi Seamount, Hawaii, in the Pacific Ocean. It is Gram negative bacillus bacterium and moves via a single polar flagellum. The strain exhibits some unique characteristic, such as the wide range of temperature (0˚C to 42˚C) which it can survive and grow (Gao et al., 2006). Respiration versatility is a prominent feature in the *Shewanella* genus and PV-4 is not an exception. To date, the list of electron acceptors than can be used by PV-4 include fumarate, MnO_2, ferric citrate, nitrate, nitrite, akaganeite, cobalt [Co(III)] EDTA, potassium chromate, uranyl carbonate, hydrous ferric oxides and trimethylamine N-oxide, although this strain is initially regarded as incapable of denitrification (Gao et al., 2006; Yoon et al., 2015). The full genome of PV-4 has been sequenced and the data is available on National Center for Biotechnology Information (NCBI).

2.4.1 Transposon mutant library fabrication and screening

After obtaining the transposon library with ~20 × coverage, screening with various types of selective conditions was conducted for isolation of colonies with interesting phenotype. Several colonies exhibited a much darker red color compared to

the wild type strain was observed on regular LB agar plates. These colonies were then chosen and cultured and the transposon insertion sites were identified. The result showed that several of these mutants have transposon insertions in Shew_2229, a gene encoding ferrochelatase, indicating the red pigmentation phenotype we observed is due to disruption in *hemH1*.

2.4.2 Verification of red pigment overproduction mutant with in-frame deletion

After obtaining the transposon mutant of *hemH1*, we attempted to verify that the red pigmentation was indeed solely due to disruption of *hemH1*. Therefore, efforts were done to create an in-frame deletion mutant of *hemH1* in PV-4. However, the transformation efficiency in PV-4 was much lower compared with some other *Shewanella* strains such MR-1. Our previous experience with *Shewanella putrefaciens* W3-18-1 suggested that the restriction systems might hinder the cloning process. The W3-18-1 strain was cumbersome in mutagenesis because it contains a restriction endonuclease system, the PstI endonuclease/PstI methylase, which targets unmethylated PstI sites in foreign DNA fragment. Similar restriction system was found in PV-4 (*pstI*, Shew_0993 and *pstM*, Shew_0992), so we decided to knock out these genes first to facilitate mutagenesis in PV-4. The result of knocking out the PstI restriction system is shown in Fig. 2.1. The DNA extracted from wild type PV-4 is immune to digestion by PstI endonuclease, whereas the DNA extracted from the *PstI* and *PstM* double mutant can be fully digested by PstI. Therefore, this double mutant with both PstI endonuclease and PstI methylase gene knocked out is used from hereon as the parental strain for later on genetic work.

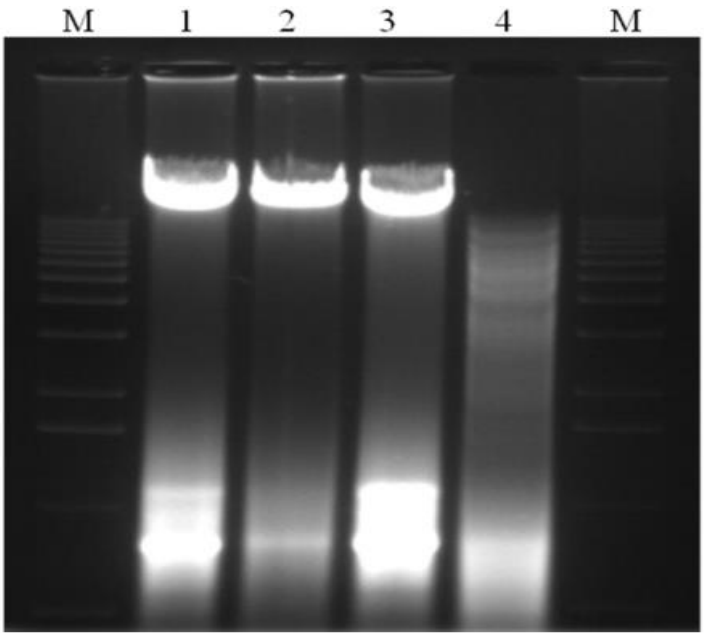

Fig. 2. 1 PtsI restriction digestion of chromosomal DNAs of the wild-type PV-4 strain (lane 2), and PV-4ΔpstIΔpstM strain (lane 4). M: 1 kb DNA markers; lanes 1 and 3 are the undigested chromosomal DNAs used as control. The chromosomal DNA of the wild-type PV-4 strain could not be digested by a commercial PstI endonuclease probably due to methylation of recognition sites.

Based on the parental strain, the *ΔhemH1* in-frame deletion mutant was obtained. Similar to the transposon insertion mutants, the *ΔhemH1* mutant exhibited the red pigmentation phenotype. Fig 2.2 shows the image of the colonies of transposon and in-frame deletion mutant of *hemH1*, and the image of cell pellets of Δ*hemH1* or wild type showing a top layer of dark red substance over the pinkish PV-4 cell pellets.

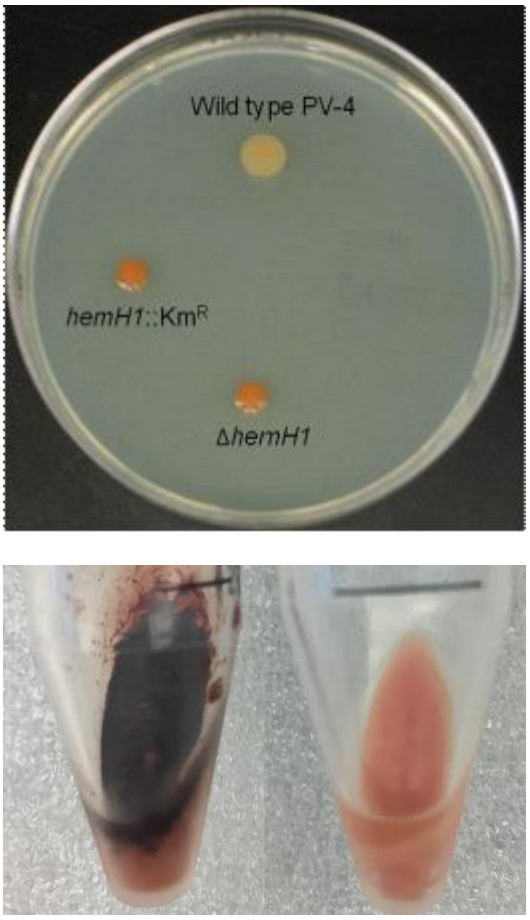

Fig. 2. 2 The colony phenotypes of PV-4 wild type, the transposon *hemH1* mutant hemH1::KmR, and the in-frame deletion *⊿hemH1* mutant (upper panel) and the cell pellets of 10ml liquid culture of Δ*hemH1* mutant or PV-4 wild type. A dark red layer lying on top of the cell pellet was observed in the Δ*hemH1* mutant.

2.4.3 The accumulated red pigment is PPIX

Due to the fact that the red pigmentation was observed in mutants with disrupted ferrocheltase gene *hemH1*, it is speculated that the red pigmentation is the precursor of the biochemical reaction catalyzed by ferrochelatase. Ferrochelatase is involved in the last stage of heme biosynthesis, by catalyzing the biochemical reaction in which a ferrous iron is incorporated into the porphyrin ring of PPIX to convert PPIX to protoheme (Fig 2.3). To verify whether the red pigmentation is PPIX, a series of

physical analysis were performed using commercial PPIX as control. PPIX belongs to the family of porphyrin compounds, with the characteristic porphyrin ring as the core structure. Such structure grants many unique physical-chemical properties to this compound that can be observed or tested, providing clues for its identification. PPIX is highly hydrophobic, which is exactly what is observed in our liquid culture. The red pigments either could form aggregates when growing in the broth, likely due to their hydrophobicity, or would disperse away from the broth surface as if it was repelled from the broth. Such observations further indicated that the red pigment might be PPIX. Besides hydrophobicity, PPIX exhibits unique feature in its absorption and fluorescence spectrum. Therefore, we performed UV-vis and fluorescence spectrum analysis and compared to PPIX standard reagent. Lastly, HPLC-MS/MS was performed on both standard and our extracted sample. The HPLC step purifies the crude extract first, while MS/MS analysis provides the most convincing evidence of whether the red pigmentation is PPIX.

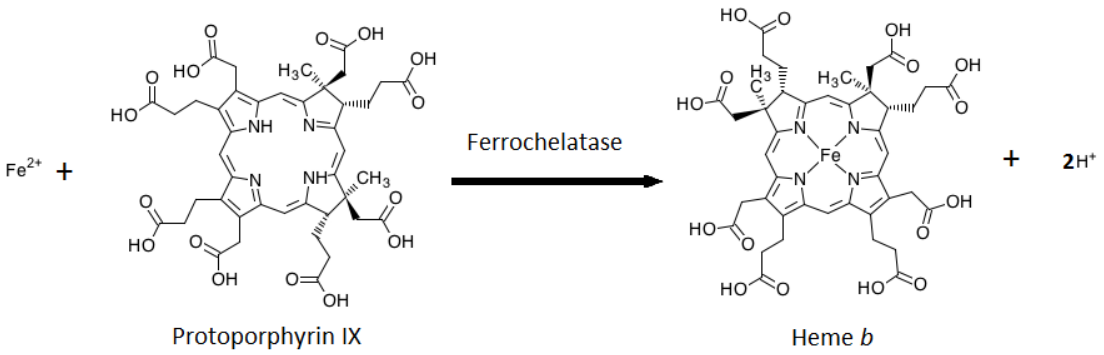

Fig. 2. 3 Biochemical reaction catalyzed by ferrochelatase, a ferrous ion is incorporated into the center of the porphyrin ring structure to produce heme *b*, which is the last step in heme *b* biosynthesis.

PPIX has a unique absorption spectrum, typically characterized by a major absorption peak at ~ 405nm. The absorption spectrum for the standard and samples extracted from wild type PV-4 and *ΔhemH1* were taken in the range of 350 nm to 750 nm. The result is shown in Fig 2.4. In consistence with previous publications, the PPIX standard showed a major absorption peak at ~ 405nm and several other minor peaks in the range of 500 nm to 670 nm. The sample extracted from the red pigment showed the exact same absorption pattern to that of the PPIX standard, as each of the peaks share the same wavelength as the PPIX standard. The lower intensity indicates a lower concentration of PPIX in the sample.

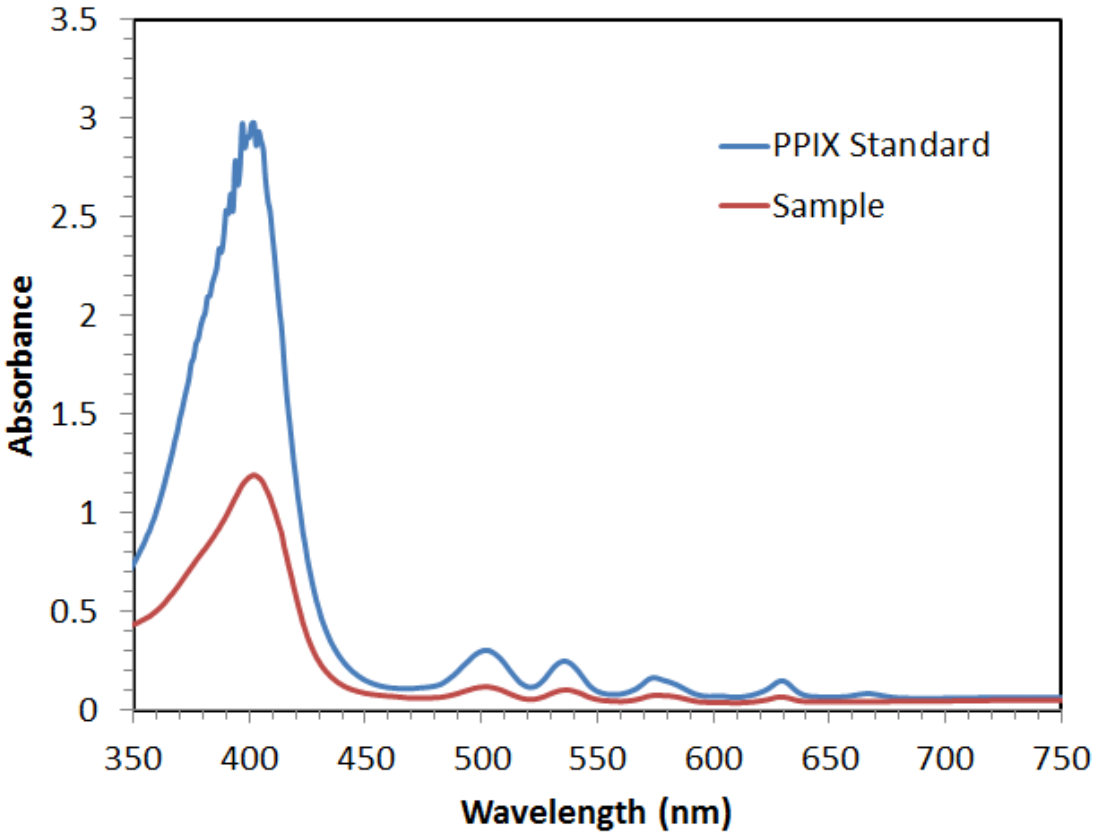

Fig. 2. 4 UV-vis spectrum of PPIX standard and sample extracted from PV-4 *ΔhemH1*.

The second analytical test performed was fluorescence spectrum in the wavelength range of 350~600 nm. The result is shown in Fig 2.5. The standard and extracted sample showed very similar fluorescence patterns, with one minor peak at ~390 nm and one major peak at ~430 nm. The peak fluorescence intensity was a bit higher in extracted samples, which might be due to the higher content of PPIX in the sample.

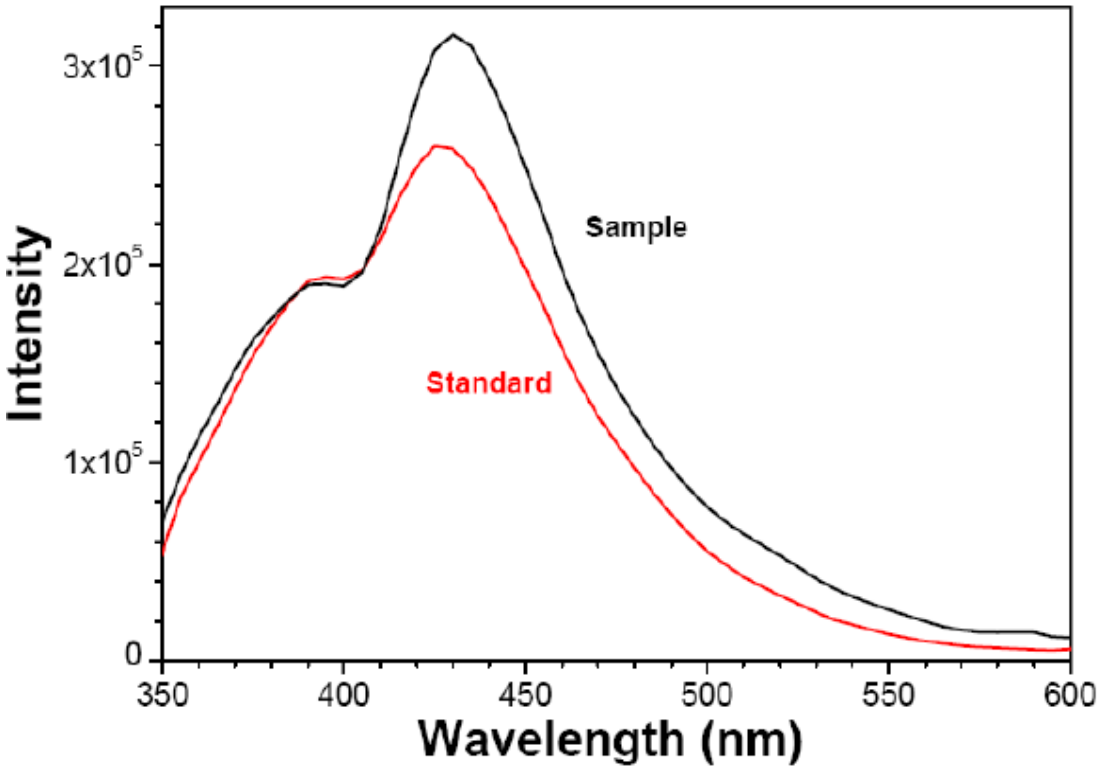

Fig. 2. 5 The fluorescence spectrum of PPIX standard and the red pigment sample extracted from PV-4 Δ*hemH1*.

Although UV-vis and fluorescence spectrum provided strong evidence that the red pigment extracted from Δ*hemH1* mutant was likely PPIX, mass spectrum can provide a more convincing evidence for the atomic composition of the chemical. Therefore, HPLC-MS/MS was performed on the PPIX standard and the extracted sample. In this procedure, the crude solution the standard and the extraction first went

through HPLC. As shown in Fig. 2.6, both the standard and extracted sample had only one peak that is eluted at the same time. This eluted portion were then analyzed with MS, which was shown in Fig 2.7 a. Both standard and extraction sample had a major peak at mass of 563.2, corresponding to the molecular weight of PPIX. This portion of mass was then further broken down with another level of MS analysis, revealing that our sample and the PPIX standard had the exact same composition, confirming that the red pigmentation is indeed PPIX.

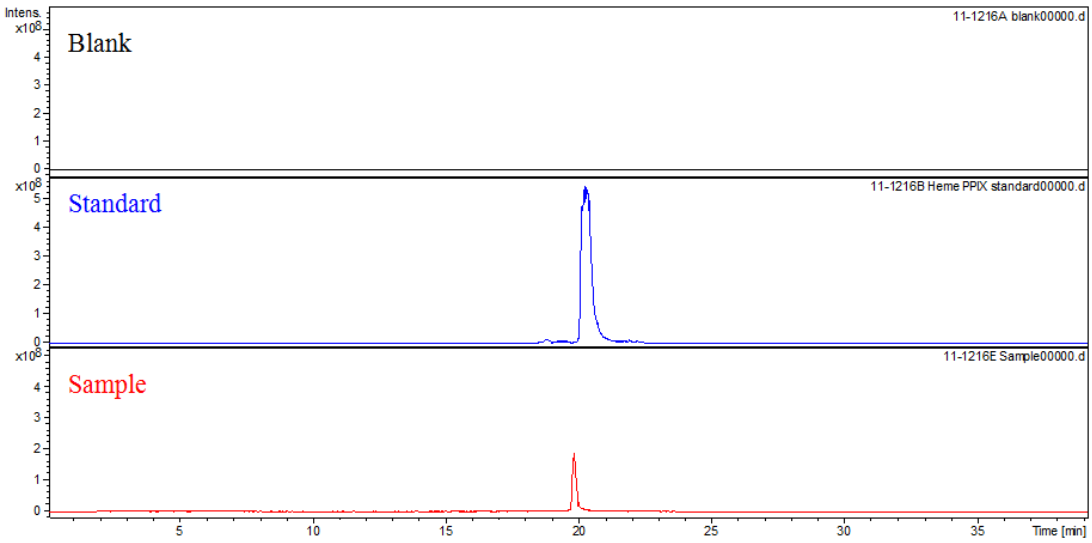

Fig. 2. 6 HPLC of PPIX standard and red pigment extraction sample, showing that there is only one major elution peak with the same time of elution.

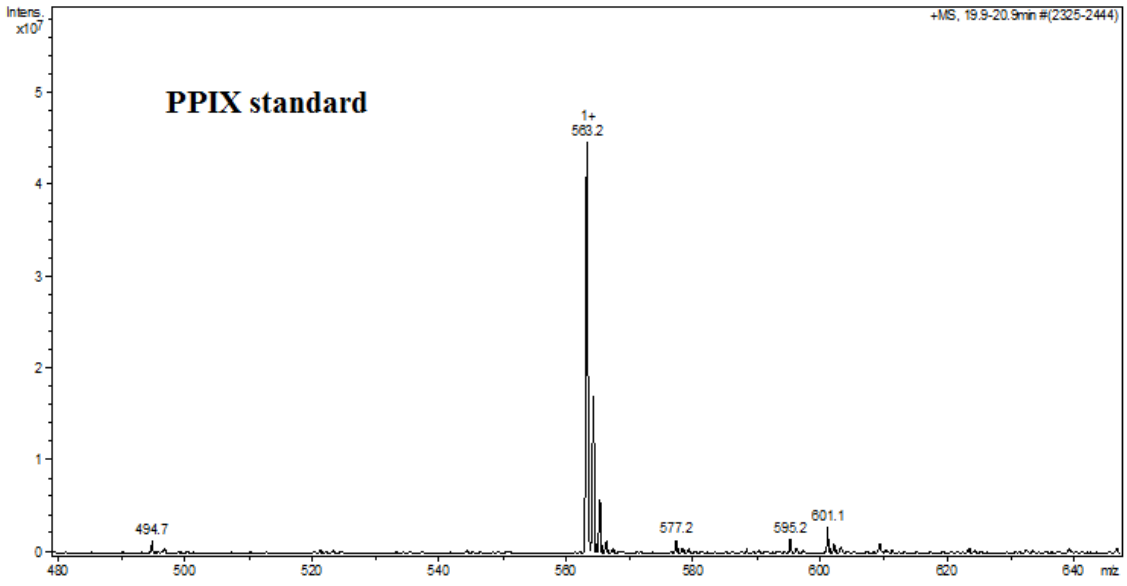
Intens.
x10^7
+MS, 19.9-20.9min #(2325-2444)
PPIX standard
1+
563.2
494.7
577.2
595.2
601.1
mz

a

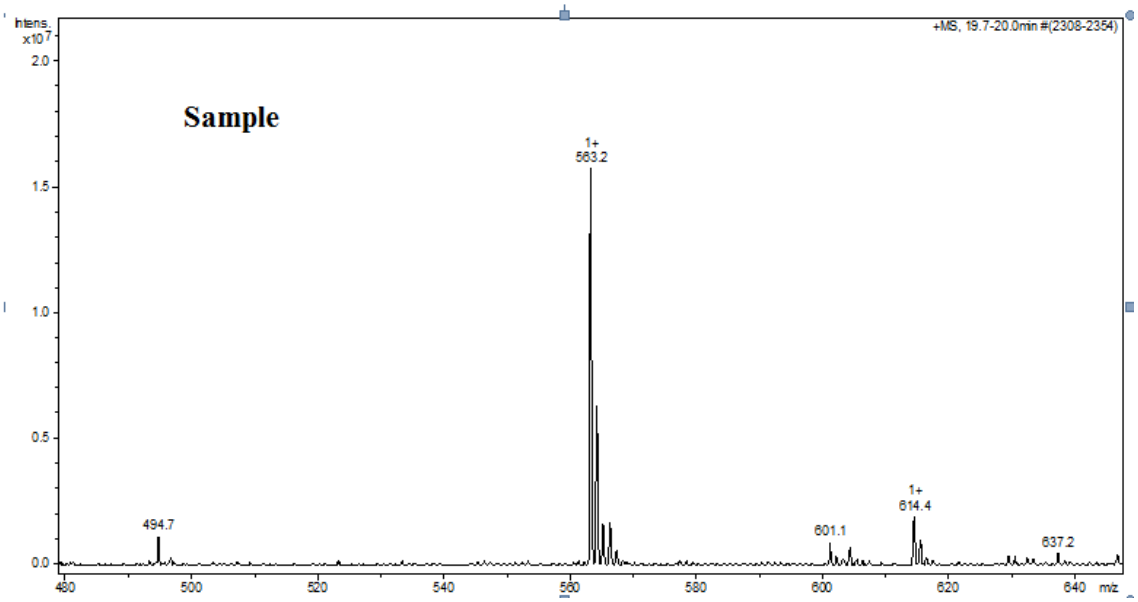
Intens.
x10^7
+MS, 19.7-20.0min #(2308-2354)
Sample
1+
563.2
494.7
601.1
1+
614.4
637.2
mz

b

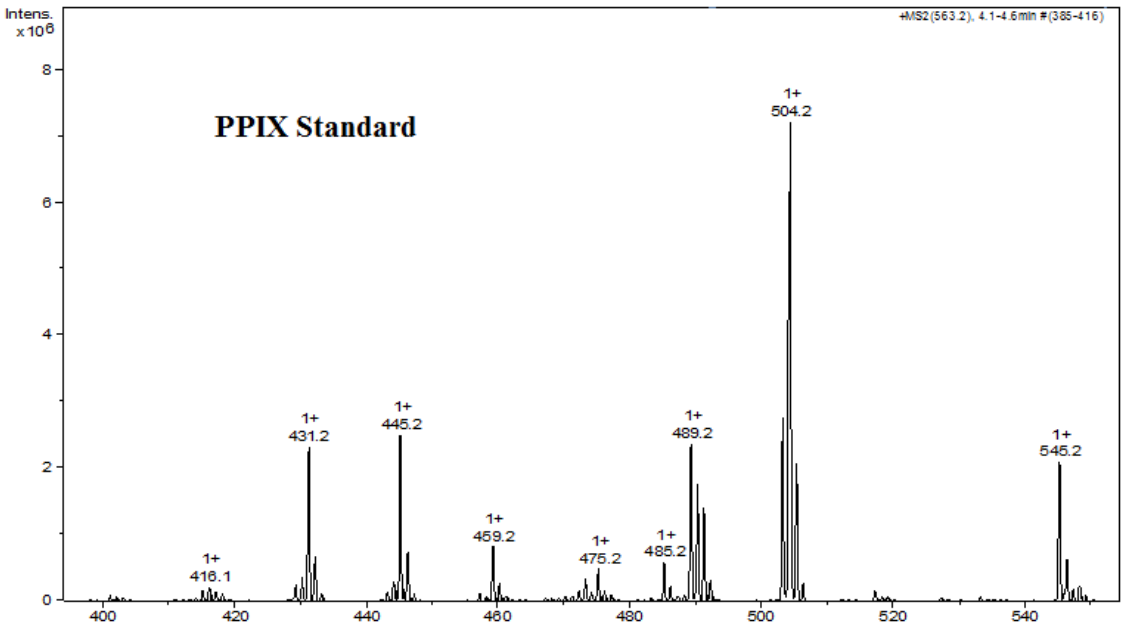

c

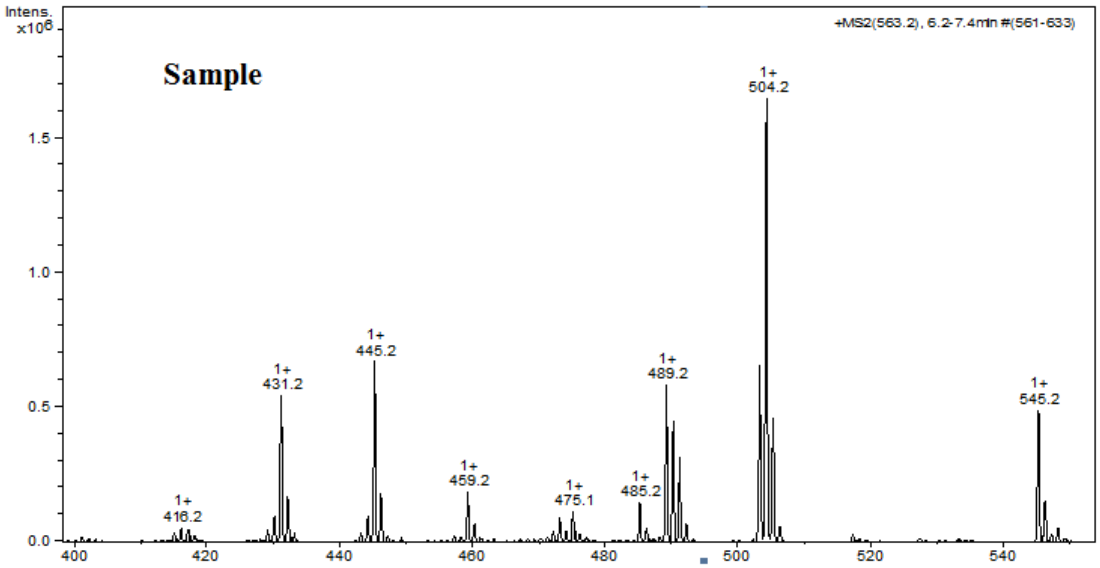

d

Fig. 2. 7 Mass spectrum of the HPLC eluted major peak from PPIX standard (a), or extracted sample (b); The m/z 563.2 peak is then went through a tandem mass spectrum analysis, showing that PPIX standard (c), and sample extracted (d) had the exact same subgroup profile.

2.4.4 Determination of PPIX yield

The yield was estimated based on HPLC-Fluorescence. As the sample passed through the fluorescence detector the PPIX was excited at 405nm and the emission at 630nm (E630) was recorded. The peak area of E630 was used for calculation. A standard curve was produced via the same procedure (Fig 2.8). The PPIX concentration in the sample was calculated based on the standard curve. Based on calculation, the yield of PPIX from *ΔhemH1* mutant was ~11.6 ± 2.5 mg per gram of dry cell weight, or about 35 mg per liter of liquid culture per day based on 20 samples, while the PPIX signal from the PV-4 wild type strain is barely detectable.

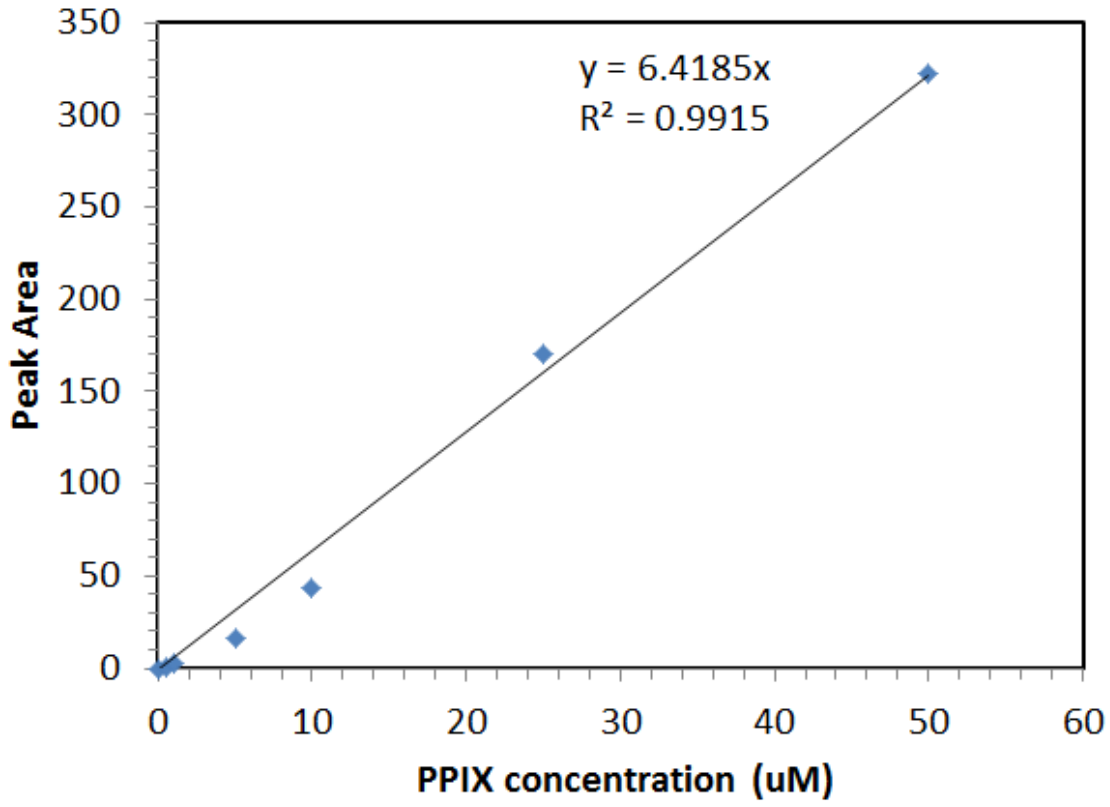

Fig. 2. 8 Representative PPIX standard curve based on HPLC-Fluorescence detection

2.5 Discussion

Industrial microbiology has become an important branch of microbiology, with more emphasis on industrial level production of valuable compounds through batch culture, semi-batch culture, and continuous culture of microorganisms. Some of the commonly known products that can be produced in industrial level include citric acid, various vitamins and amino acids, hormones, and enzymes. Typically the organisms involved in industrial production are traditional fermentation organisms that human have been utilizing since ancient time, such as various lactobacillus strains and yeasts, as well as model organisms such as *E. coli*, *Bacillus*, *Pseudomonas*, etc. Production of valuable compound using environmental microbes is relatively rare due to the less understood genetics, physiology, and regulation. However, with increased knowledge, and combined with modern molecular biology and engineering, some unique features of certain environmental organisms have great potential for industrial productions of chemicals or compounds that are of great value.

Members in the *Shewanella* genus are renowned mostly due to their flexibility to survive in wide gradient of various environmental factors. Their psychrotolerance and extraordinary respiration capability are two signature features. The cold resistance is largely attributed to the ability of modifying the cellular membrane properties under cold temperature by producing unsaturated fatty acids, such as EPA and DHA (Wang et al., 2009; Yin and Gao, 2011) . Very high yield of EPA production was reported in a pioneer study of *Shewanella* isolated from sea water samples (Yazawa et al., 1988). These studies have led to the efforts to produce EPA and DHA using recombinant biotechnology, using gene or gene clusters from *Shewanella* or other marine bacterium

(Amiri-Jami and Griffiths, 2010). Some of these findings were published as patents (US 8829274 B2, US7939305 B2, CA2647150 A1, etc.)

Regarding the respiratory versatility, the broad range of electron acceptors *Shewanella* can use for respiration is largely attributed to the diversified cytochromes in these organisms. Among the 20 + fully sequenced *Shewanella* strains, around 40 cytochrome encoding genes were typically found in their genomes. Many of these cytochromes need more than one heme molecule for proper functioning. For example, some of best characterized cytochromes that play critical roles in anaerobic reduction all need multiple heme molecules. The membrane anchored cytochrome CymA is tetraheme. The sulfite reductase cytochrome c is octaheme. A series of cytochromes involved in dissimilatory metal reduction, MtrA, MtrC, MtrD, MtrF and OmcA, are all decaheme. It is the expression of the numerous cytochromes that gaves the unique orange or pink color of these organisms and allows for switching to different types of electron acceptors with change of redox potential in its environment. In order to produce these cytochromes, the correct function of the heme synthesis pathway is necessary to guarantee sufficient heme supply. In this study, the capability of heme synthesis in PV-4 is used for production of heme precursor, PPIX, an important molecule with great applications in various fields, especially as basal materials for synthesis of metalloporphyrins and for PDT.

Based on our experience and previous publications, the PPIX overproduction phenomenon in the PV-4 *hemH1* mutant strain may be a unique feature amongst *Shewanella*. Firstly, the transposon library of several other *Shewanella* strains, such as *Shewanella oneidensis* MR-1, *Shewanella putrefaciens* strain CN-32 and strain W3-18-

1, *Shewanella frigidimarina* NCIMB400, etc., were prepared in our lab and with similar coverage. However, red pigmented mutants such as the PV-4 mutant were never observed. Secondly, when the *hemH1* gene was knocked out in MR-1 via in-frame deletion, no red pigmentation phenotype was observed, indicating no PPIX accumulation. It is possible that the *hemH* paralogues in these strains may take up the role for converting PPIX to heme. A detailed study regarding the redundancy of this *hemH* paralogue system is summarized in Chapter 3. Thirdly, there are no other publications reporting PPIX overproduction in other *Shewanella* strains.

When evaluating the potential of industrial application for producing valuable compounds with bacteria, the yield, ease of processing, and efforts needed to reach desired purity of product, etc., must be taken into consideration. In terms of yield, the mutants reported in this study were the highest in reported literature using bacterial mutants, at least hundreds of times higher than reported from other studies (Meinecke et al., 2010); three times higher than a yeast mutant which needs to be cultivated on solid media to achieve highest yield (JOHN BASSEL, 1975); and reached similar level as a previously published patent in which a recombinant *E. coli strain* harboring multiple vectors was used for PPIX production (patent No. US20050089972). However, in this patent the engineered *E. coli* strain needs to be cultured with supplementation of three types of antibiotics to ensure expression of the recombinant enzymes, whereas in the in-frame deletion mutant no antibiotics is needed during fermentation. Currently, the production of PPIX is mainly based on extraction from livestock blood. This process is complicated, expensive, and with apparent biosafety concerns during the collection and processing of blood. The procedure of chemical synthesis of PPIX is complicated and

the product is likely to be a mixture of isomers, and only a certain portion of the product is of biological use because of the chirality of PPIX. These drawbacks make large scale production of PPIX virtually impossible. However, with the mutant strain from this study, large scale production of PPIX can be realized easily with the current fermentation industry. The fact that the PPIX produced were secreted out of the cell makes the separation/extraction procedure much easier as simple centrifuge can separate the cell pellets with PPIX aggregates so that no cell lysis is necessary. The crude PPIX produce is with high level of purity. If higher purity is desired, the crude product can be dissolved with a favored solvent and further purified by a simple HPLC procedure.

Chapter 3: Environmental implications of the differential regulation of *hemH* paralogues in *Shewanella*

3.1 Abstract

It has been an intriguing task to understand the functions and regulations of paralogous genes in microorganisms. In chapter 2 was described a ferrochelatase (*hemH1*, Shew_2229) mutant of *Shewanella loihica* PV-4 that can accumulate significant level of PPIX. A paralogous ferrochelatase gene, Shew_1140, named *hemH*2, was annotated in PV-4. Existence of the ferrochelatase paralogues were also found in the majority of sequenced *Shewanella* strains. In PV-4, single knock out of *hemH2* did not exhibit the PPIX accumulation phenotype. However, efforts to create double deletion mutant *ΔhemH1ΔhemH2* were not successful, likely due to the fact that heme was essential for the survival and growth of PV-4. The expression pattern of the two paralogues differed significantly based on RT-PCR and qRT-PCR analysis. *hemH*1 expression level was consistently high, while expression of *hemH2* was barely detectable in the wild type strain. However, the expression of *hemH2* became significant in the *ΔhemH1* mutant, indicating that *hemH2* might play a supplementary role for producing ferrochelatase under extreme conditions, such as low heme supply. The function of *hemH2* as ferrochelatase was further supported by the fact that the PPIX accumulation phenotype was reverted when the expression of *hemH2* was boosted artificially. Differences in the promoter sequences of the two paralogues suggested that the paralogues were under different regulation. While it is apparent that *hemH1* is the dominant ferrochelatase gene whose expression is driven by the housekeeping sigma factor rpoD, expression of *hemH2* may be driven by the ECF sigma factor rpoE. This speculation is supported by a

series of bioinfomatic analysis and experiments. Our results showed that expression level of *hemH2* was dependent on the expression level of *rpoE*, whose expression was upregulated under oxidative stress. Instead of inducing *hemH2* expression by cloning, exposing the wild type strain to oxidative stress led to significant increase of the expression of both *rpoE* and *hemH2*. Interestingly, in the *ΔhemH1* mutant, the PPIX accumulation was reverted by exposing the culture to light. The reason might be that initial accumulation of PPIX led to production of oxygen radicals upon light exposure. The oxidative stress imposed by the oxygen radicals triggered the upregulation of *rpoE*, which in turn, drove up the expression of *hemH2*, producing more ferrochelatase to convert PPIX to heme, reverting the phenotype. The qRT-PCR result showed that indeed, the expression of *rpoE* and *hemH2* were much higher when *ΔhemH1* mutant was exposed to light than cultured under dark condition. In summary, the differential regulation of the two *hemH* paralogues has important environmental implications. Although under aerobic culture conditions with LB medium *hemH1* alone is enough to ensure the heme synthesis, the two paralogues likely works in concert under stress conditions to ensure enough heme supply for this bacterium.

Keywords: ferrochelatase paralogues; gene redundancy; expression regulation; rpoD, rpoE, oxidative stress, photosensitizer, comparative genomics

3.2 Introduction

Heme is a critical cofactor involved in a wide range of important biological processes, such as respiration, detoxification, gas sensing and transport, and signal transduction. The biosynthesis pathway of heme has been well characterized. The intermediates in the heme biosynthesis pathway are conserved across prokaryotes and eukaryotes, possibly due to the fundamental nature of many of the biochemical processes that require involvement of heme (Obornik and Green, 2005). An incomplete heme synthesis pathway usually results in heme auxotrophy, such as in *Haemophilus influenza* or *Buchnera* (Baumann et al., 1995). In humans, abnormal heme synthesis can lead to anemia or porphyria (Iolascon et al., 2009; Moore, 1998).

Despite the high level of conservation, variations in the enzymes that actually carry out heme biosynthesis were observed among different organisms. Eukaryotic cells use oxygen dependent coproporphyrinogen oxidase encoded by *hemF*, while some bacteria use an oxygen independent counterpart encoded by *hemN* (Panek and O'Brian, 2002). More recently, two new sub-pathways for heme biosynthesis were validated: one involves the production of heme from siroheme, and the other does not use protoporphyrin as an intermediate (Bali et al., 2011; Dailey et al., 2015). However, most heme biosynthesis or heme homeostasis studies in prokaryotes were conducted in pathogenic or symbiotic microorganisms, relevant knowledge in environmentally important microorganisms is still lacking. Therefore, study of genes involved in the heme biosynthesis pathway in environmental microorganisms is very important for our understanding of the cellular response to fluctuation in environmental conditions and manipulation of microorganisms for industrial, medical and environmental applications.

Shewanella species, frequently isolated from redox-stratified environments, are renowned for their respiratory versatility. Members of the *Shewanella* genus are capable of carrying out dissimilatory reduction of various organic compounds, metals, and nitrate, which are critical steps in the global cycling of carbon, metals, and nitrogen (Fredrickson et al., 2008; Hau and Gralnick, 2007). The ability to use such a diverse group of electron acceptors is largely attributed to the great variety of *c*-type cytochromes, many of which contain more than one heme (Fredrickson et al., 2008; Hau and Gralnick, 2007). Therefore, there is a strong demand of heme for the biosynthesis of *c*-type cytochromes and other proteins that require heme as a prosthetic group. However, excessive heme or its closely related porphyrin compounds are toxic (Cox GS, 1982; Miyamoto et al., 1992; Nakahigashi et al., 1991), resulting in tight control of the intracellular heme/porphyrin pool in *Shewanella* species. Bacteria employ various strategies to control intracellular heme levels, such as the regulation of heme biosynthesis or uptake, exportation, sequestration, and degradation (Anzaldi and Skaar, 2010). We employ *Shewanella* species as an ideal system to study heme biosynthesis and homeostasis for environmental microorganisms.

Shewanella loihica PV-4 was isolated from iron-rich microbial mats at an active, deep sea, hydrothermal Naha Vent (1325 m below sea level), located on the South Rift of Loihi Seamount, Hawaii, in the Pacific Ocean (Gao et al., 2006). Two *hemH* genes, *hemH1* (Shew_2229) and *hemH2* (Shew_1140) are annotated in the PV-4 genome. Both genes encode the enzyme ferrochelatase, which catalyzes the last step of heme synthesis by inserting a ferrous ion into the porphyrin ring of protoporphyrin IX to form heme *b*. These two ferrochelatase paralogues share 47% amino acid sequence identity although

DNA sequences vary significantly. We hypothesize that both *hemH* paralogues function in heme biosynthesis but might be differentially regulated for sustaining the heme homeostasis in the *Shewanella* strains encoding a number of *c*-type cytochromes for flexible respirations. We conducted the molecular genetics analyses, including transposon mutant library screening, genetic complementation, in-frame gene deletion, and functional genomics analyses on the mutants by transcriptional profiling with quantitative reverse transcription PCR and microarray technology, heme staining, chemical analyses, and comparative genomics analyses to test our hypothesis. Disruption of *hemH1* resulted in extremely high concentrations of extracellular PPIX, which was not observed when *hemH2* was disrupted. In Δ*hemH1*, the biosynthesis of heme and cytochromes were observed. However, the double knockout mutant of *hemH1* and *hemH2* could not yet be generated. More importantly, the transcription of two *hemH* paralogues was regulated differentially in response to environmental stresses. Besides *hemH*, numerous genes involved in the heme synthesis pathway possess paralogues in *Shewanella*. Although gene redundancy is a common phenomenon, to the best of our knowledge, existence of paralogues of multiple genes belonging to heme biosynthetic pathway is not reported yet. These data suggested the importance of the ancient heme synthesis pathway and their particular biological significance in these respiratory microbes, providing important insights into the mechanisms underlying bacterial adaptation to ever-changing environmental conditions via differential regulation of paralogues for concerted gene expression, and the understanding of genetic redundancy, a phenomenon widely found in all life domains and in almost every gene category.

3.3 Materials and Methods

3.3.1 Strains, plasmids, and culture conditions.

The strains and plasmids used in this study is listed in Table 3.1 and Table 3.2, respectively. Unless otherwise noted, the PV-4 and its derivative strains were cultured aerobically at 30˚C with 200 rpm shaking.

Table 3. 1 Bacterial strains used in this study

Strain	Description	Reference
Shewanella loihica PV-4	Wild-type strain isolated from the iron-rich microbial mat at a hydrothermal vent of Loihi Seamount, Pacific Ocean	(Gao et al., 2006)
Escherichia coli WM3064	*thrB1004 pro thi rpsL hsdS lacZDM15 RP4-1360 (araBAD)567 dapA1341::[erm pir(wt)]*	W. Metcalf
Shewanella loihica PV-4 parental strain	The *PstI* (Shew_0993) and *pstM* (Shew_0992) double deletion double mutant of PV-4	This study
PV-4 Δ*hemH1*	*hemH1* (Shew_2229) deletion mutant derived from the PV-4 parental strain	This study
PV-4 ΔhemH2	*hemH2* (Shew_1140) deletion mutant derived from PV-4	This study
E. coli TOP10	F ¯*mcrA* Δ(*mrr-hsdRMS-mcrBC*) ϕ80d*lacZ*ΔM15 Δ*lacX74 deoR recA1 araD139*Δ (*ara-leu*)*7697 galU galK rpsL* (Str^r) *endA1 nupG*	Invitrogen
E. coli EC100D+	F ¯ *mcrA* Δ (*mrr-hsdRMS-mcrBC*) ϕ80d*lacZ*ΔM15Δ*lacX74 recA1 endA1 araD139*Δ (*ara, leu*)*7697 galU galK*λ^- *rpsL* (Str^r) *nupG pir*$^+$(DHFR)	Epicentre Technologies

Table 3. 2 Plasmids used in this study

Plasmid	Description	Reference
pDS3.0	Suicide vector derived from pCDV224; Ampr Gmr sacB	reference
pDS3.0-PV-hemH2ko	Suicide plasmid for deletion of *hemH2* derived from PV-4	This study
pHERD30T	Shuttle vector with pBAD promoter, Gmr	(Qiu et al., 2008)
pHERD30T-PV-hemH1	pHERD30T containing the *hemH1* derived from PV-4, Gmr	This study
pHERD30T-PV-hemH2	pHERD30T containing the *hemH2* derived from PV-4, Gmr	This study
pHERD30T-PV-rpoE2	pHERD30T containing the *rpoE2* derived from PV-4, Gmr	This study
pHERD30T-MR-hemH1	pHERD30T containing the *hemH1* derived from MR-1, Gmr	This study
pDS3.0	Suicide vector derived from pCDV224; *Amp^r, Gm^r, sacB*	(Wan et al., 2004)
pDS3.0-PV-hemH1ko	Suicide plasmid for deletion of *hemH1* derived from PV-4	This study
pDS3.0-PV-hemH2ko	Suicide plasmid for deletion of *hemH2* derived from PV-4	This study
pHERD30T	Shuttle vector with pBAD promoter, *Gm^r*	(Qiu et al., 2008)
pHERD30T-PV-hemH1	pHERD30T containing the *hemH1* derived from PV-4, Gm^r	This study
pHERD30T-PV-hemH2	pHERD30T containing the *hemH2* derived from PV-4, *Gm^r*	This study
pHERD30T-PV-rpoE2	pHERD30T containing the *rpoE2* derived from PV-4, Gm^r	This study
pHERD30T-MR-hemH1	pHERD30T containing the *hemH1* derived from MR-1, Gm^r	This study

pHERD30T-MR-hemH2	pHERD30T containing the *hemH2* derived from MR-1, Gm^r	This study
pHERD30T-MR-rpoE2	pHERD30T containing the *rpoE2* derived from MR-1, Gm^r	This study
pHERD30T-PV-gltX	pHERD30T containing the *gltX* derived from PV-4, Gm^r	This study
pHERD30T-PV-hemA	pHERD30T containing the *hemA* derived from PV-4, Gm^r	This study

3.3.2 RT-PCR and qRT-PCR

Total RNA was extracted using RNAisoPlus (Takara) and RNAprep pure Cell/Bacteria Kit (TIANGEN BIOTECH (Beijing) CO., LTD.) followed by DNase I treatment. To prepare cDNA, 2 μg of total RNA was reverse-transcribed using the PrimeScript® RT reagent Kit with gDNA Eraser (Takara) and TIANscript RT Kit (TIANGEN BIOTECH (Beijing) CO., LTD.). Reverse-transcription PCR (RT-PCR) was carried out as described previously. Quantitative real-time PCR (qRT-PCR) was performed in 20μl total volume with 1μl template cDNA from 10-fold diluted reverse transcription products. Relative gene expression levels were quantified using SYBR Premix Dimer Eraser (Takara) on a Roche Light Cycler 480 II Real-Time PCR system (Roche Diagnostics, Penzberg, Germany) with triplicates. Gene expression was normalized against the 16S rRNA gene using the $2^{-\Delta Ct}$ calculation: $\Delta Ct = Ct_{\text{gene of interest}} - Ct_{\text{16s rRNA.}}$.

Table 3. 3 Primers used in this study

Primer	Sequence (5' to 3')
PV4-hemH1-F	GGAATTCTAAAGTGAAGCGCTATATGAGC
PV4-hemH1-R	GCTCTAGAGCAGTGATTTATGCCGTTTACC
PV4-hemH2-F	GGAATTCGTGGCGATTGATCTCTAAG
PV4-hemH2-R	GCTCTAGACAAGTTAAAGATACGGCCTC
PV4-rpoE2-F	GGAATTCAAGGGTCATACGTGAGTACAG
PV4-rpoE2-R	GCTCTAGAATTAATCATGCTGCTGGTCTCC
MR1-hemH1-F	GTGAGCTCTATGCGACTGAATGTTAGCC
MR1-hemH1-R	GCTCTAGATCATTCTGCACTTATCCAAG
MR1-HemH2-F	GGAATTCAGAAATGGGTCACGCTGC
MR1-HemH2-R	GCTCTAGAGCTTACAGATACGGCTTCACC
MR1-rpoE2-F	AGAATTCCGAACGGGGTTGAACCTTA
MR1-rpoE2-R	AGTCGACGGGGGTGATGTTTAATCATGT
PV4-gltX-F	GCGAATTCTCGATAACAGGTTACTGTCCC
PV4-gltX-R	GCTCTAGAACACCCAAAAGTGTCAACTCG
PV4-hemA-F	GCGAATTCCTAGAGACCAGAAAGAGTCAG
PV4-hemA-R	GCTCTAGAGAACGCTAACCTTAGTCTTTATC
PV4-pstko_5O	AGAGCTCCCTGCCCTCAATGACTTGTT
PV4-pstko_5I	TGCATCGAGTTGATTGTCGCGCAACAAGTGACCCACTCAA
PV4-pstko_3I	GCGACAATCAACTCGATGCACCCAAAATTTCCGCATCATA
PV4-pstko_3O	AGAGCTCGGCCTTAAGCCCTTTGATCT
PV4-hemH1_5O	AGAGCTCGTACGTTCACCGCACTCTGA
PV4-hemH1_5I	TGCATCGAGTTGATTGTCGCATCACTGCCCGATGCTATTT
PV4-hemH1_3I	GCGACAATCAACTCGATGCATAGGCTAGCACCCACCCTTG
PV4-hemH1_3O	AGAGCTCGTTAAAGCGGGAACGCCTCT
PV4-hemH2_5O	GTGAGCTCATAGATACCGACTCGTTCG
PV4-hemH2_5I	GCGGTCAATTACGTGCTGTCTTAGAGATCAATCGCCACA
PV4-hemH2_3I	GACAGCACGTAATTGACCGCTTCTATCAATTGCCTGTGG
PV4-hemH2_3O	CAGAGCTCTGGTTCTGGGTATCAAAATG
QRT-PV4-hemH1-F	CAGTGTCAACGTACTGCCGA
QRT-PV4-hemH1-R	ATAAAGCTCTCCTTGCCGCC
QRT-PV4-hemH2-F	ATTTCTGCATGCGTTACGGC
QRT-PV4-hemH2-R	GCCAGCGCCGCAATATAATC
QRT-16S-F	TAATGGCTCACCAAGGCGAC
QRT-16S-R	GGAGTTAGCCGGTCCTTCTTC
PV4-hemH1-RTF	CCGTAGCCAAGCTCTATGAG
PV4-hemH1-RTR	GTCACCCTCGGTCACATAAC
PV4-hemH2-RTF	GCTGGTGTGGATGCTGATAC
PV4-hemH2-RTR	TTAGCGATAGAGTCAGCCAG
PV4-rpoE2-RTF	GCTTAGGCGCGTCAAGGCCAAG
PV4-rpoE2-RTR	ATTAATCATGCTGCTGGTCTCC
16S rRNA-RT-F	GTTGGAAACGACTGCTAATACC
16S rRNA-RT-R	GGTCCTTCTTCTGTAGGTAACG
oligodT	GCCAGTCTTTTTTTTTTTTTTT

P-PV4-hemH1-1R	CATAACTCATCCCCAACTCCACC
P-PV4-hemH1-2R	CCTCGGGCCACCAGATAGACT
P-PV4-hemH2-1R	CACTGCCATTTTCACTCAGCTTTTG
P-PV4-hemH2-2R	CCTGCTCCGTCCAGATAGACTG

3.3.3 Microarray analysis

The whole genome microarray of *S. loihica* PV-4 covers 3857 of the 3869 annotated coding sequences. 65-mer nucleotide probes were designed with CommonOligo 2.0 (He et al., 2007). If possible, three probes were designed for each ORF, and each probe was randomly localized on the array with 3 replicates. The microarray was synthesized by Roche NimbleGen (Madison, WI). Cell cultures grown in LB were collected at late-log phase when substantial PPIX accumulation occurred. Genomic DNA of the PV-4 strain was extracted using a Bacterial Genomic DNA Extraction kit (Sigma, St. Louis, MO). Cy5-labeled cDNA (2μg of total RNA per sample/labeling reaction) and Cy3-labeled gDNA (150ng of gDNA/labeling reaction, and 1/12 of the labeling product was used for each hybridization) were co-hybridized in each array. Cy3-labeled gDNA was used as a control for microarray hybridization and data analysis. Details about the labeling, hybridization, array scanning, and data processing were performed as previously described (Tu et al., 2014; Zhou et al., 2013).

3.3.4 Determination of transcription start sites

Terminal deoxynucleotidyl transferase (TdT, Takara) was used to catalyze the incorporation of single deoxynucleotides (dATPs) into the 3'-OH terminus of cDNA to make the dA-tailed cDNA according to the manufacturer's protocol. Touchdown and nested PCR were used to amplify the dA-tailed cDNA by using an oligodT primer and a

gene-specific primer (Mendoza-Vargas et al., 2009). The PCR product was cloned into the pMD18-T vector (Takara, Dalian, China) for sequencing.

3.3.5 Nitrate reduction and hydrogen peroxide tolerance test

Nitrate reduction was examined in PV-4 and mutants cultured in modified M1 medium with sodium nitrate as the electron acceptor. The cultures were incubated under anaerobic or microoxic conditions (without shaking). Nitrate and nitrite concentrations were measured with a standard colorimetric assay (China, 2002). Hydrogen peroxide sensitivity was tested by monitoring the $OD_{600\ nm}$ of relevant strains cultured in LB broth with a gradient of hydrogen peroxide concentrations (0, 0.1, 0.3, 0.5, 0.7 and 1mM) (Won et al., 2001).

3.3.6 SDS-PAGE and heme staining

Mid-log phase cell cultures (OD_{600} 0.6 ~ 0.8) grown in LB were collected and homogenized by applying high pressure (JN-02C low temperature ultra-high pressure continuous flow cell disrupter, Juneng Biol. & Technol. Co., Guangzhou, China) or Ultrasonic Cell Disruption System (SCIENTZ-IID, Ningbo Xingzhi Biotechnology Co., China). After centrifugation at 13000 rpm at 4°C, the supernatants containing the cellular protein fraction were resuspended in SDS loading buffer and separated by SDS-PAGE using 12% polyacrylamide gels. Heme stains were performed using 3, 3′, 5, 5′-tetramethyl benzidinedihydrochloride as the substrate as previously described (Thomas et al., 1976). Images of the stained gels were taken with the Gel DocTM XR+ system (Bio-Rad Laboratories, Inc. United Kingdom).

3.3.7 Bioinformatics analysis

Amino acid and nucleotide sequences were retrieved from the NCBI database. The ClustalW2 package (http://www.ebi.ac.uk/Tools/msa/clustalw2/) was used for amino acid and nucleotide sequence alignments and Weblogo (http://weblogo.berkeley.edu) was applied to nucleotide sequences for promoter motif identification.

3.4 Results

3.4.1 Disruption of hemH1 led to PPIX accumulation, reduced level of heme containing proteins and impairment in nitrate reduction in PV-4

As mentioned in Chapter 2, disruption in *hemH1* of PV-4 led to significant accumulation of PPIX. In this study, we first tested whether such PPIX accumulation would negatively affect the growth of PV-4. The growth test was conducted under aerobic conditions and result is shown in Fig. 3.1. Based on the growth curve, there is no impairment in terms of growth for the single knock out of *hemH1* or *hemH2* compared to the PV-4 parental strain, suggesting that neither of the two *hemH* paralogues is essential in PV-4 under aerobic respiration. However, a double mutant knocking out both genes were not able to be obtained, indicating that heme is necessary for growth of PV-4 under the conditions tested. When both genes were disrupted, there is no ferrochelatase to convert PPIX to heme, an essential component in cytochrome based respiration. In addition, supplementation of hemin in the medium did not lead to successful generation of the double knockout mutant *ΔhemH1ΔhemH2*, indicating that PV-4 does not have the machinery for active uptake of hemin.

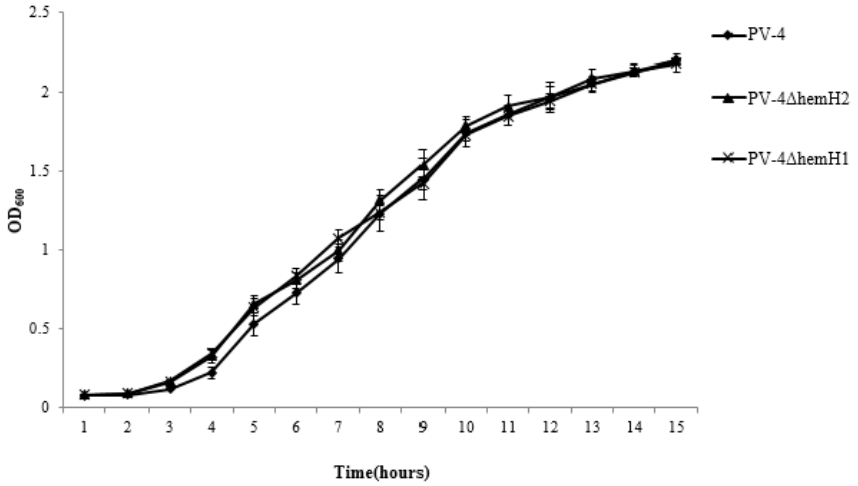

Fig. 3. 1 Growth curve of PV-4, ΔhemH1 and ΔhemH2 in LB medium aerobically

Conventional aerobic respiration with oxygen as electron acceptor only requires the use of several classical cytochromes, which may explain why there is no growth deficiency in *ΔhemH1* under aerobic conditions. Although disruption of *hemH1* did not lead to growth impairment, the amount of heme containing proteins was indeed much less in *ΔhemH1* than wild type, as shown in Fig 3.2a. Therefore, less heme-containing proteins was synthesized in *ΔhemH1* strain, which was not observed in *ΔhemH2*. Consistently, in nitrate reduction test under anaerobic condition, similar trends were observed (Fig 3.2b). The rate of nitrate reduction in the wild type strain was significantly higher than *ΔhemH1* strain and the complementation strain PV-*4ΔhemH1*/pHERD30T-*hemH1*. Complementation of *hemH1* with plasmid bourn native *hemH1* only showed certain extent of restoration, but not to the full level of the nitrate reduction, which might be due to the level of *in-trans* gene expression.

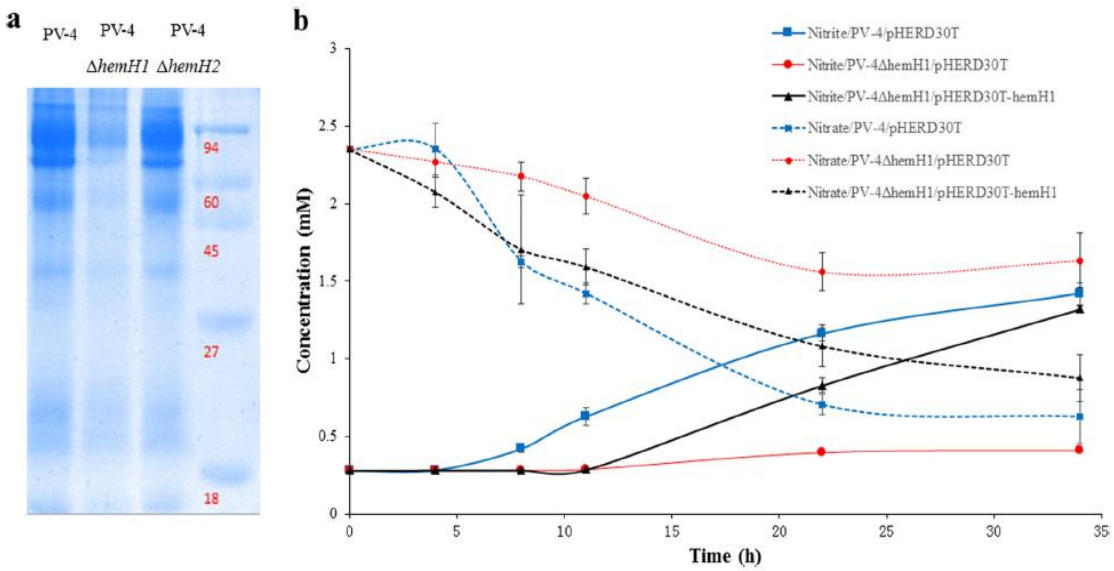

Fig. 3. 2 Heme stain of PV-4 wild type, *ΔhemH1* and *ΔhemH2* strain (a) and nitrate reduction rate of PV-4, *ΔhemH1* and complementation strain PV-*4ΔhemH1*/pHERD30T-*hemH1*

Taken together, deletion of *hemH1* in PV-4 resulted in dramatic extracellular accumulation of PPIX, decreased intracellular cytochrome *c* level, and impaired nitrate reduction. Deletion of *hemH2*, on the contrary, did not lead to any of these significant changes under the same conditions tested. However, it appeared that *hemH2* also encodes a functional ferrochelatase, because 1) Δ*hemH1* showed normal growth and still produced cytochromes despite at a lower level, indicating some PPIX was still converted to heme; 2) plasmid-borne *hemH2* fully restored heme synthesis despite loss of *hemH1* and 3) we were unable to generate a Δ*hemH1*Δ*hemH2* double mutant even with supplemented hemin, indicating that heme synthesis is essential for growth of this bacterium. The transcription of the two paralogues was compared in the wild-type and mutant strains to further elucidate their cellular functions.

3.4.2 Different expression pattern for hemH1 and hemH2

Temporal expression patterns of *hemH1* and *hemH2* were monitored with RT-PCR and qRT-PCR. In the parental strain, *hemH1* showed constitutive expression, while the expression of *hemH2* was undetectable (Fig. 3.3a) in RT-PCR, and at basal level from qRT-PCR data. However, in the Δ*hemH1* strain, the expression of *hemH2* was detected in both exponential (OD_{600} 0.6) and early stationary (OD_{600} 1.3) phases. The qRT-PCR analysis validated the results of the RT-PCR, showing a mild increase (~2 fold) of *hemH2* expression in Δ*hemH1* strain compared to the basal level expression in PV-4 parental strain (Fig. 3.3b). These results indicated that *hemH1* was the dominant gene under standard growth conditions and *hemH2* may play a supplementary role when *hemH1* was disrupted, so that ferrochelatase can still be produced to ensure conversion of PPIX into heme.

3.4.3 hemH1 and hemH2 are regulated differently

To determine how the expression of *hemH1* and *hemH2* is regulated, the upstream regions of each gene were examined to identify potential transcriptional regulator binding motifs. A transcriptional start site was identified using a primer extension assay. For *hemH1*, the +1 site was determined to be nucleotide A downstream of the -10 (TAGCCT) and −35 (GGCTTT) promoter motifs (Fig 3.4a). Sequence analysis identified a RpoD binding motif (-10/-15 sites) and a putative OxyR (shew_1035) binding motif (TTCTCATATTTGAAAAAGC) upstream of -10/-15 sites in the promoter region of *hemH1* (Fig 3.4b). Therefore, expression of *hemH1* might be dependent on the housekeeping sigma factor RpoD and possibly regulated by the

oxidative stress response regulator OxyR (Fig 3.4b). A previous study in *S. oneidensis* MR-1 identified the gene *pgpD*, encoding gluotathione peroxidase, belonging to a regulon of sigma factor RpoE2, an extracytoplamsic function (ECF) sigma factor involved in oxidative stress response(Dai et al., 2015). Coincidentally, *hemH2* in MR-1 is in the same operon as *pgpD*, and a similar RpoE2-dependent promoter motif was identified upstream of *hemH2* in PV-4 (Fig.3.5). A primer extension assay also showed that *hemH2* was transcribed from the nucleotide A (+1) downstream of the −35 (TGATCT) and −10 (CGTACT) promoter motifs, recognized by RpoE2.

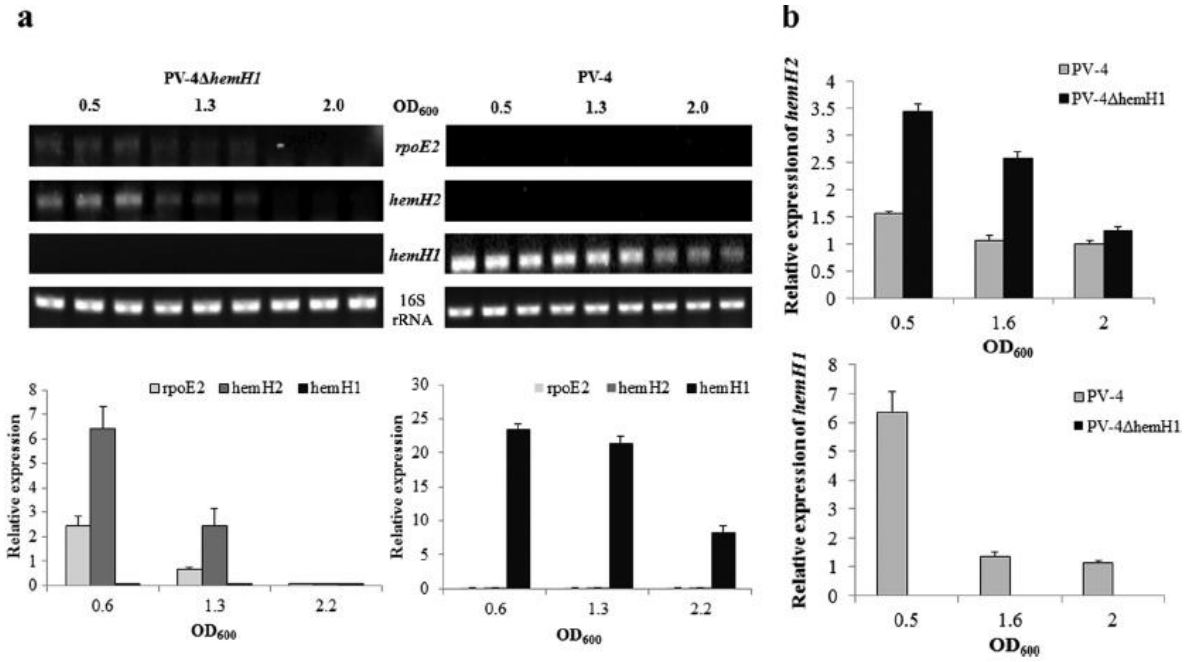

Fig. 3.3 Transcriptional analyses of *rpoE2* and *hemH* paralogues in the wild-type strain and the *hemH1*-null mutants of PV-4. (a) Semiquantitative RT-PCR analyses of *rpoE2* and *hemH2* expression in PV-4 and PV-4 Δ*hemH1* strains. (b) qRT-PCR analyses of *hemH2* transcripts in PV-4 and PV-4 Δ*hemH1* strains. Transcription of the 16S rRNA genes was analyzed and used as the loading control. The assays were performed in triplicate. The error bars represent the standard deviations (SD) of the results from triplicate independent samples.

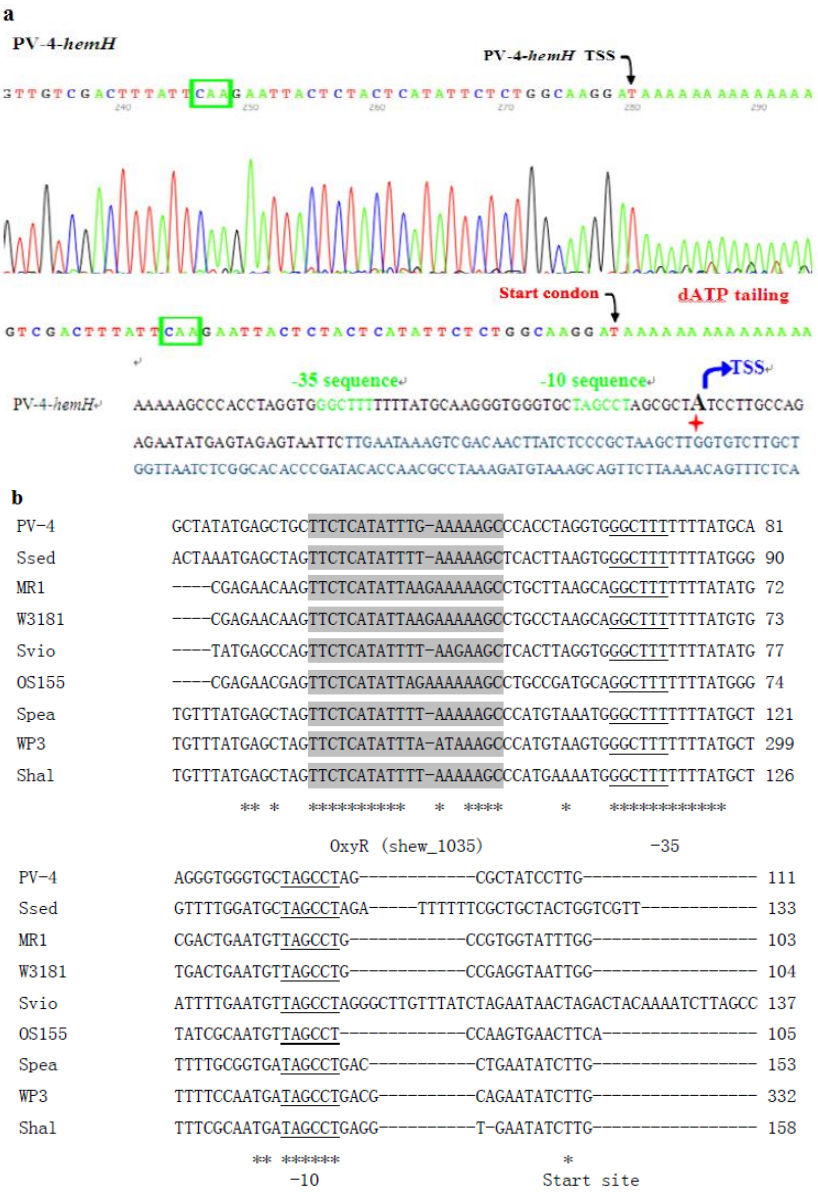

Fig. 3.4 Analysis of the promoter of the *hemH1* in *Shewanella* strains. (a)Primer extension analysis of transcriptional start site (TSS) of *hemH1* (Shew_2229) in *S. loihica* PV-4 via 5' RACE. (b) Multiple alignment analysis on the nucleotide sequences upstream of the *hemH1* gene of *Shewanella* strains using ClustalW2 to identify the promoter motifs and the putative OxyR (encoded by Shew_1035)-recognized motif. The shadowed motifs are supposedly predicted OxyR-recognized elements, and the underlined motifs are RpoD-recognized elements.

To verify the regulation of *hemH1* expression by OxyR, the expression of *oxyR* is induced *in-trans* in the parental strain. The result showed that *hemH1* transcription was significantly induced due to the higher level of *oxyR* expression (Fig. 3.6a). To validate the regulation of *hemH2* by RpoE2, the expression of *hemH2* was monitored in PV-4 harboring a vector pHERD30T with a native *rpoE2* gene driven by an arabinose inducible promoter. Under control conditions, both *rpoE2* and *hemH2* exhibited a basal level expression. After a 2-hour induction with arabinose, the expression of *rpoE2* increased 9-fold and the expression of *hemH2* increased about 8-fold. Induction of *rpoE2* in Δ*hemH1* completely reversed the red color phenotype of the Δ*hemH1* mutant (Fig. 3.7). These results suggested that expression of *hemH2* was regulated by RpoE2.

Fig. 3.5 Promoter prediction of *hemH2* and *rpoE2*. Transcription start site (TSS) and promoter prediction for PV-4 *hemH2* via 5'-RACE (a). Similar promoter sequence is also identified upstream of operon *rpoE2-ChrR* (b). The *rpoE2* exhibits the typical arrangement of Extracytoplasmic Functioning (ECF) sigma factor in the manner of self-regulation. The *rpoE2-chrR* operon and promoter region in PV-r is very similar to that of *Shewanella oneidensis* MR-1.

3.4.4 Functions of the hemH paralogues under oxidative stress

Protoporphyrin IX is a long-known photosensitizer and produces reactive oxygen species (ROS) upon light exposure, leading to cell damage or even death (Bouhenni et al., 2005). To uncover the roles of *hemH* paralogues under oxidative stress, gene expression and phenotypes in PV-4 parental strain or the *hemH1* mutant

were examined under visible light or with added hydrogen peroxide in the medium. The introduction of hydrogen peroxide to the medium partially suppressed the red-colored phenotype of the Δ*hemH1* mutant. Interestingly, light exposure completely reversed the red-colored phenotype (Fig. 3.8). The qRT-PCR results demonstrated an increased expression of *rpoE2* and *hemH2* in the Δ*hemH1* mutant but not in the parental strain under light exposure (Fig. 3.9). Also, increased expression of *rpoE2* and *hemH2* was observed in both PV-4 and the Δ*hemH1* mutant after the addition of hydrogen peroxide (Fig. 3.9). Additionally, the Δ*hemH1* mutant appeared to be more sensitive to hydrogen peroxide than the Δ*hemH2* mutant or PV-4 (Fig. 3.10), indicating more important role of *hemH1* for oxidative stress response.

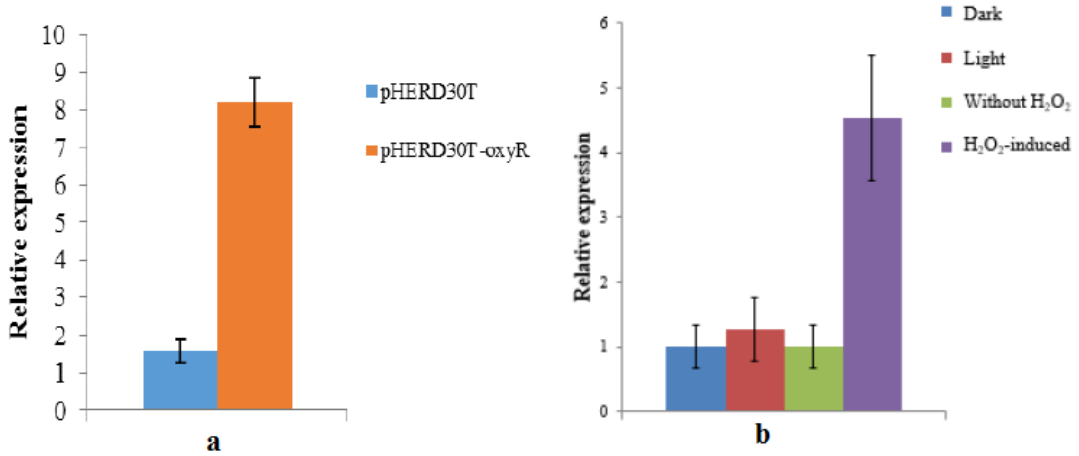

Fig. 3.6 Expression of *hemH1* in PV-4 harboring empty vector pHERD30T or pHERD30T containing the native *oxyR*, whose expression is induced by arabinose, showing that expression of *hemH1* is positively regulated by expression level of OxyR. (b) Expression of *hemH1* in PV-4 parental strain under various conditions.

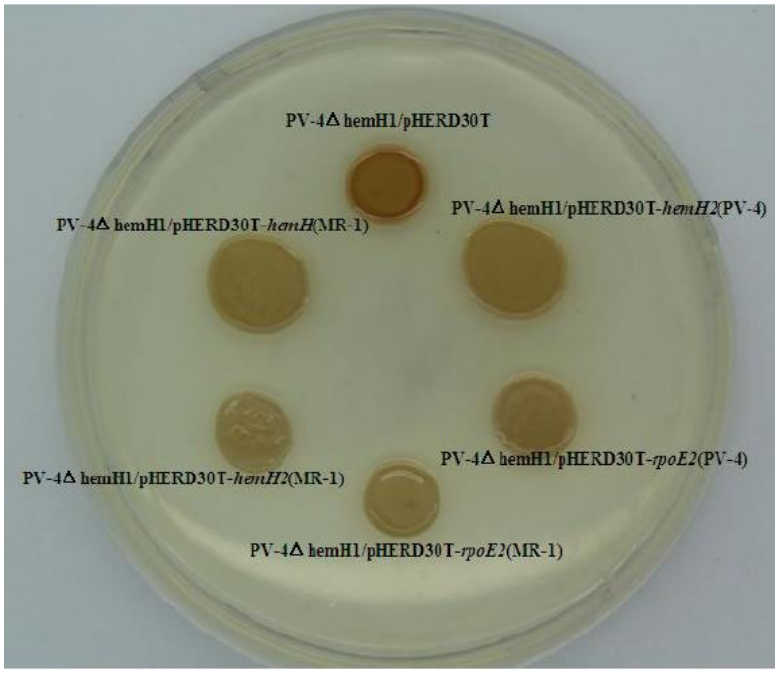

Fig. 3. 7 Induced expression of *hemH1*, *hemH2*, or *rpoE2* from MR-1 or PV-4 can fully suppress the PPIX overproduction in PV-4 *ΔhemH1*.

Under the oxidative stress conditions, *hemH1* exhibited significant upregulation, which was likely dependent on the transcription factor OxyR as overexpression of *oxyR in-trans* led to the enhanced expression of *hemH1* in PV-4 parental strain (Fig. 3.5a). These results suggested that *hemH1* plays an important role in response to oxidative stress. Upregulation of *hemH2* expression was also observed under oxidative stress due to either the addition of hydrogen peroxide or the ROS produced from PPIX under light exposure. But its expression was regulated by RpoE2. With their unique regulations, *hemH1* and *hemH2* can work in concert to sustain heme homeostasis under oxidative stresses.

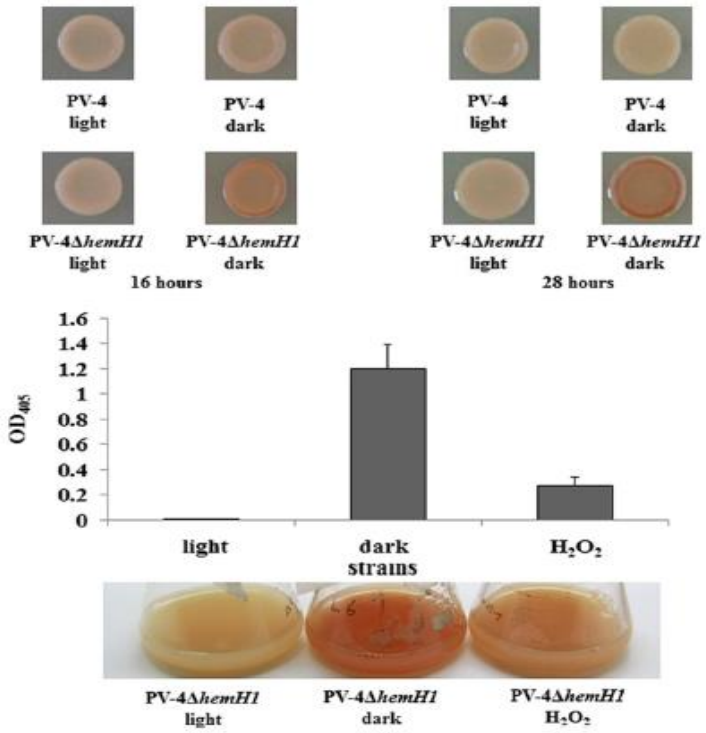

Fig. 3. 8 PPIX accumulating or non-accumulating strains in response to light or hydrogen peroxide stress conditions

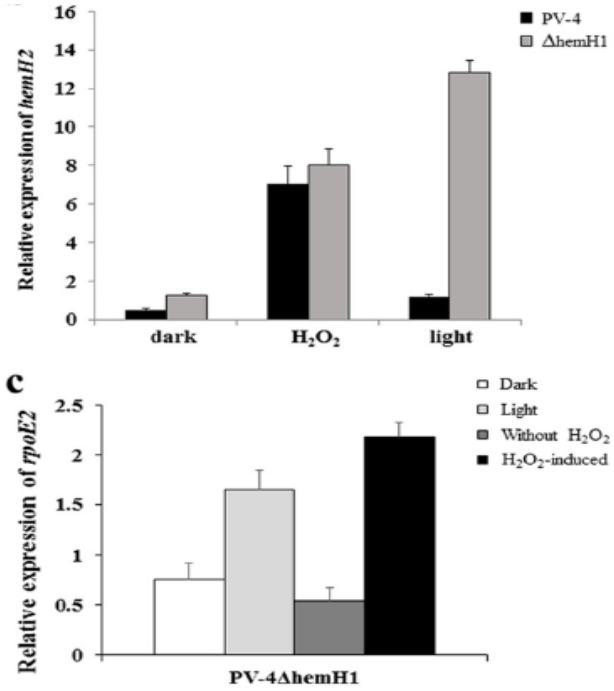

Fig. 3. 9 Expression of *hemH2* and *rpoE2* in PV-4 or *ΔhemH1* under dark, light, or oxidative stress condition with hydrogen peroxide via qRT-PCR.

*3.4.5 Increased expression of iron uptake genes and decreased expression of PPIX synthesis genes in the Δ*hemH1* mutant.*

Genome-wide gene expression changes in the Δ*hemH1* mutant at the late-log phase were examined with microarray analysis. Compared with PV-4 (Table 3.4), genes involved in iron uptake exhibited significantly increased expression (log_2R >3) in Δ*hemH1*. These included two siderophore receptor genes (Shew_3097 and Shew_3841), one ferric iron binding protein (Shew_0861), two ferrous iron transporter genes Shew_2517 (*feoA*) and Shew_2518 (*feoB*), and a bacterioferritin-associated ferrodoxin gene Shew_0552. Considering the substantial accumulation of PPIX at the late-log phase and the need for ferrous iron in the biosynthesis of heme from PPIX, it was reasonable that iron uptake was enhanced in order to counteract PPIX accumulation in the Δ*hemH1* mutant.

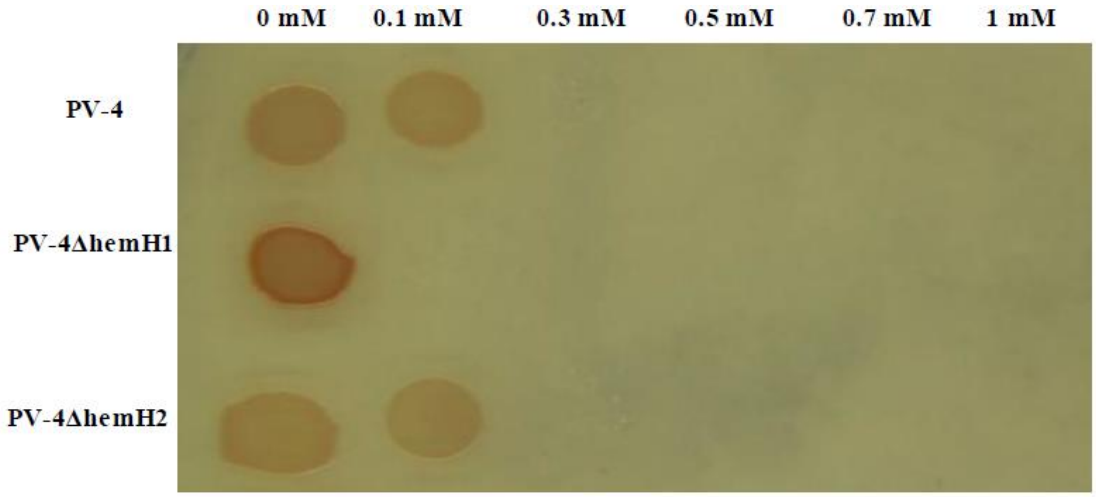

a

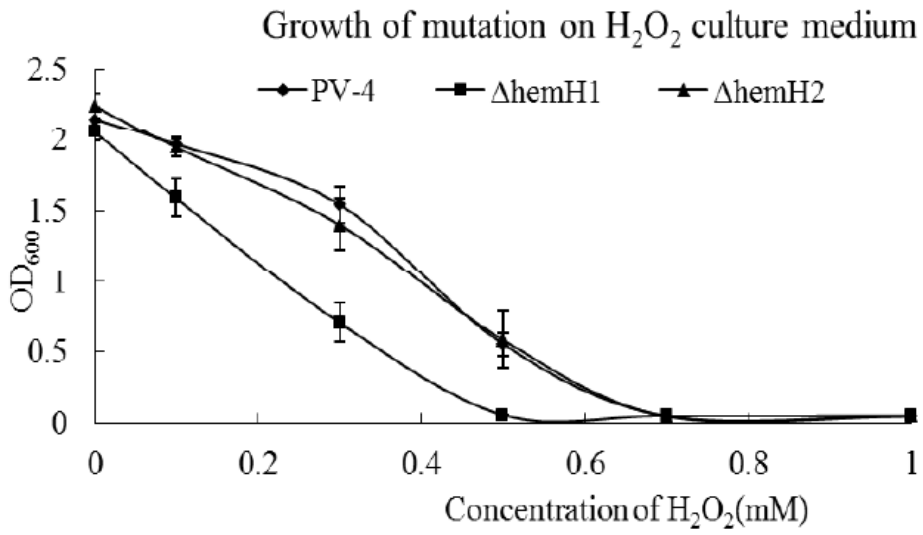

b

Fig. 3. 10 Growth of PV-4 parental strain, *ΔhemH1*, or *ΔhemH2* under oxidative stress imposed by hydrogen peroxide concentration gradient. (a), Cell patched onto LB agar plates; (b) OD600 after cultured in LB containing hydrogen peroxide with a concentration gradient of 0, 0.1, 0.3, 0.5, 0.7, and 1mM for 18 hours.

In contrast to increased expression of iron uptake genes, the expression of genes involved in the heme biosynthesis pathway prior to the PPIX production step significantly decreased. These included glutamyl-tRNA reductase gene (Shew_2913) and delta-aminolevulinic acid dehydratase (Shew_3382) genes involved in the synthesis of early precursors of heme (5-aminolevulinate and porphobilinogen, respectively), *hemF* (Shew_0073) and *hemG* (Shew_0025) involved in the synthesis of protoporphyrinogen and PPIX, respectively. In addition, the expression of several cytochrome *c* genes, including two decaheme cytochrome *c* genes, *omcA* and *mtrC* (Shew_0918 and Shew_2525), were significantly decreased. These results suggest that a potential negative feedback effect of accumulation of PPIX on heme biosynthesis. Significant repression of flagella synthesis genes was also detected, possibly as a cellular response to stresses imposed by PPIX accumulation.

Table 3. 4 Genes with significant change in expression revealed by microarray analysis

Function	Gene	Log2R	Z-score	Annotation
Iron uptake	Shew_3097	7.29	9.42	TonB-dependent siderophore receptor
	Shew_0861	7.04	7.67	extracellular solute-binding protein
	Shew_3841	7.69	5.15	TonB-dependent siderophore receptor
	Shew_3166	6.02	7.3	extracellular solute-binding protein
	Shew_1181	5.87	7.26	putative iron regulated membrane protein
	Shew_2517	4.45	5.46	ferrous iron transport protein B
	Shew_2518	4.19	4.18	ferrous iron transport protein A
	Shew_0552	4.47	3.11	Bacterioferritin associated ferrodoxin
Cytochrome c	Shew_3112	-3.77	-5.09	flavocytochrome c
	Shew_0572	-3.51	-2.53	cytochrome c1
	Shew_2526	-3.19	-4.51	cytochrome c family protein
	Shew_2525	-2.98	-3.85	decaheme cytochrome c
	Shew_0918	-6.75	-5.25	decaheme cytochrome c
PPIX and heme biosynthesis	Shew_0678	-4.21	-7.71	protoporphyrinogen oxidase (hemG)
	Shew_0073	-4.38	-4.16	coproporphyrinogen III oxidase (hemN)
	Shew_2913	-3.54	-4.5	Glutamyl-tRNA reductase (hemA)
	Shew_3382	-3.4	-3.17	ALA dehydratase (hemB)
Flagella synthesis	Shew_1345	-7.20	-6.69	flagellar basal body rod protein FlgB
	Shew_1346	-6.76	-7.3	flagellar basal body rod protein FlgC
	Shew_1347	-6.73	-7.75	flagellar basal body rod modification protein
	Shew_1348	-6.12	-6.47	flagellar hook protein FlgE
	Shew_1350	-5.20	-7.19	flagellar basal body rod protein FlgG
	Shew_1352	-5.08	-7.69	flagellar basal body P-ring protein
	Shew_1354	-6.26	-8.17	flagellar hook-associated protein FlgK
	Shew_1355	-4.22	-5.58	flagellar hook-associated protein FlgL
	Shew_1356	-5.79	-3.96	flagellin domain-containing protein

3.4.6 Genetic redundancy of the heme synthesis pathway in Shewanella

It is found that the existence of two ferrochelatase encoding genes is a rarely observed feature in other bacteria but is commonly seen in *Shewanella*. In fact, 19 out of the 24 sequenced *Shewanella* strains showed two *hemH* paralogues in their genomes (Table 3.5). To evaluate the evolutionary relatedness of these *hemH* paralogues, a distance tree based on the DNA sequence of the *hemH* genes were constructed (Fig. 3.11). The *hemH* genes were clearly divided into two clusters, with one branch harboring the *hemH1* homologues and the other branch harboring the *hemH2*

homologues. The *hemH1* gene was also clustered with the reference *hemH* gene from *E. coli*, which is in consistence with the dominant role and regulatory control as aforementioned.

It is intriguing that, the gene redundancy is not restricted in *hemH* gene only. Many other genes in the heme synthetic pathway also possess paralogues genes in the genus of *Shewanella*. Based on KEGG pathway annotation and BLAST analysis, out of the 10 genes directly responsible for biosynthesis of heme, 5 genes (*hemL, hemB, hemN, hemG,* and *hemH*) possess paralogues in multiple *Shewanella* species. Two other genes that are involved in synthesis of heme O (*cyoE*) and siroheme synthesis (*cysG*) also have paralogues. A detailed summary of the paralogues genes in each species were listed in table 3.6.

3.5 Discussion

The great respiratory flexibility found in *Shewanella* species is achieved through expression of multiple *c*-type cytochromes (around 40), which requires sufficient heme supply (Konstantinidis et al., 2009). Therefore, heme homeostasis is critical in *Shewanella* species which predominantly conduct a respiratory lifestyle (Pinchuk et al., 2011). There are two ferrochelatase genes in 19 out of 24 sequenced *Shewanella* genomes (Table 3.5). Heme synthesis could be regulated by the differential expression of the paralogues, which in turn, has profound impact on critical cellular processes like respiration and tolerance to stresses. In this study we demonstrated that two *hemH* paralogues, *hemH1* and *hemH2,* both encode a functional ferrochelatase, but are under different transcriptional regulation for sustaining heme homeostasis in *S. loihica* PV-4.

Although it has long been known that PPIX could accumulate due to inactivation of ferrochelatase in *Escherichia coli* (Baysse et al., 2001; Miyamoto et al., 1991), the level of PPIX accumulation in PV-4Δ*hemH1* mutant was at least two orders of magnitude higher, conferring a red color to bacterial colonies and broth, than those of previous studies (Miyamoto et al., 1992; Nakahigashi et al., 1991; Yang et al., 1996). The high yields of PPIX in PV-4 mutants could potentially be exploited for commercial production. The photosensitivity of PPIX is utilized in the photodynamic therapy (PDT) against different forms of cancers. Protoporphyrin IX disodium salt is also used as a health care supplement and hepatic protectant (*e.g.* the Prolmon table (Tokyo Tanabe Co. Ltd. Tokyo, Japan)) for patients with infective hepatitis and chronic liver diseases. Nowadays the commercial production of PPIX and related products are mainly based on the extraction from livestock bloods. Bacterial fermentation-based bioprocess may reduce the cost and is expected to be more environmentally friendly because the extraction and purification of the secreted PPIX will be simple, using less chemical reagents, and/or may be achieved by simple physical processes.

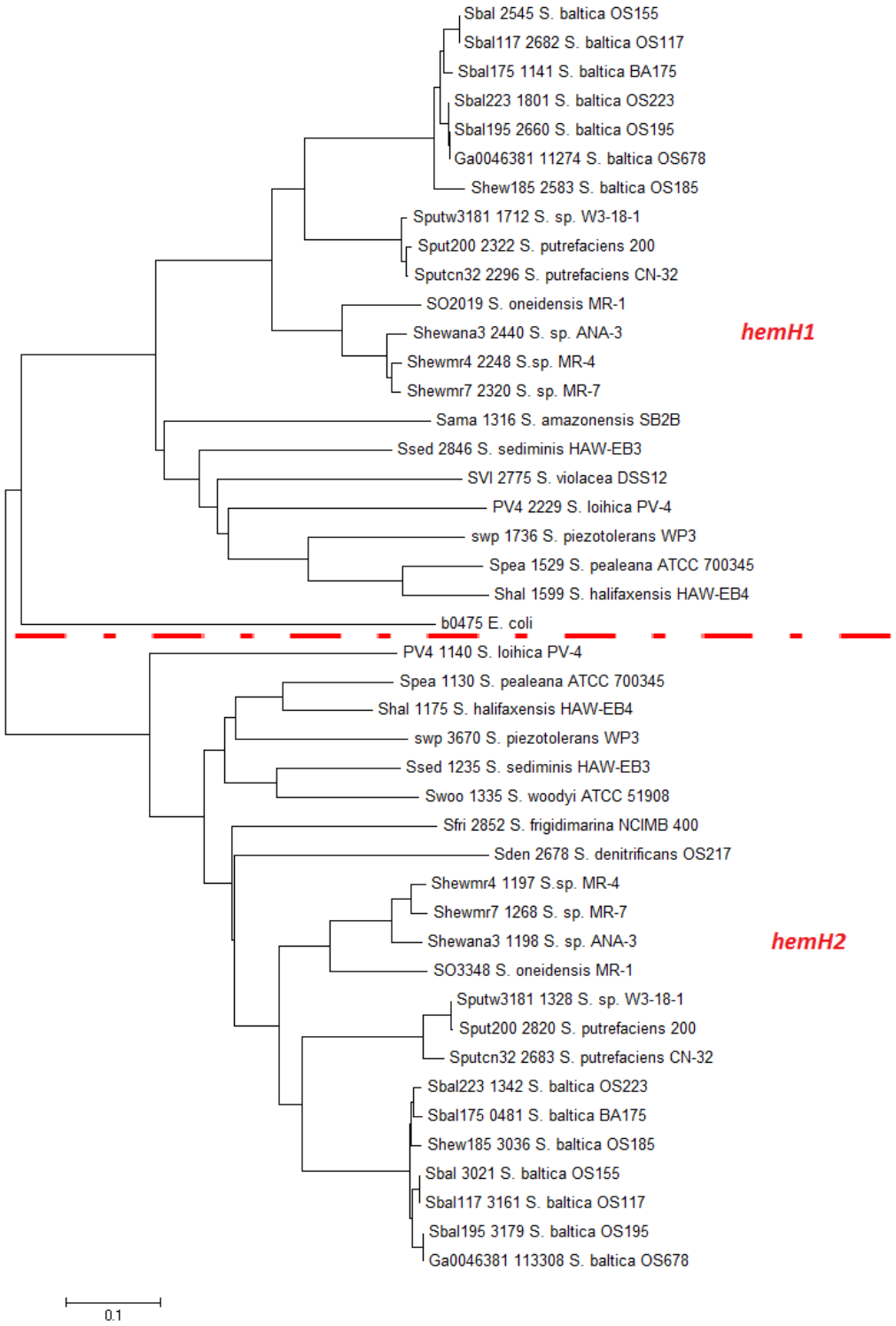

Fig. 3. 11 Distance tree of *hemH* genes in *Shewanella* based on DNA sequence, with *hemH* in E. coli as a reference. The *hemH* gene sequences were clustered into two groups as indicated by the red dashed line. All *hemH1* homologues and *hemH2* homologues were clustered in their own group.

Table 3. 5 *hemH, chrR, rpoE2* homologues in sequenced *Shewanella* strains

Strains	Genes				
	chrR	***rpoE2***	***pgpD***	***hemH2***	***hemH1***
S. oneidensis	SO_1985	SO_1986	SO_3348	SO_3349	SO_2019
S. denitrificans	Sden_3373	Sden_3374	Sden_2679	Sden_2678	
S. frigidimarina	Sfri_2319	Sfri_2318	Sfri_2853	Sfri_2852	
S. amazonensis	Sama_2037	Sama_2036	Sama_2474		Sama_1316
S. baltica OS155	Sbal_2598	Sbal_2597	Sbal_3022	Sbal_3021	Sbal_2545
S. baltica OS185	Shew185_2637	Shew185_2636	Shew185_3037	Shew185_3036	Shew185_2583
S. baltica OS195	Sbal195_2712	Sbal195_2711	Sbal195_3180	Sbal195_3179	Sbal195_2660
S. baltica OS223	Sbal223_1748	Sbal223_1749	Sbal223_1341	Sbal223_1342	Sbal223_1801
S. baltica OS678	Sbal678_2717	Sbal678_2716	Sbal678_3186	Sbal678_3185	Sbal678_2663
S. baltica OS117	Sbal117_2734	Sbal175_1733	Sbal175_1323	Sbal175_1324	Sbal117_2682
S. baltica BA175	Sbal175_1732	Sbal175_1733	Sbal175_1323	Sbal175_1324	Sbal175_1783
S. loihica	Shew_1477	Shew_1476		Shew_1140	Shew_2229
S. putrefaciens CN-32	Sputcn32_2323	Sputcn32_2322	Sputcn32_2684	Sputcn32_2683	Sputcn32_2296
S. putrefaciens 200	Sput200_2349	Sput200_2348	Sput200_2821	Sput200_2820	Sput200_2322
S. sediminis				Ssed_1235	Ssed_2846
S. pealeana				Spea_1130	Spea_1529
S. sp. MR-4	Shewmr4_2276	Shewmr4_2275	Shewmr4_1196	Shewmr4_1197	Shewmr4_2248
S. sp. MR-7	Shewmr7_2348	Shewmr7_2347	Shewmr7_1267	Shewmr7_1268	Shewmr7_2320
S. sp. ANA-3	Shewana3_2466	Shewana3_2465	Shewana3_1197	Shewana3_1198	Shewana3_2440
S. sp. W3-18-1	Sputw3181_1685	Sputw3181_1686	Sputw3181_1327	Sputw3181_1328	Sputw3181_1712
S. halifaxensis				Shal_1175	Shal_1599
S. woodyi	Swoo_2779	Swoo_2780		Swoo_1335	
S. piezotolerans				swp_3670	swp_1736
S. violacea					SVI_2775

Interestingly, the PPIX-accumulating phenotype was only observed in Δ*hemH1*, but not in Δ*hemH2*, indicating expression of *hemH1* alone could be sufficient to meet the demand for heme under tested conditions. However, multiple lines of evidence

showed that *hemH2* was also functional, as the *hemH2* expression *in trans* could complement the loss of *hemH1*. The fact that a deletion mutant of both *hemH1* and *hemH2* could not be achieved in PV-4 suggested that heme might be essential for growth of PV-4. Alignment of the amino acid sequences of the ferrochelatase paralogues in PV-4 with other organisms (Fig. 3.12) revealed conserved motifs and amino acid residues, such as the invariant residues His235 and Glu314 of the *Saccharomyces cerevisiae* ferrochelatase (Karlberg et al., 2002) and the conserved residues His183 and Glu264 from *Bacillus subtilis* (Hansson et al., 2007). However, another well conserved Ser residue of HemH2 (Shew_1140) was substituted by Ala167 in PV-4. In addition, an essential [2Fe–2S] cluster coordinated by cysteine residues in the C-terminus of the mammalian ferrochelatases was not present in the bacterial homologues (Dailey et al., 1994). These results indicate that HemH1 and HemH2 are functional ferrochelatases and have conserved motifs and amino acid residues, providing a forward study direction in the crystal structures of HemH1 and HemH2, especially the protein structure-activity analysis.

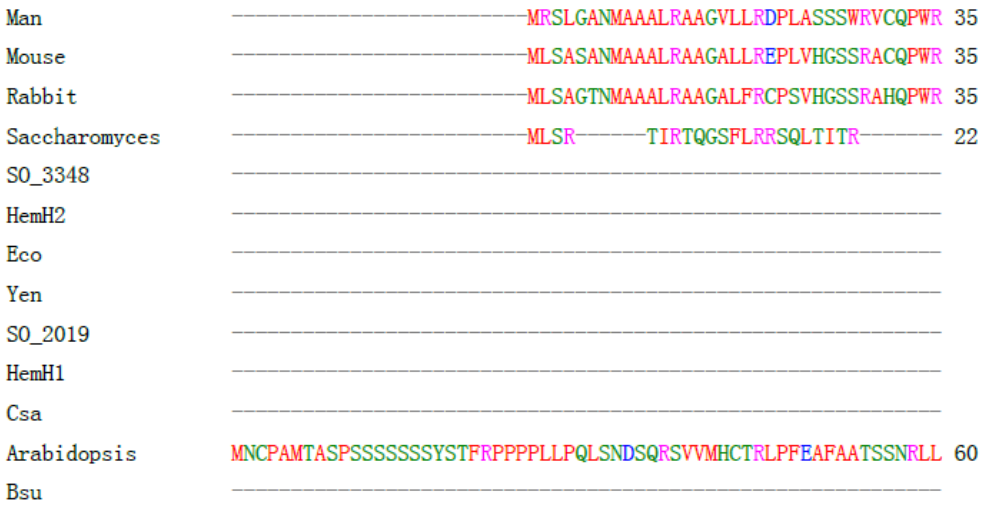

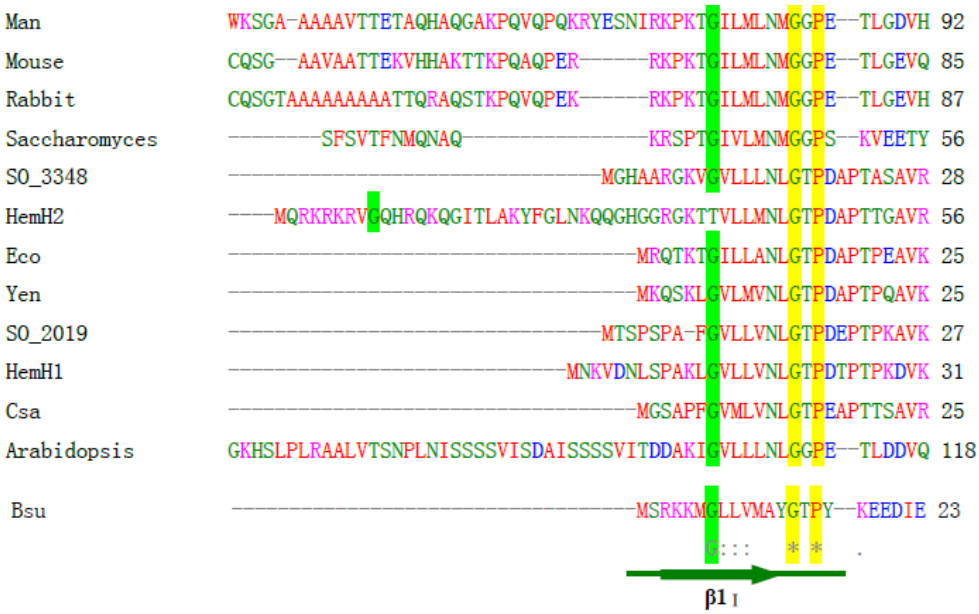
Man WKSGA-AAAAVTTETAQHAQGAKPQVQPQKRYESNIRKPKTGILMLNMGGPE--TLGDVH 92
Mouse CQSG--AAVAATTEKVHHAKTTKPQAQPER-------RKPKTGILMLNMGGPE--TLGEVQ 85
Rabbit CQSGTAAAAAAAAATTQRAQSTKPQVQPEK-------RKPKTGILMLNMGGPE--TLGEVH 87
Saccharomyces ---------SFSVTFNMQNAQ----------------KRSPTGIVLMNMGGPS--KVEETY 56
SO_3348 ----------------------------------MGHAARGKVGVLLLNLGTPDAPTASAVR 28
HemH2 -----MQRKRKRVGQHRQKQGITLAKYFGLNKQQGHGGRGKTTVLLMNLGTPDAPTTGAVR 56
Eco ----------------------------------MRQTKTGILLANLGTPDAPTPEAVK 25
Yen ----------------------------------MKQSKLGVLMVNLGTPDAPTPQAVK 25
SO_2019 ----------------------------------MTSPSPA-FGVLLVNLGTPDEPTPKAVK 27
HemH1 ----------------------------------MNKVDNLSPAKLGVLLVNLGTPDTPTPKDVK 31
Csa ----------------------------------MGSAPFGVMLVNLGTPEAPTTSAVR 25
Arabidopsis GKHSLPLRAALVTSNPLNISSSSVISDAISSSSVITDDAKIGVLLLNLGGPE--TLDDVQ 118
Bsu ----------------------------------MSRKKMGLLVMAYGTPY--KEEDIE 23
β1
Man DFLLRLFLDRDLMTLP------IQNKLAPFIAKRRTPKIQEQYRRIG--GGSPIKIWTSKQ 145
Mouse DFLQRLFLDRDLMTLP------IQNKLAPFIAKRRTPKIQEQYRRIG--GGSPIKMWTSKQ 138
Rabbit DFLLRLFLDRDLMTLP------VQSKLGPFIAKRRTSKIQEQYRRIG--GGSPIKMWTSKQ 140
Saccharomyces DFLYQLFADNDLIPISA----KYQKTIAKYIAKFRTPKIEKQYREIG--GGSPIRKWSEYQ 111
SO_3348 RYLAEFLSDPRVVEIPKLLWML--ILYGIVLRVRPAKSAALYQKVWTEAGSPLMDISLRQ 86
HemH2 RYLAEFLSDPRVVEIPKLVWML--ILHGIILRIRPAKSAALYQSIWTEQGSPLMAITQAQ 114
Eco RYLKQFLSDRRVVDTSRLLWWP--LLRGVILPLRSPRVAKLYASVWMEGGSPLMVYSRQQ 83
Yen RYLAEFLSDRRVVDTSPWLWWP--LLRGVILPIRSPRVAKLYQSVWMDEGSPLLVYSRRQ 83
SO_2019 RFLKQFLSDPRVVDLSPWLWQP--ILQGIILNTRPKKVAKLYQSVWTEQGSPLMVISQCQ 85
HemH1 QFLKQFLSDPRVVDLNPWIWKP--ILNGIILNTRPKAVAKLYESIWWPEGSPLMVISERQ 89
Csa RYLAEFLGDPRVIDLPRVKWLP--ILHGIILRIRPPRVAKAYASVWQDEGSPLLAIGRRQ 83
Arabidopsis PFLFNLFADPDIIRLPPVFQFLQKPLAQFISVARAPKSKEGYASIG--GGSPLRHITDAQ 176
Bsu RYYTHIRRGR----------KPEPEMLQDLKDRYEAIG--GISPLAQITEQQ 63
α1
α2
α3

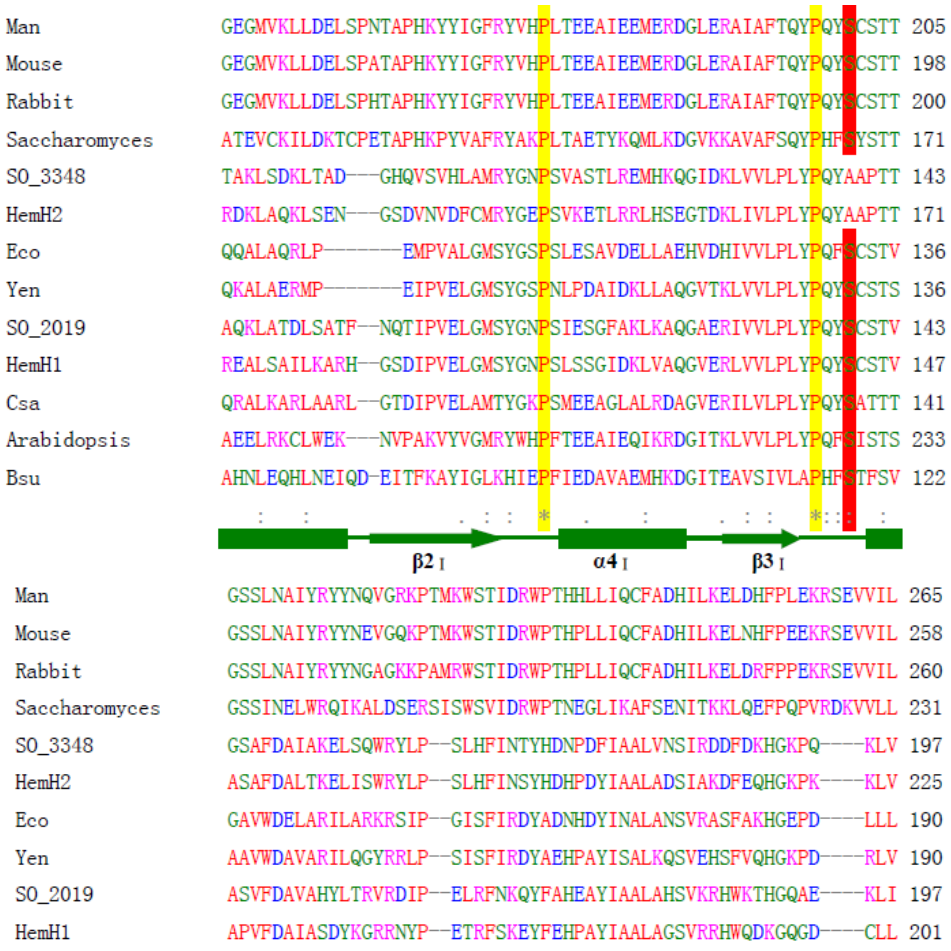
Man GEGMVKLLDELSPNTAPHKYYIGFRYVHPLTEEAIEEMERDGLERAIAFTQYPQYSCSTT 205
Mouse GEGMVKLLDELSPATAPHKYYIGFRYVHPLTEEAIEEMERDGLERAIAFTQYPQYSCSTT 198
Rabbit GEGMVKLLDELSPHTAPHKYYIGFRYVHPLTEEAIEEMERDGLERAIAFTQYPQYSCSTT 200
Saccharomyces ATEVCKILDKTCPETAPHKPYVAFRYAKPLTAETYKQMLKDGVKKAVAFSQYPHFSYSTT 171
SO_3348 TAKLSDKLTAD---GHQVSVHLAMRYGNPSVASTLREMHKQGIDKLVVLPLYPQYAAPTT 143
HemH2 RDKLAQKLSEN---GSDVNVDFCMRYGEPSVKETLRRLHSEGTDKLIVLPLYPQYAAPTT 171
Eco QQALAQRLP--------EMPVALGMSYGSPSLESAVDELLAEHVDHIVVLPLYPQFSCSTV 136
Yen QKALAERMP--------EIPVELGMSYGSPNLPDAIDKLLAQGVTKLVVLPLYPQYSCSTS 136
SO_2019 AQKLATDLSATF---NQTIPVELGMSYGNPSIESGFAKLKAQGAERIVVLPLYPQYSCSTV 143
HemH1 REALSAILKARH---GSDIPVELGMSYGNPSLSSGIDKLVAQGVERLVVLPLYPQYSCSTV 147
Csa QRALKARLAARL---GTDIPVELAMTYGKPSMEEAGLALRDAGVERILVLPLYPQYSATTT 141
Arabidopsis AEELRKCLWEK---NVPAKVYVGMRYWHPFTEEAIEQIKRDGITKLVVLPLYPQFSISTS 233
Bsu AHNLEQHLNEIQD-EITFKAYIGLKHIEPFIEDAVAEMHKDGITEAVSIVLAPHFSTFSV 122
β2 I
α4 I
β3 I
Man GSSLNAIYRYYNQVGRKPTMKWSTIDRWPTHHLLIQCFADHILKELDHFPLEKRSEVVIL 265
Mouse GSSLNAIYRYYNEVGQKPTMKWSTIDRWPTHPLLIQCFADHILKELNHFPEEKRSEVVIL 258
Rabbit GSSLNAIYRYYNGAGKKPAMRWSTIDRWPTHPLLIQCFADHILKELDRFPPEKRSEVVIL 260
Saccharomyces GSSINELWRQIKALDSERSISWSVIDRWPTNEGLIKAFSENITKKLQEFPQPVRDKVVLL 231
SO_3348 GSAFDAIAKELSQWRYLP---SLHFINTYHDNPDFIAALVNSIRDDFDKHGKPQ-----KLV 197
HemH2 ASAFDALTKELISWRYLP---SLHFINSYHDHPDYIAALADSIAKDFEQHGKPK-----KLV 225
Eco GAVWDELARILARKRSIP---GISFIRDYADNHDYINALANSVRASFAKHGEPD-----LLL 190
Yen AAVWDAVARILQGYRRLP---SISFIRDYAEHPAYISALKQSVEHSFVQHGKPD-----RLV 190
SO_2019 ASVFDAVAHYLTRVRDIP---ELRFNKQYFAHEAYIAALAHSVKRHWKTHGQAE-----KLI 197
HemH1 APVFDAIASDYKGRRNYP---ETRFSKEYFEHPAYIAALAGSVRRHWQDKGQGD-----CLL 201

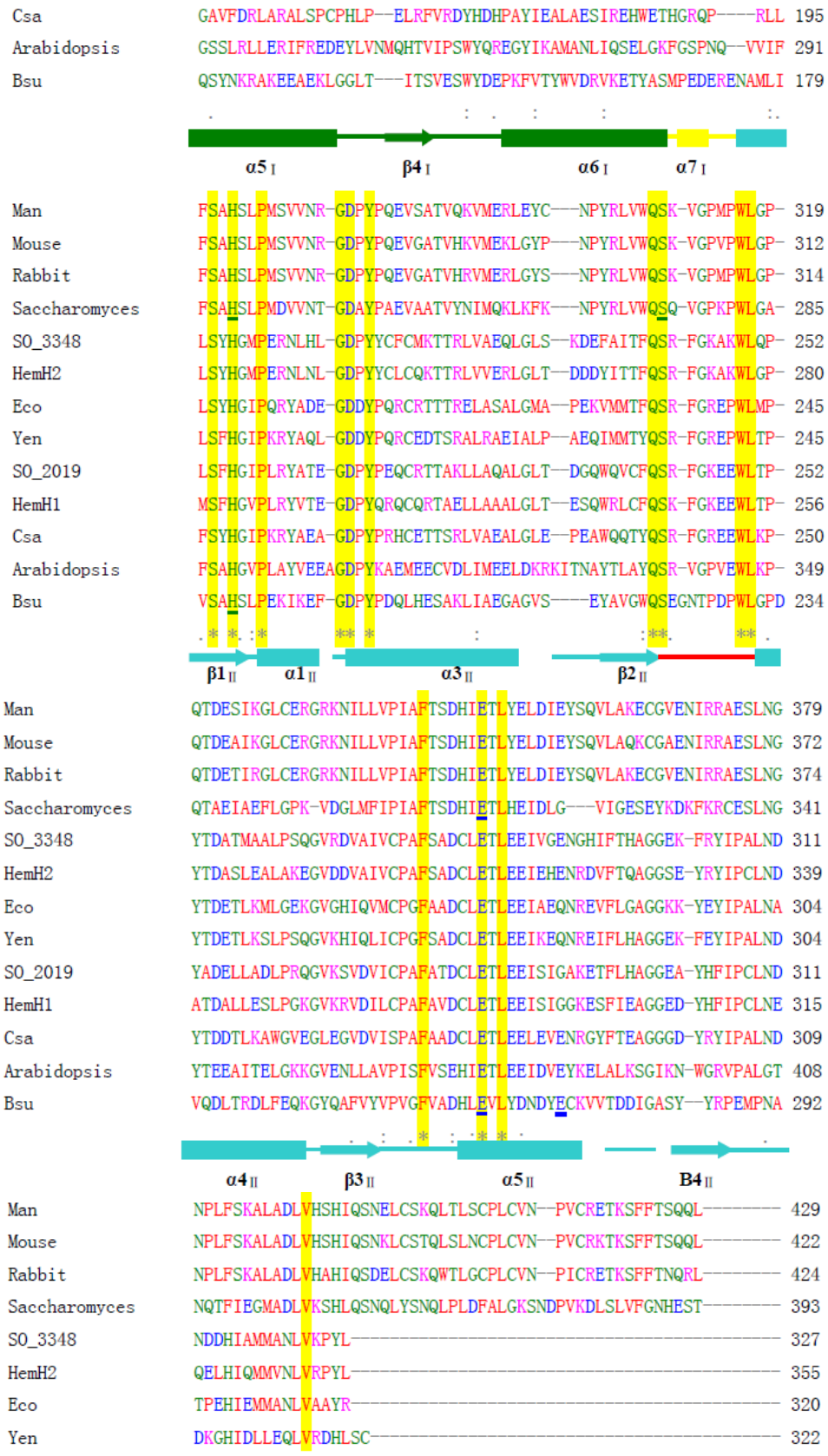
Csa GAVFDRLARALSPCPHLP---ELRFVRDYHDHPAYIEALAESIREHWETHGRQP-----RLL 195
Arabidopsis GSSLRLLERIFREDEYLVNMQHTVIPSWYQREGYIKAMANLIQSELGKFGSPNQ---VVIF 291
Bsu QSYNKRAKEEAEKLGGLT----ITSVESWYDEPKFVTYWVDRVKETYASMPEDERENAMLI 179
α5 I β4 I α6 I α7 I
Man FSAHSLPMSVVNR-GDPYPQEVSATVQKVMERLEYC---NPYRLVWQSK-VGPMPWLGP- 319
Mouse FSAHSLPMSVVNR-GDPYPQEVGATVHKVMEKLGYP---NPYRLVWQSK-VGPVPWLGP- 312
Rabbit FSAHSLPMSVVNR-GDPYPQEVGATVHRVMERLGYS---NPYRLVWQSK-VGPMPWLGP- 314
Saccharomyces FSAHSLPMDVVNT-GDAYPAEVAATVYNIMQKLKFK---NPYRLVWQSQ-VGPKPWLGA- 285
SO_3348 LSYHGMPERNLHL-GDPYYCFCMKTTRLVAEQLGLS---KDEFAITFQSR-FGKAKWLQP- 252
HemH2 LSYHGMPERNLNL-GDPYYCLCQKTTRLVVERLGLT---DDDYITTFQSR-FGKAKWLGP- 280
Eco LSYHGIPQRYADE-GDDYPQRCRTTTRELASALGMA---PEKVMMTFQSR-FGREPWLMP- 245
Yen LSFHGIPKRYAQL-GDDYPQRCEDTSRALRAEIALP---AEQIMMTYQSR-FGREPWLTP- 245
SO_2019 LSFHGIPLRYATE-GDPYPEQCRTTAKLLAQALGLT---DGQWQVCFQSR-FGKEEWLTP- 252
HemH1 MSFHGVPLRYVTE-GDPYQRQCQRTAELLAAALGLT---ESQWRLCFQSK-FGKEEWLTP- 256
Csa FSYHGIPKRYAEA-GDPYPRHCETTSRLVAEALGLE---PEAWQQTYQSR-FGREEWLKP- 250
Arabidopsis FSAHGVPLAYVEEAGDPYKAEMEECVDLIMEELDKRKITNAYTLAYQSR-VGPVEWLKP- 349
Bsu VSAHSLPEKIKEF-GDPYPDQLHESAKLIAEGAGVS-----EYAVGWQSEGNTPDPWLGPD 234
β1 II α1 II α3 II β2 II
Man QTDESIKGLCERGRKNILLVPIAFTSDHIETLYELDIEYSQVLAKECGVENIRRAESLNG 379
Mouse QTDEAIKGLCERGRKNILLVPIAFTSDHIETLYELDIEYSQVLAQKCGAENIRRAESLNG 372
Rabbit QTDETIRGLCERGRKNILLVPIAFTSDHIETLYELDIEYSQVLAKECGVENIRRAESLNG 374
Saccharomyces QTAEIAEFLGPK-VDGLMFIPIAFTSDHIETLHEIDLG---VIGESEYKDKFKRCESLNG 341
SO_3348 YTDATMAALPSQGVRDVAIVCPAFSADCLETLEEIVGENGHIFTHAGGEK-FRYIPALND 311
HemH2 YTDASLEALAKEGVDDVAIVCPAFSADCLETLEEIEHENRDVFTQAGGSE-YRYIPCLND 339
Eco YTDETLKMLGEKGVGHIQVMCPGFAADCLETLEEIAEQNREVFLGAGGKK-YEYIPALNA 304
Yen YTDETLKSLPSQGVKHIQLICPGFSADCLETLEEIKEQNREIFLHAGGEK-FEYIPALND 304
SO_2019 YADELLADLPRQGVKSVDVICPAFATDCLETLEEISIGAKETFLHAGGEA-YHFIPCLND 311
HemH1 ATDALLESLPGKGVKRVDILCPAFAVDCLETLEEISIGGKESFIEAGGED-YHFIPCLNE 315
Csa YTDDTLKAWGVEGLEGVDVISPAFAADCLETLEELEVENRGYFTEAGGGD-YRYIPALND 309
Arabidopsis YTEEAITELGKKGVENLLAVPISFVSEHIETLEEIDVEYKELALKSGIKN-WGRVPALGT 408
Bsu VQDLTRDLFEQKGYQAFVYVPVGFVADHLEVLYDNDYECKVVTDDIGASY---YRPEMPNA 292
α4 II β3 II α5 II B4 II
Man NPLFSKALADLVHSHIQSNELCSKQLTLSCPLCVN---PVCRETKSFFTSQQL--------- 429
Mouse NPLFSKALADLVHSHIQSNKLCSTQLSLNCPLCVN---PVCRKTKSFFTSQQL--------- 422
Rabbit NPLFSKALADLVHAHIQSDELCSKQWTLGCPLCVN---PICRETKSFFTNQRL--------- 424
Saccharomyces NQTFIEGMADLVKSHLQSNQLYSNQLPLDFALGKSNDPVKDLSLVFGNHEST--------- 393
SO_3348 NDDHIAMMANLVKPYL---------- 327
HemH2 QELHIQMMVNLVRPYL---------- 355
Eco TPEHIEMMANLVAAYR---------- 320
Yen DKGHIDLLEQLVRDHLSC---------- 322

Fig. 3. 12 Alignment of ferrochelatase amino acid sequences of various organism. Conserved regions of the sequence are highlighted in yellow, and minor differences are boxed in green (Thr and Gly) and red (Ser and Ala). Secondary structure elements are shown as determined from the *B. subtilisenzyme* (1). The alignment was generated by ClustalW2. The aligned sequences were from ferrochelatase amino acid sequences of a variety of organisms: Eco (*Escherichia coli*), Yen (*Yersinia enterocolitica*), Csa (*Cucumis sativus*), man, mouse, Rabbit (*Oryctolagus cuniculus*), Saccharomyces (*Saccharomyces cerevisiae*), Arabidopsis (*Arabidopsis thaliana*), Bsu (*B. subtilis*), the two HemH paralogues of the *S. loihica* PV-4 and the *S. oneidensis* MR-1.

The different roles of *hemH* paralogues in PV-4 was also supported by the dissimilar gene expression regulation, leading to their distinctive expression patterns. The *hemH1* gene was regulated by more general regulators RpoD and OxyR, consistent with its constitutive expression. Expression of *hemH2* was controlled by ECF sigma factor RpoE2, which was an self-regulated oxidative stress response regulator and operates with an anti-sigma factor ChrR (Shew_1477) (Bashyam and Hasnain, 2004). Sequence analysis and transcriptional start site mapping revealed the existence of conserved RpoE2 regulatory motif upstream of *rpoE2* and *hemH2* in multiple

Shewanella strains other than PV-4, indicating this is a common feature in this genus. Under non-stress conditions, the anti-sigma factor ChrR binds to RpoE2, preventing the latter from binding to recognition sites on the genome. In the case of oxidative stress, ChrR undergoes a conformational change and RpoE2 is released, resulting induction in its regulon members including *rpoE2* itself (Kazmierczak et al., 2005). In accordance with previous studies that RpoE2 is an oxidative stress response regulator, *hemH2* expression is conditionally induced under oxidative stress due to hydrogen peroxide or ROS generated from light exposure upon PPIX producing Δ*hemH1*. Without a functioning *hemH* paralogue, light radiance on in PPIX-export deficient *Streptococcus agalactiae* mutants or PPIX-accumulating *E. coli hemH* mutant was harmful or even lethal (G. Sidney Cox et al., 1982; Miyamoto et al., 1992; Nakahigashi et al., 1991). Because *hemH2* "backed up" the loss of *hemH1*, instead of killing the cells, light exposure of Δ*hemH1* reverted the PPIX accumulation phenotype to wild type.

Table 3. 6 Genetic redundancy in other heme synthesis genes in *Shewanella*

Strains	**Locus tag**					
	hemB	***hemL***	***hemN***	***hemG***	***cysG***	***cyoE***
S. oneidensis	_2587, _4208		_3359, _4730	_0025, 0027, _3720	_3728, _4315	
S. denitrificans	_0303, _0452		_2687, _3626		_0386, _0958, _3717	
S. frigidimarina			_0042, _2866	_0017, _0019, _0813	_0438, _1506, _3188	_0220, _0250
S. amazonensis			_0086, _2483	_0036, _0038, _2882	_2892, _3256	
S. baltica OS195	_0422, _1892		_3189, _4239, _4493	_0024, _0026, _0973	_0961, _4096	
S. loihica			_1131, _3720	_0023, _0025, _0678	_0316, _0672	_0117, _0370
S. putrefaciens CN-32	_0497, _1755		_2693, _3913	_0017, _0019, _3038	_3044, _3589	_3789, _3862

S. sediminis	_1088, _3708	_0090, _1226, _4414	_0027, 0029, _3790	_2768, _3797, _4135	
S. pealeana		_0096, _1121, _3339	_0022, _0026, _0673	_0371, _0662, _1808	
S. halifaxensis	_1021, _2957	_0116, _1166, _3411, _4226	_0020, 0022, _3525	_3534, _3919	
S. woodyi		_0053, _1326, _2002		_0481, _0787, _1872	_0170, _0429
S. piezotolerans	_0974, _1129	_3679, _3985, _5079	_0049, _0051, _4046	_0399, _2921, _4059	_1427, _4836
S. violacea	_0895, _3511	_0082, _1037, _3565		_0588, _3522, _3843	_0182, _4323

Genetic redundancy is a common phenomenon observed in all life domains and happens in almost every gene category, including housekeeping, functional, and regulatory genes (Zhang, 2012). It remains an intriguing subject to understand the function, regulation, and fate of the paralogues during the evolutionary course. In terms of the *hemH* paralogues in PV-4, it seems that transcriptional reprogramming due to feedback effects (*e.g.* reduced heme and PPIX accumulation) or environmental stresses (*e.g.* oxidative stress) played a key role in maintaining heme homeostasis and thus the selection and necessity for the two paralogues. We propose a model to depict the roles of *hemH1* and *hemH2* in heme biosynthesis and their regulation in context with respiration and oxidative stress (Fig. 3.13). Under anaerobic/microoxic and dark conditions, the RpoD-dependent *hemH1* is constitutively expressed and plays a primary role in heme and *c*-type cytochrome synthesis. Inactivation of *hemH1* blocks the biosynthesis of heme and cytochromes and results in accumulation of PPIX, which may mediate the production of ROS under aerobic and light exposure conditions. The presence of ROS is sensed by ChrR, resulting in the release and activation of RpoE2 to drive the transcription of *hemH2* for heme synthesis. Additionally, synthesis of heme

precursors decreased and uptake of iron increased by feedback regulation. Under oxidative stress, the OxyR transcriptional factor may also act to enhance the transcription of *hemH1*. Overproduction of PPIX in Δ*hemH1* suggests a yet to be identified PPIX/heme export system similar to those reported in pathogens such as *Streptococcus agalactiae* to prevent an excessive intracellular porphyrin pool (38), which is currently under investigation.

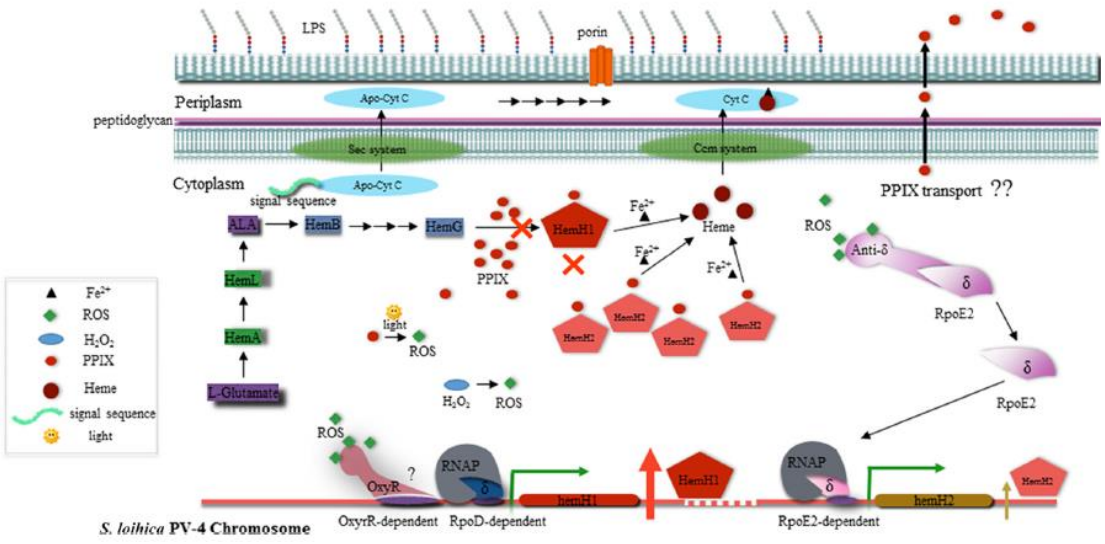

Fig. 3. 13 Schematic diagram illustrating the biosynthesis pathway of heme and cellular function and transcriptional regulation of two ferrochelatase paralogues in *S. loihica* PV-4 strain. LPS, lipopolysaccharide; Sec, secretion; Ccm, cytochrome *c* maturation.

Rather surprisingly, a further look at the heme synthesis genes in *Shewanella* revealed an extremely high level of genetic redundancy than expected. Besides *hemH*, 4 genes directly involved in heme synthesis, and two gene involved in synthesis of heme O (cyoE) and siroheme (cysG), were found to possess paralogues in multiple *Shewanella* species. Many of these genes have more than one paralogue. While paralogues of hemN and cysG were more commonly seen in various microbes, such as

E. coli, *Shigella*, *Enterobacter*, and *Pseudomonas*, etc., paralogues for the other genes were not as frequent, let alone showing up in the same organism. Such convergence of gene redundancy is very rare among prokaryotes. To the best of our knowledge, *Shewanella* may be the only genus that display such diversified gene redundancy in the heme synthesis pathway. This phenomenon may be associated with the respiratory versatility of *Shewanella*, to ensure synthesis of heme under various redox conditions. Therefore, it is an intriguing task to elucidate the function and regulation of these paralogues. The availability of abundant genome sequences and a mature mutagenesis platform make *Shewanella* an ideal model organism for studying genetic redundancy and its implication in the physiology, ecology, as well as stress response for environmental microbes using comparative genomics.

Chapter 4: Investigation of population level fitness change, salt stress tolerance, and the underlying mechanisms for *Shewanella putrefaciens* CN-32 via experimental evolution

4.1 Abstract

Environmental microbiology and its associated methods have shown great potential for pollution treatment and sustainable energy source. Understanding the long term microbial stress response mechanism is critical for boosting the functionality and sustainability of such applications. In this study, we investigated the phenotypic changes and mechanism for long term salt stress response with a model environmental strain, *Shewanella putrefaciens* CN-32, using experimental evolution strategy. After evolving for one thousand generations under control or salt stress conditions with additional NaCl, significant phenotypic changes were observed among the evolved populations, reflecting the change of fitness after exposing to a consistent environment. These populations showed significantly higher growth rate and peak biomass than the ancestor, indicating gain of fitness during the course of evolution. Populations evolved from salt stress condition showed significant advantage in growth rate and peak biomass compared to ancestor and populations evolved in control media. In addition, all evolved populations showed significant impairment in motility compared to the ancestor, suggesting a tradeoff for other phenotypical advantages gained during evolution. The metabolite profiles showed a clear shift among the three groups of populations that are evolved in salt stress, evolved in control condition, and the ancestor. Detrended Correspondence Analysis (DCA) showed that culture condition and the evolution condition are the two major factors shaping the distinct metabolite profiles. Detailed

analysis at individual metabolites revealed several distinctive patterns among ancestor, control, and treatment populations. Significant accumulation of ectoine and proline were found in treatment populations under salt stress, indicating that these two known compatible solutes may play critical role for long term salt stress response. Micorarray analysis was conducted on the ancestor and two populations from the control and treatment group, respectively, under control or salt stress conditions. The result showed that genes responsible for uptake/synthesis of proline, were significantly upregulated when exposed to salt stress, which is in consistence with metabolite analysis. Whole genome level population resequencing revealed a total of Single Nucleotide Polymorphisms (SNPs) in the evolved populations, with control populations showing significantly higher number of SNPs. Particularly interesting SNPs were those that only found in the treatment populations, which may indicate their role in boosting the fitness of the population.

Keywords*: Shewnella putrefaciens* CN-32, salt stress, experimental evolution, fitness, metabolite profile, microarray analysis, single nucleotide polymorphism

4.2 Introduction

Environmental microbiology and its associated technologies have shown great potential application for monitoring environment, treating various types of pollution, and providing sustainable energy (Diplock et al., 2010; Du et al., 2007; Kirkbride et al., 1992; Wasi et al., 2013). One of the major factors perturbing environmental microbiology applications is the various kinds of stresses these organisms may encounter, which adversely affect their growth and function. Knowledge of how these organisms cope with unfavorable conditions is critical for improving the efficiency and sustainability of desired function. Although our understanding of mechanisms bacterial employ to respond to a great variety of stresses have been enhanced greatly thanks to studies imposing short term stress conditions (shock) and investigate cellular response (Berrier et al., 1992; Chastanet et al., 2003; Michel et al., 1997; Yura et al., 1993), in natural environments it is very common for such stress conditions to persist for months to years. The cellular response and the strategies microorganisms use to cope with long term stresses can be different from short term exposure. Knowledge about these long-term stress response strategies and the underlying mechanisms can provide important implications for bioremediation or industrial applications. Because of this, there has been growing interest and endeavor in understanding the long term stress response of microbes that are of environmental importance. Because of the long time span during which hundreds and thousands of bacterial generation will proliferate, perspective of adaptation and evolution became critical.

In recent decades, directed experimental evolution with model microorganisms has emerged as an important strategy to test important evolutionary biology theories and

for engineering purposes for various applications (Barrick and Lenski, 2013; Kawecki et al., 2012). Combined with rapid development in molecular biology technology and DNA sequencing, there is unprecedented opportunity to understand how microbes adapt to environmental stress in the long term from the point of views of genetics, physiology, ecology, and evolution. Intriguing results were obtained from various bacteria such as *E. coli*, *Pseudomonas*, and *Enterococcus*, etc. (King et al., 2016; Tenaillon et al., 2016; Wong et al., 2012). For example, an *E. coli* strain that originally cannot use citrate as carbon source developed such capability after 30,000 generations of incubation in medium containing both glucose and citrate (Blount et al., 2012). In contrast, there are relatively few studies focusing on microbes with great potential in environmental applications. In recent years, our laboratory has published a number of experimental evolution studies using *Desulfovibrio vulgaris* Hildenbourough as a model organism. Interesting findings, such as shift in the transcriptome profile, increased amount of compatible solutes, and fast sweep of pre-existed polymorphism during early stage of adaptation but slow fixation of new mutations, were observed (Zhou et al., 2013; Zhou et al., 2015).

Bacteria in the *Shewanella* genus are bacillus facultative anaerobes that are frequently isolated from various fresh and salt water bodies. Their habitats encompass a wide gradient of various environmental factors, such as redox potential, temperature, salinity and pressure (Fredrickson et al., 2008). Besides, these bacteria are renowned for the broad spectrum of substances that they can use as electron acceptors. These include organic molecules, such as fumarate, dimethyl sulfoxide and trimethylamine N-oxide; inorganic salts, such as nitrate and thiosulfate; and various metals both in the

form of ions and oxides, such as ferric iron, manganese, uranium, chromium, etc., (Fredrickson et al., 2008; Hau and Gralnick, 2007). Because of this, there have been extensive research endeavors to try to understand the physiology, genetics, and ecology of *Shewanella*, with the aim to explore the potential of using this genus for bioremediation or as alternative energy source through Microbial Fuel Cells.

In this study, we use one of the better characterized strains among the *Shewanella* genus, *Shewanella putrefaciens* CN-32, as our target organism. CN-32 is a metabolically versatile strain capable of reducing various contaminants such as Chromium, Uranium, Arsenate, and nitrobenzene (Huang et al., 2011; Luan et al., 2015). In an effort to improve our understanding toward the effect of long term exposure of salt stress on CN-32, experimental evolution with parallel populations with different salinity levels by altering the sodium chloride concentration was set up. Salt stress is commonly associated with natural environments and contamination sites. It could also be introduced during bioremediation processes, such as addition of alkaline chemicals to neutralize sites with low pH. It was hypothesized that the populations evolved under salt stress will show improved fitness under higher salt concentrations compared with control groups and the ancestor, but with certain tradeoffs. Such fitness gain is an overall reflection of the changes at molecular level during the course of evolution. The fitness, metabolite profile, transcriptomes, and mutations occurred after 1 thousand generations of evolution were examined to explore the mechanisms for long term adaptation under osmotic pressure imposed by sodium chloride.

4.3 Materials and Methods

4.3.1 Strain and culture conditions

The strain used in this study is a lab stock. One colony from revived stock culture of CN-32 was picked and grown in LB medium overnight and designated as ancestor (An). 100µl of this fresh culture is used as seed to found 12 populations. These populations were divided into 2 groups, evolved control (EC) and evolved salt (ES), each with 6 parallel populations. Each population was cultured in a 30ml glass tube in 10ml anaerobic medium with butyl stopper and aluminum seal. The medium used in this experiment is M1 medium. A small amount of tryptone (0.2g/l) was added in all evolution medium as nutrient to stimulate bacterial growth. For experimental evolution propagations, EC lines were cultured in modified anaerobic M1EC medium (total Na+ concentration is 150mM). The ES lines were cultured in M1ES medium supplemented with additional 200mM of NaCl. All the populations were transferred every other day with a 1: 100 dilution, which corresponds to approximately 6.7 generations with each transfer. In this report, all EC and ES populations were evolved 1 thousand generations.

4.3.2 Growth test for 1 thousand generation

For testing growth of evolved lines and ancestor, all the evolved lines were revived from frozen stock, transferred one time in the medium they evolved from before inoculating into test medium, which are anaerobic M1TC (M1 Test Control; M1 control medium without tryptone), M1TS1 medium (M1 Test Salt 1; M1 control medium +200 NaCl, without tryptone), or M1TS2 medium (M1 Test Salt 2; M1 control medium +300 NaCl, without tryptone). At least three biological replicates were used for growth

curves. Biomass yield comparison is directly based on the maximum optical density measured at 600nm (OD600) during the course of growth. Growth rate is calculated using the formula K=2.303S, where S is the slope of the linear portion of the growth curve obtained by plotting log10 (OD600) with time.

4.3.3 Metabolite profiling experiment

To obtain the metabolite profile of evolved populations and ancestor under control and NaCl stress conditions, ancestor and each evolved population were revived and cultured in anaerobic M1TC and M1TS medium. 50ml of late log phase culture in M1TC or M1TS testing medium was centrifuged. The supernatant was discarded and cell pellets were immediately frozen in liquid nitrogen and kept frozen in -80ºC until assay performed. The profiling was performed in Dr. Trent Northen laboratory with protocol as previously published(Baran et al., 2013).

4.3.4 Motility test

Ancestor and evolved populations were revived from frozen stock as in growth comparison test. Mid-log phase liquid cultures were adjusted to similar optical density. Then, 5µl of each population was dropped onto the surface of M1TC and M1TS soft agar plates containing 0.4% (w/v) of agar with three replicates. The plates were then incubated anaerobically at 30°C for one week. Cell motility was compared by measuring the diameter of each cell patch.

4.3.4 Microarray analysis

The following populations were chosen for microarray analysis, An, ES2, ES6, EC5 and EC1. The four evolved populations were selected because of the better salt tolerance compared with other ES or EC lines based on growth data. These populations were revived from frozen stock using the medium in which they evolved from. The revived cultures were then inoculated into 100ml of anaerobic M1TC medium and M1TS medium. 50ml cells were collected at mid-log phase and frozen immediately in liquid nitrogen and stored in -80°C until RNA extraction. A Trizol based RNA extraction protocol is performed for extraction of total RNA, as previously reported (Hurt et al., 2001). The quality of the RNA extracted is checked by gel electrophoresis. RNA quantitation, A260/280, and A260/230 were obtained using Nanodrop 1000. 1.5µg of total RNA is used for labeling of each sample with Cy5 dye, while 150ng of genomic DNA of each population was labeled with Cy3. The microarray used in this study is a customized pure culture array designed in our lab with CommonOligo 2.0 and manufactured by NimbleGen. Array hybridization, scanning, raw data extraction, data processing were adopted from previous publication (Tu et al., 2014).

4.3.5 Detection of SNPs via population level genome sequencing

To extract population genomic DNA, ancestor and 1K generation frozen stocks were revived their respective evolution medium. The cell pellets were collected after 48 hours and the genomic DNA was extracted using a Bacterial Genomic DNA Extraction Kit (Sigma Aldrich) following manufacturer instructions. Concentration and quality of the prepared DNA was examined using Nanodrop 1000 and electrophoresis. 60ng of

genomic DNA is sent for population genome DNA sequencing, using Illumina Hiseq2500 platform in Oklahoma Medical Research Foundation. The SNP detection was conducted by mapping each sequence to the reference genome of *Shewanella putrefaciens* CN-32 using the SNP detection pipeline under the Galaxy sequence analysis platform developed in our lab.

4.4 Results

4.4.1 Phenotypical changes in evolved populations

The growth test of ancestor and evolved populations are conducted in media with same composition, except the different NaCl concentration to impose a control (no extra supplement of NaCl, M1TC), medium salt stress conditions (extra 200mM of NaCl, M1TS1), and high salt stress condition (extra 300mM of NaCl, M1TS2). Fig 4.1 shows the growth curves for the AN, EC, and ES populations under the three conditions. Generally, the average growth of the three populations was not significantly different in M1TC. With increased NaCl concentration and moderate salt stress, ES populations became more advantageous than EC and AN in M1TS1 media. The advantage of ES was most significant when cultured under high salt stress, in M1TS2 media.

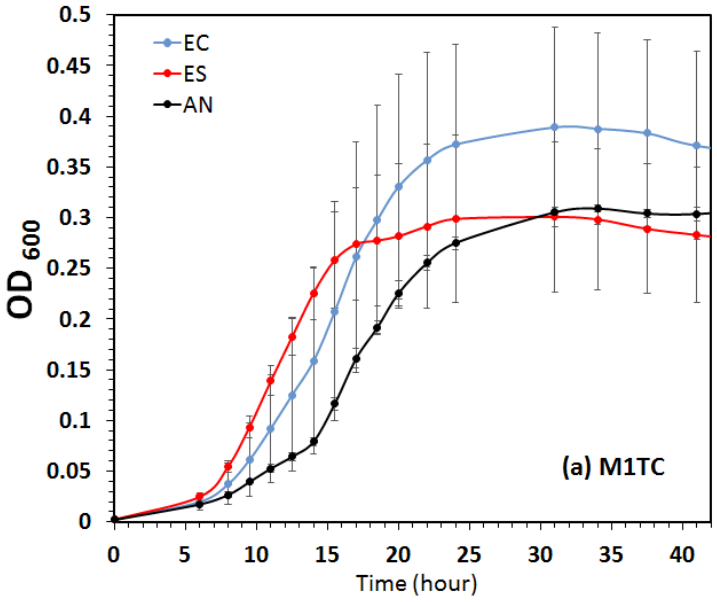

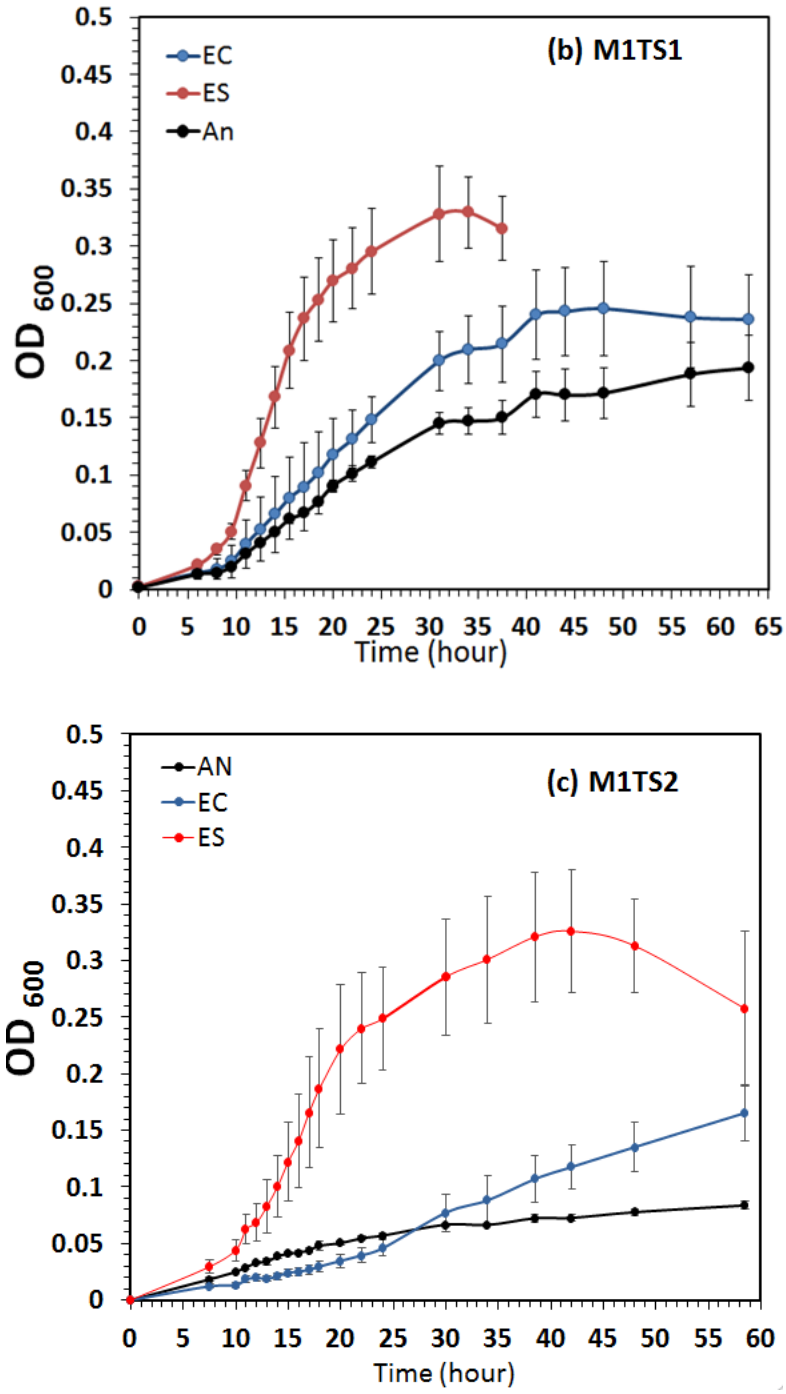

Fig. 4. 1 Growth curve of AN, EC, and ES in media with different osmotic conditions, M1TC (a), M1TS1 (b), or M1TS2 (c).

Growth rate and peak biomass are two key phenotypic features depicting the fitness of a bacterial population. The growth rate for the three groups, AN, EC, and ES in M1TC, M1TS1, and M1TS2 were extrapolated from the growth curve data. Analysis

of variance (ANOVA) was conducted to test for statistical significance. The results were summarized in a bar plot as shown in Fig. 4.2. A bit to our surprise, ES showed the highest growth rate in M1TC media, followed by EC and then AN, with statistical significance. When cultured in M1TS1 media, all evolved populations showed a decrease in growth rate. The average growth rate decreased from 0.35 to 0.31 for ES lines, from 0.3 to 0.23 for EC lines, while the growth rate of An only decreased slightly, from 0.22 to 0.2. When cultured in M1TS2 media, growth rate of all populations further decreased to 0.2, 0.08, and 0.11 for ES, EC, and An, respectively. In both M1TS1 and M1TS2 media, the growth rate of ES lines was significantly higher than EC and AN, with the latter two populations not significantly different from each other. Apparently, one thousand generations of propagation under moderate salt stress conditions allowed the ES lines to adapt to such conditions better than EC or AN, who were not exposed to salt stress conditions.

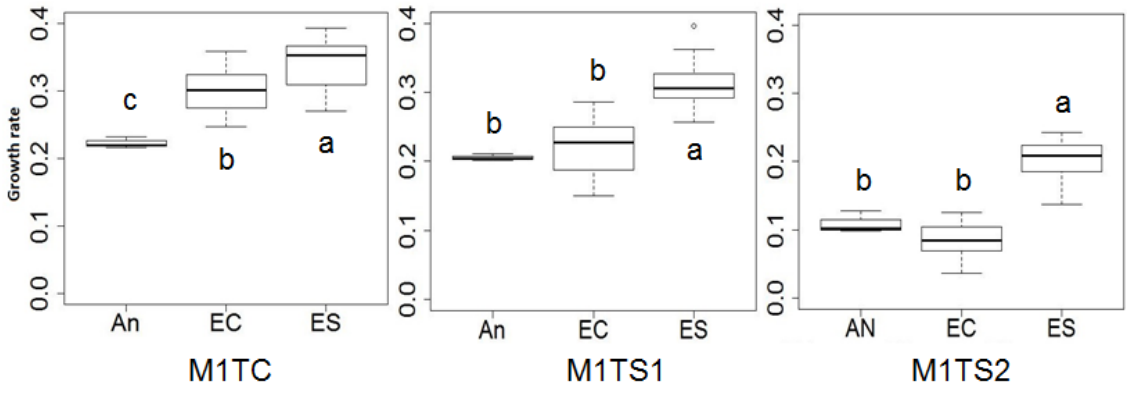

Fig. 4. 2 Average growth rate of An, EC, and ES lines in M1TC, M1TS1, and M1TS2 media. Letters a, b, and c represent statistically significant difference ($P<0.05$) based on ANOVA. The middle horizontal bar represent the median. The upper and lower horizontal bars of the box represent 25 and 75 percentiles, error bars represent standard deviation

The peak biomass of AN, EC, and ES were also compared and the result is presented in a bar plot, as shown in Fig. 4.3. When cultured in M1TC, EC populations showed the highest peak biomass, significantly higher than ES or An, which are not similar with each other, reflecting that the EC populations were more adapted to the control medium. With an increase in salt stress in M1TS1 and M1TS2 media, ES populations were obviously more advantageous, with peak biomass significantly higher than EC, which in turn, is significantly higher than An. Therefore, ES populations grew faster and can accumulate higher peak biomass under salt stress. Interestingly, although the growth rate of ES decreased under higher salt stress with culture media in the order of M1TC>M1TS1>M1TS2, the average peak biomass for ES populations stayed virtually at the same level of OD600 around 0.3 under in all three media, whereas the peak biomass for EC and An dropped significantly with increased salt stress.

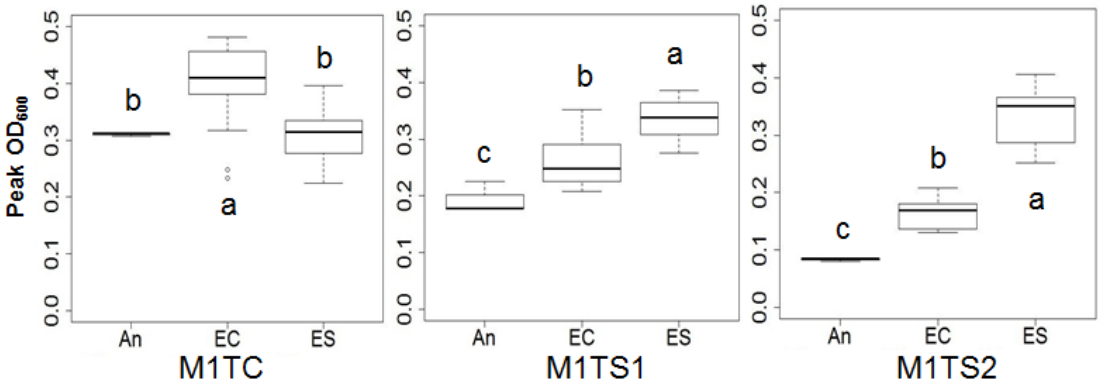

Fig. 4. 3 Average peak biomass of An, EC, and ES populations cultured in M1TC, M1TS1, and M1TS2 media, letters a, b, and c represent statistically significant difference (P<0.05) based on ANOVA. The middle horizontal bar represent the median. The upper and lower horizontal bars of the box represent 25 and 75 percentiles, error bars represent standard deviation

Motility is an important parameter for fitness assessment as the ability to move is critical for exploitation of favorable habitats or avoiding harsh conditions. It would be

interesting to see whether the evolved populations will exhibit improved or impaired motility. The motility test was conducted on soft M1TC or M1TS1 agar plates and the motility was recorded as the difference in the diameter of the bacteria lawn after incubation and the initial lawn inoculated (5µl of liquid culture with similar OD600). The result by treatment level is shown in Fig. 4.4. The motility of EC and ES were both significantly lower than that of An on both M1TC plate and M1TS1 plate, although An was inferior in growth rate or peak biomass in both cases. Therefore, this impairment of motility represents a major tradeoff for the fitness gain of the EC and ES lines under their evolved condition.

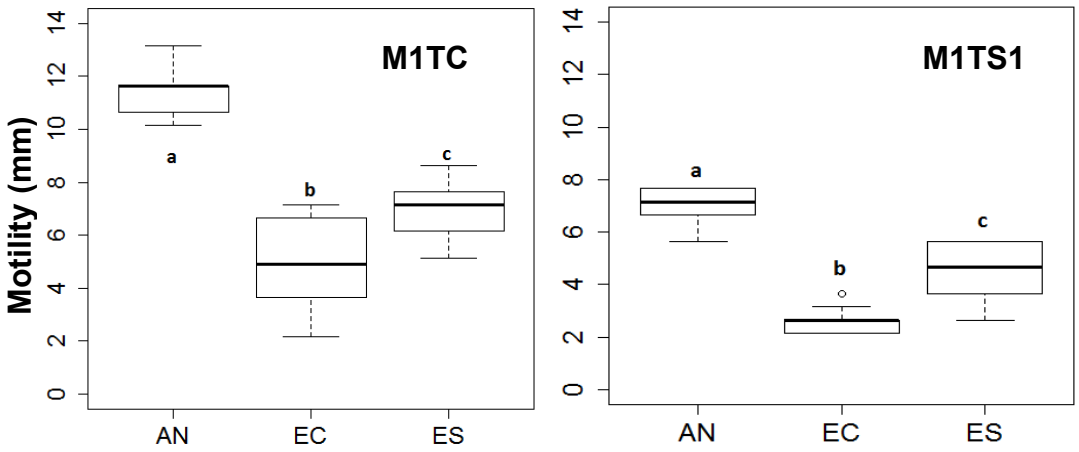

Fig. 4. 4 Motility of An, EC and ES populations cultured in M1TC or M1TS1 soft agar plate. Motility is calculated by subtracting the diameter of the inoculated cell plaque from the overall diameter of the cell plaque after incubation. Letters a, b, and c represent statistically significant difference ($P<0.05$) based on ANOVA. The middle horizontal bar represent the median. The upper and lower horizontal bars of the box represent 25 and 75 percentiles, error bars represent standard deviation

The bar charts shown in Fig. 4.2, Fig. 4.3, and Fig. 4.4 provided an overview toward growth rate, peak biomass, and motility at the treatment level, i.e., EC, ES, or

An, under different culture conditions. Although such observation provides useful indication regarding the effect of evolution condition on growth, information toward the variance among the parallel populations was not as clear. As previously reported, even under the same environmental conditions, each parallel population may show similar trend or take different routes to achieve better fitness. Therefore, it would be noteworthy to look at the growth rate and peak biomass for each of the populations. Fig. 4.5, Fig. 4.6, and Fig. 4.7 showed the growth rate, peak biomass, and motility for each of the individual populations, along with the ancestor, in M1TC, M1TS1, and/or M1TS2. Generally, there was a great difference in growth rate, peak biomass, and motility among populations within the same treatment. But such variance decreased as the salt stress increases. For EC populations, noticeably, in M1TC, the growth rate of EC lines were divided into two groups, with EC1, EC3, and EC6 showing the higher growth rate (>0.3), and EC2, EC4, and EC5 showing lower growth rate (<0.25 and similar to that of An). Considering M1TC was the medium that the EC lines have evolved from, this variance in growth rate indicates that the EC lines may have undertaken different routes during their course of propagation. ES lines generally showed less variance for growth rate, peak biomass, and motility compared to EC lines, suggesting the salt stress condition in which they evolved from may cause certain constraint on phenotypes.

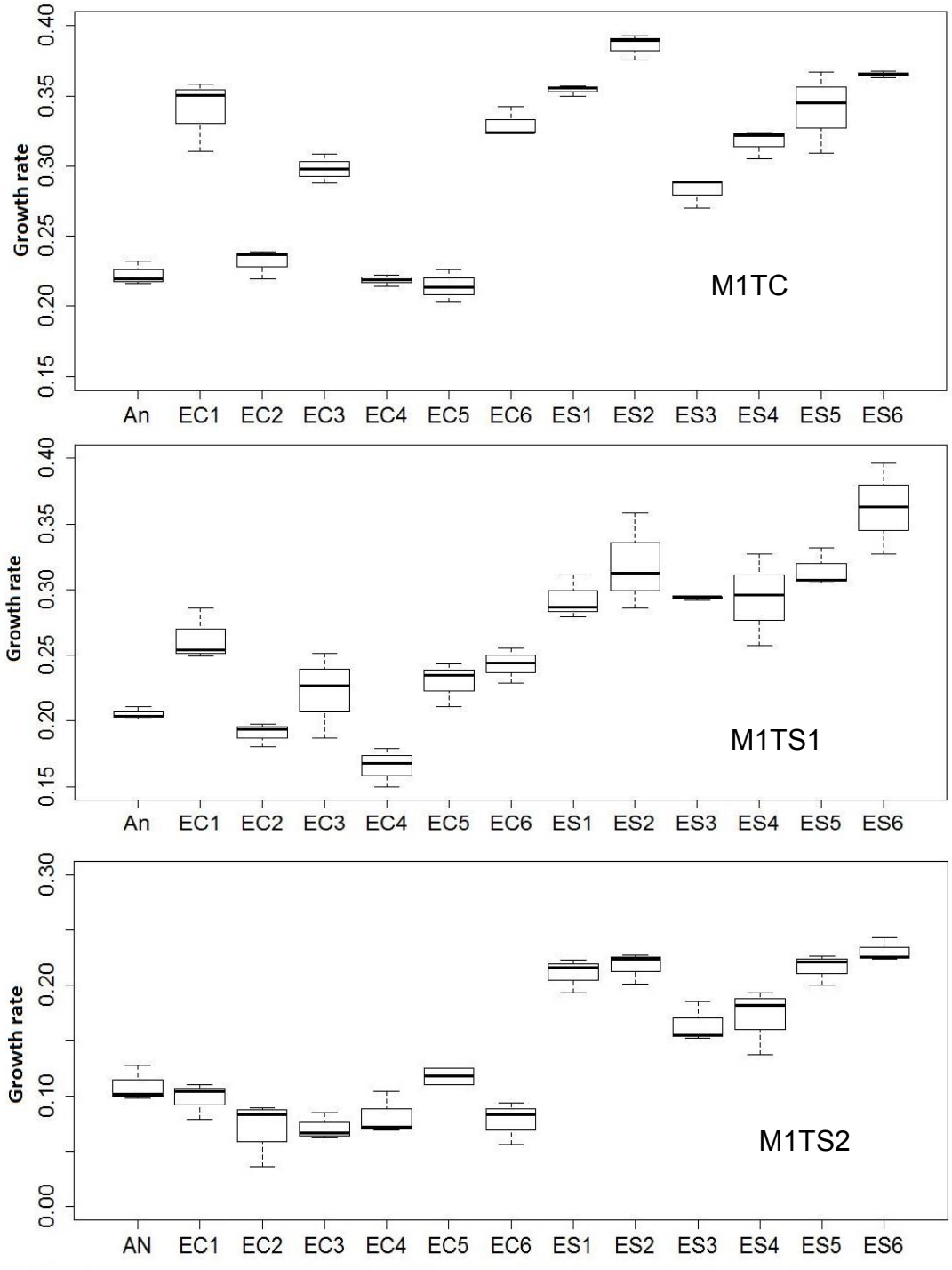

Fig. 4. 5 Growth rate of each individual populations from An, EC, or ES under control condition (M1TC), moderate salt stress (M1TS1), and high salt stress (M1TS2)

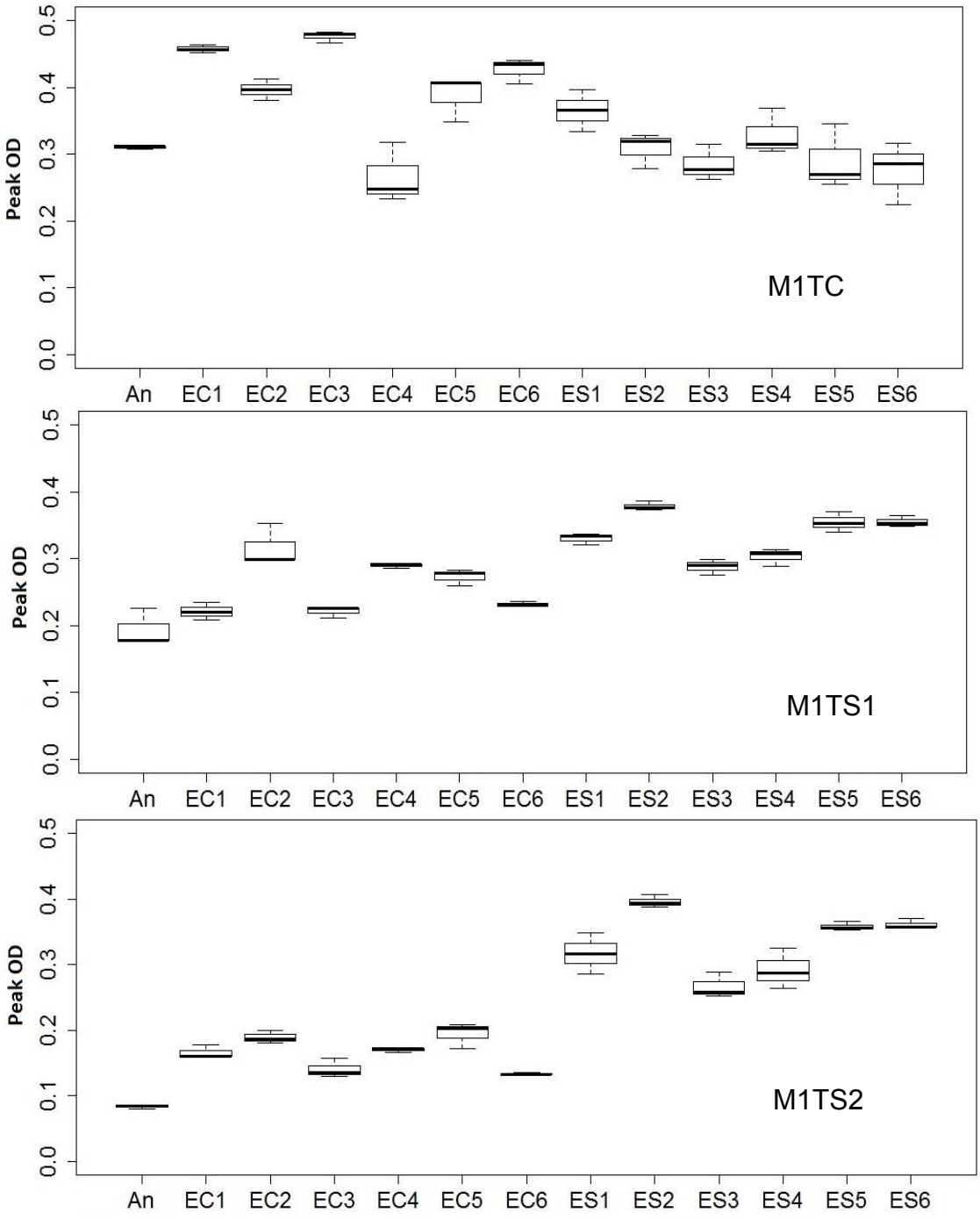

Fig. 4. 6 Peak biomass (OD600) for individual populations cultured in M1TC, M1TS1 or M1TS2 media.

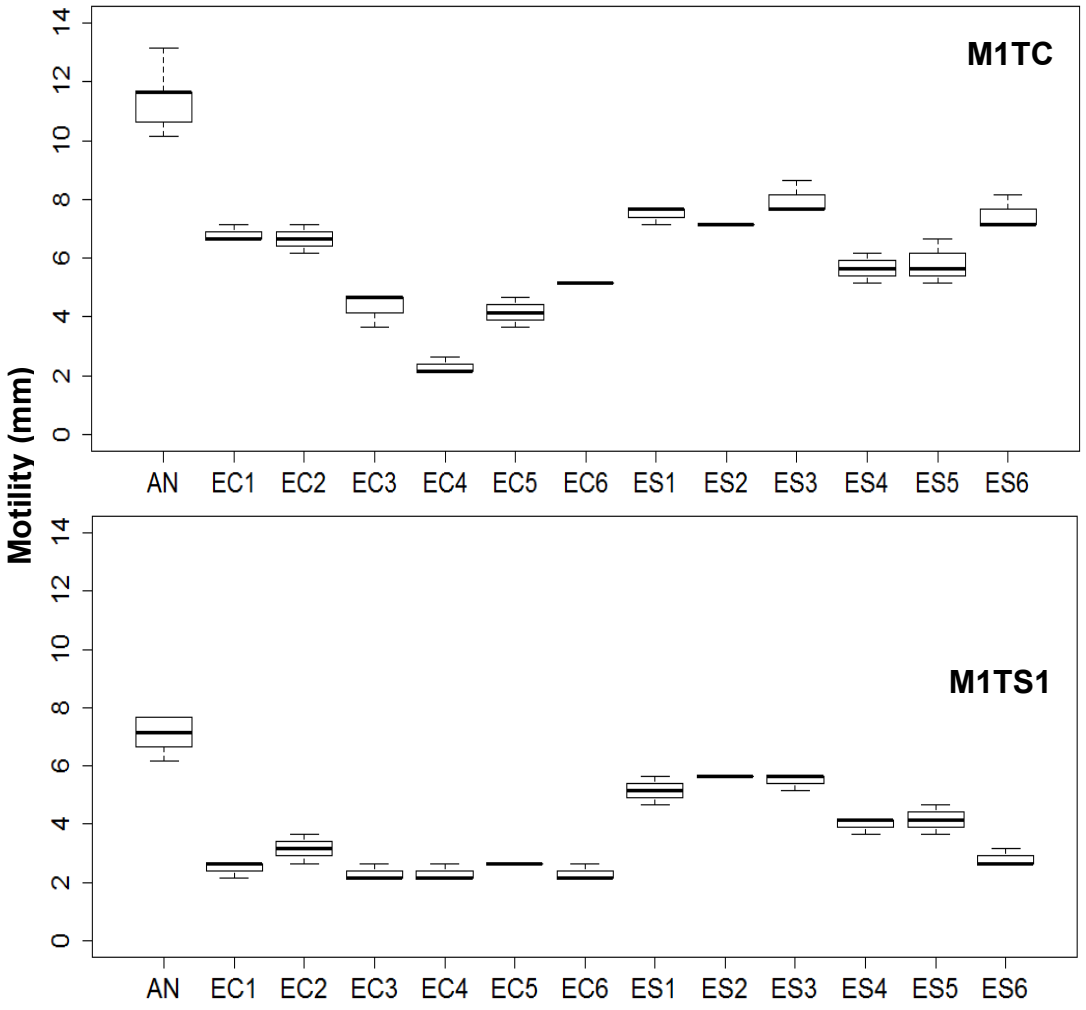

Fig. 4. 7 Motility of individual cell lines on M1TC or M1TS1 soft agar.

4.4.2 Shifted metabolite profile in evolved populations

In an effort to better understand the underlying mechanism contributing to the phenotypic advantage of ES lines under salt stress, the metabolome of An, EC, and ES lines were analyzed with sample taken from each population cultured in M1TC or M1TS1 media. In total, 32 metabolites were identified and quantified. Detrended Correspondence Analysis (DCA) was conducted to visualize the overall metabolite profile for samples taken from different population and culture conditions. The DCA result is shown in Fig. 4.8. Some obvious clustering patterns can be observed from the

result. The first important pattern was that there is a clear separation between samples cultured in M1TC and samples cultured in M1TS1 media, along the DCA1 axis, indicating the concentration of NaCl, and the resulting osmotic condition of the media, was the major factor shaping the metabolite profile among all populations. The second pattern was the clustering of samples based on the treatment level. Under M1TC condition, An samples were clustered together, while all the EC and ES samples were mixed and formed another cluster, with EC samples more scattered and ES samples more converged. Under M1TS1 condition, the cluster and their separation became more apparent. The populations of different treatment level formed their own clusters and shifted toward the lower right corner on 2-D space of the DCA chart, with only one EC populations mixed with An samples. This result indicated that the treatment level, i.e. the culture condition where these populations have evolved from, is another critical factor determining the composition of the overall metabolite profile.

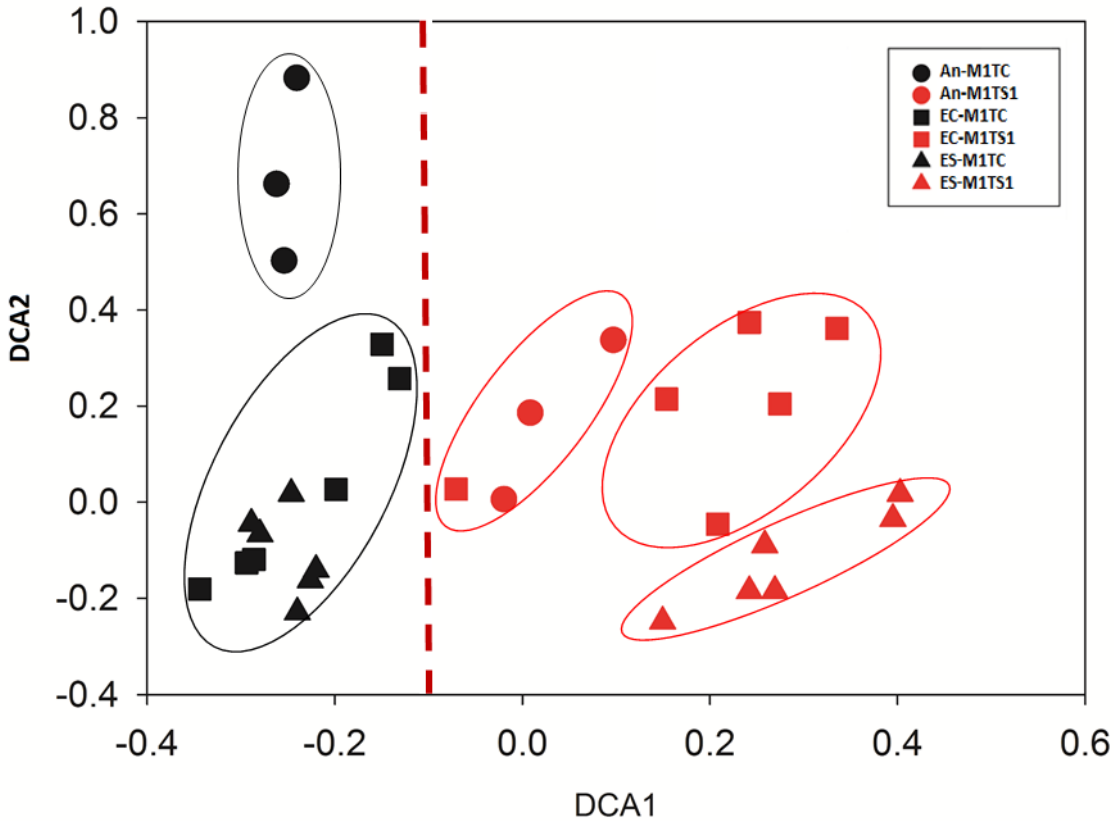

Fig. 4. 8 DCA analysis of the metabolite profile based on the 32 metabolites identified in sample from different populations and cultured in M1TC (black symbols) or M1TS1 media (red symbols). The red dashed line indicates separation of samples based on the culture conditions, whereas the ovals showed that the samples are clustered according to their evolution condition.

4.4.3 Critical patterns of change in key metabolites

Although the different overall metabolite profile revealed that both culture condition and evolution condition are critical in shaping the metabolite composition, the specific amount of important metabolites can potentially provide important clues for understanding the mechanism of long term salt stress. The protective roles of osmoprotectants, or compatible solutes, toward salt stress in bacteria have been well documented. However, different bacteria have their own set of preferred compatible solutes. Besides, studies on compatible solutes in bacteria populations underwent long

term salt stress is very limited. In this study, we analyzed the change in quantity of the metabolites identified in An, EC, and ES populations, when cultured in M1TC or M1TS1. Although most of the metabolites showed patterns without a clear trend, there were a few metabolites that did show very interesting patterns. For example, glutamate is regarded as a key compatible solute in numerous bacteria and it is usually among the earliest compatible solutes to be synthesized when exposed to salt stress. The change of glutamate is shown in Fig. 4.9. In An replicates, it can be seen that the amount of glutamate showed significant increase when cultured in M1TS1 compared to M1TC, which is expected and in consistence with previous publications. Although the amount of glutamate also increased when cultured in M1TS1 than in M1TC for EC and ES populations, the mean amount of glutamate actually decreased under M1TS1 in the order of An>EC>ES, suggesting that glutamate may be play as important role in the evolved populations as in the ancestor.

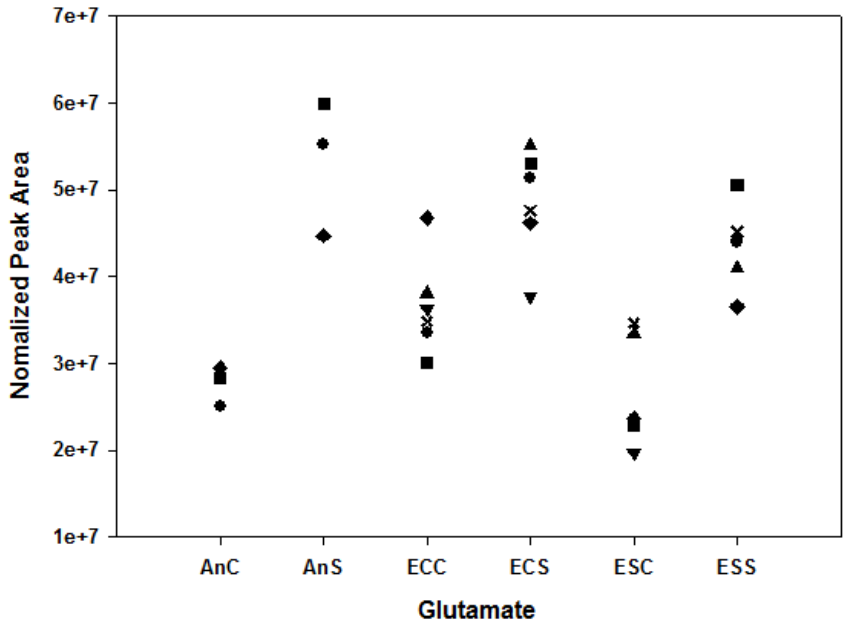

Fig. 4. 9 Amount of Glutamate in An, EC and ES populations, AnC indicate An samples from M1TC, AnS indicate An samples from M1TS1, etc. Each symbol

represents one population in EC or ES, while shown in An are the three biological replicates.

Among the 32 metabolites, two osmolytes proline and ectoine, showed significant increase in evolved populations, especially in ES, when cultured in M1TS1. As shown in Fig. 4.10, An, EC, and ES showed very similar levels of proline under M1TC condition. When cultured in M1TS1, all populations were accumulating proline, but to a different extent. The level of proline in An and EC populations were still at a similar level in M1TS1, with EC populations showing greater variance. In ES lines, however, the accumulation of proline reached a different level, with the mean peak area close to 4 times of An and EC. Besides, proline is among one of the most abundant metabolites detected, as reflected by its peak area. This dramatic increase in proline is very interesting and really suggests that proline may be one of the most important machineries for the ES populations to withstand salt stress and achieve high biomass under such condition. For Ectoine, similar trend like proline was observed in all populations. Despite the huge variance in the ES lines with M1TS1, the mean peak area of ectoine in ES populations was more than 3 folds of An and EC. However, the quantity of ectoine, as reflected by the peak area, was much lower than proline. In fact, ectoine is one of the detected metabolites with the least abundance. But this pattern of accumulation still suggests that ectoine may also be an important factor contributing to salt stress tolerance in ES populations.

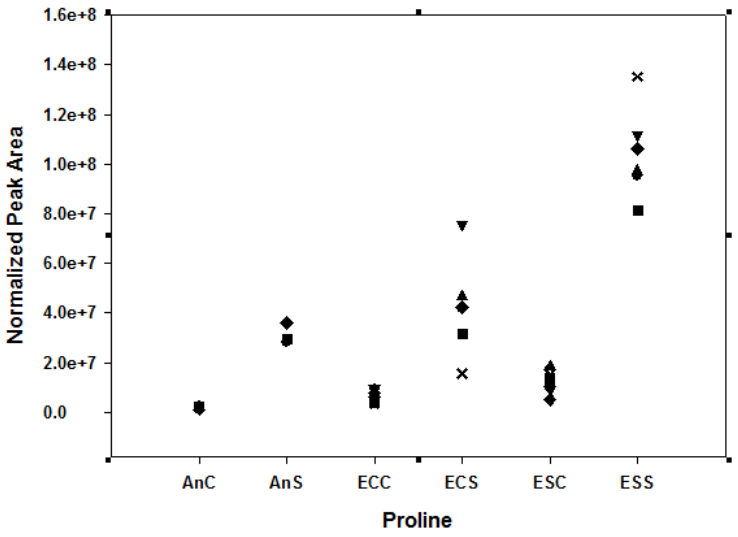

Fig. 4. 10 Amount of proline in An, EC and ES populations under M1TC or M1TS1 conidtions

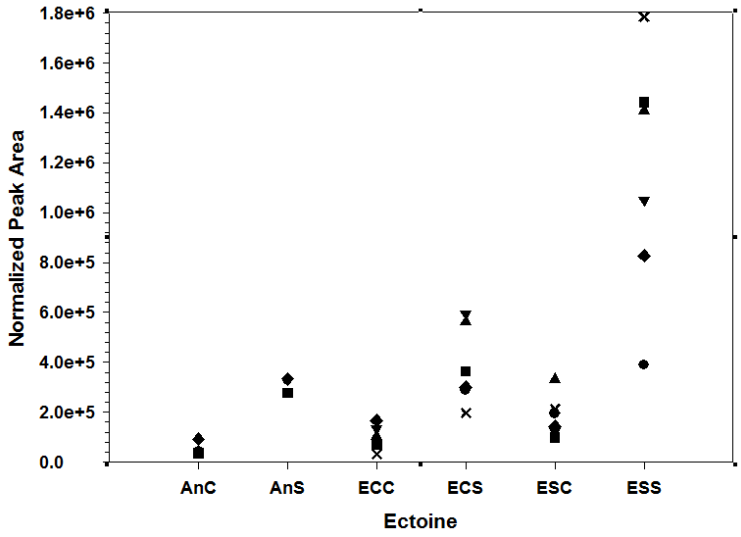

Fig. 4. 11 Amount of ectoine in An, EC and ES populations under M1TC or M1TS1 conditions

It is noteworthy to mention that other patterns of metabolites were also observed. For example, leucine and isoleucine, two closely related amino acid and can be interchanged via one biochemical reaction, showed very similar trend among the populations. As shown in Fig. 4.12, the An and EC populations showed similar level of

both amino acids under M1TC and M1TS1 conditions, with a bit less amount of leucine than isoleucine. For the ES lines, the mean quantity of leucine and isoleucine is ~3 fold higher under M1TC than An and EC, but falls lower to ~2 fold higher than An and EC when cultured in M1TS1. Another amino acid, arginine, is most abundant in ES populations under both control and salt stress conditions, but it remained at similar level under these two conditions. Similar situation is found in EC populations. Only in An the level of arginine is increased when exposed to salt stress.

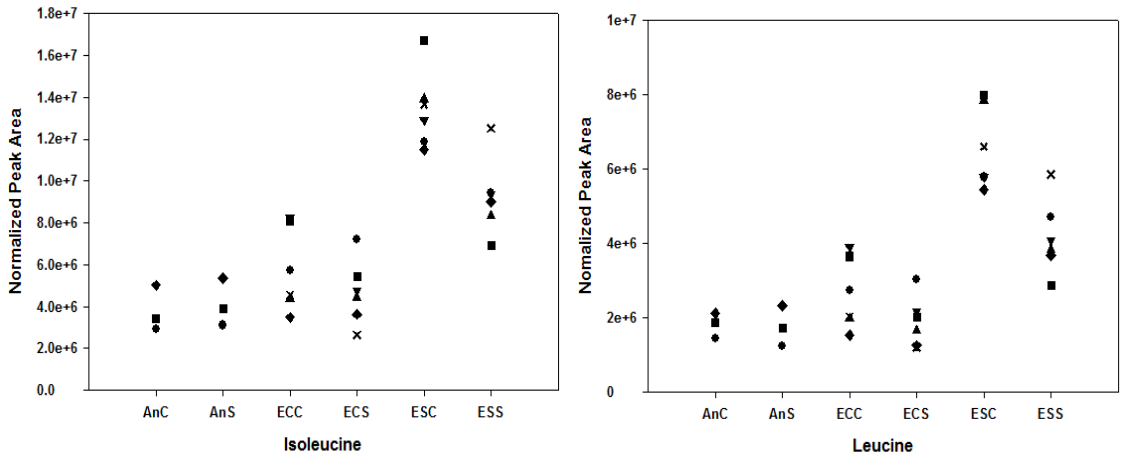

Fig. 4. 12 Amount of isoleucine and leucine in An, EC, and ES under M1TC or M1TS1 conditions

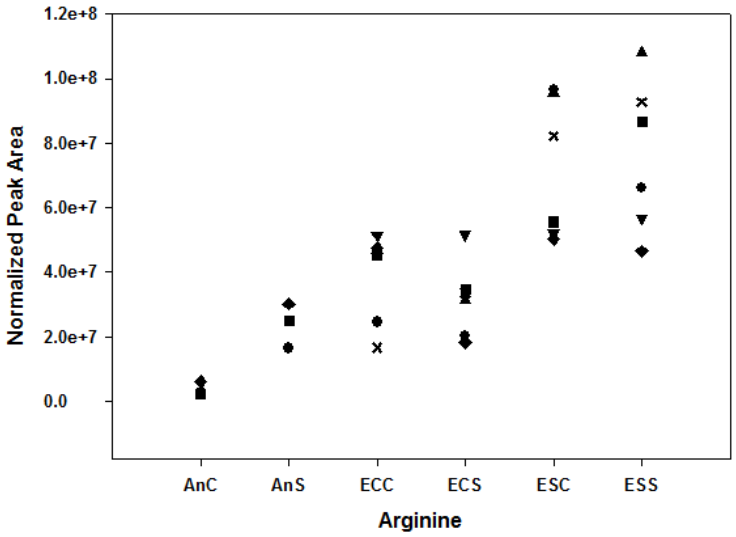

Fig. 4. 13 Amount of arginine in An, EC, and ES under M1TC or M1TS1 conditions

4.4.4 Upregulation in proline uptake/synthesis as revealed in transcriptome analysis

To investigate the potential change in gene expression regulations among evolved population versus the ancestor, particularly in the salt stress resistance mechanism, five populations, An, EC1, EC5, ES2, and ES6 were chosen for analysis of their transcriptome under M1TC or M1TS1 conditions (see materials and methods section for population selection). The transcriptome of each population under M1TS1 was compared with M1TC. Interestingly, we observed some shared trend of change in gene expression across all populations. First and foremost is the upregulation of the proline uptake/synthesis operon (Sputcn32_0081-Sputcn32_0083), encoding gamma glutamyl phosphate reductase (ProA), glutamate glutamyl kinase (ProB) and a sodium:proline symporter (PutP), respectively. ProA catalyzes the first and rate limiting step in proline synthesis, while the PutP can be activated under salt stress conditions. Among all tested populations, there was >2 fold increase in expression of both genes in this operon, suggesting the critical role of proline accumulation for salt stress tolerance. The significant upregulation of the proline synthesis/uptake genes was also consist with

the metabolite assay dataset, which showed that all the populations were accumulating proline when cultured in M1TS1. Secondly, several genes involved in flagella synthesis showed down-regulation in tested populations, which was also consist with our motility assay result showing impaired motility of these populations.

Other than these shared expression changes, there are interesting and unique changes in gene expression among the An, and the selected EC and ES populations. For example, upregulation of the potassium uptake gene *kdpA*, the transcriptional regulator *rpoE*, and a glutamate/sodium symporter is only observed in An. In the two ES populations upregulation in a hypothetical membrane protein, outer membrane porin, peptidoglycan transglycosylase, and acetolactate synthase is observed. Expression of these genes can pose critical effect on the membrane/cell wall properties, and alternate synthesis of amino acid, indicating the role of these genes for providing the salt stress tolerance observed in the ES populations. While the expression profiles of the two EC lines were more varied and does not have significant similarity.

4.4.5 SNPs developed in one thousand generation populations

Whole genome resequencing of all the populations revealed that SNP occurred in every one of the evolved populations. After quality check of the raw sequence, the SNPs were detected using a customized SNP detection pipeline developed in our laboratory. In total, 865 SNPs were detected in all evolved populations, with 757 SNPs detected in coding region and 108 SNPs detected in intergenic region. Table 4.1 summarizes the number of SNPs in each population. The EC populations had significantly more SNPs (625 total SNPs) than ES population (240 total SNPs). The

number of SNPs also varied greatly among the evolved populations. 5 of the evolved populations showed 35 or less SNPs, 4 populations showed SNPs number between 50 and 70, while 3 of the EC populations showed SNPs from 117 to as high as 178. Mutations in genes involved in DNA replication and repair may be responsible for the significantly higher number of SNPs. For example, among the 5 populations with 35 or less SNPs, only one population (ES4) has one mutation in DNA mismatch repair (mutS), while all other 4 populations did not have any such mutations. The number of SNPs involved in DNA replication/repair increased with higher number of SNP detected. EC1 had an SNP in DNA topoisomerase IV and in DNA polymerase IV, while ES3, ES5, and ES6 all have SNPs in mutS. For populations with highest numbers of SNPs, EC2 has two SNPs detected in the chromosome replication initiation protein, and one SNP in DNA polymerase III. EC4 and EC5 both have 3 SNPs in their mutS genes, along with other SNPs detected in DNA primase, DNA helicase, DNA polymerase, or chromosome replication initiation protein.

Table 4. 1 Summary of SNPs by population

Population	No. SNPs	No. SNPs in coding region	No. SNPs in intergenic region
EC1	66	56	10
EC2	117	101	16
EC3	30	28	2
EC4	131	114	17
EC5	178	156	22
EC6	14	13	1
ES1	12	12	0
ES2	23	22	1
ES3	61	53	8
ES4	35	33	2
ES5	56	50	6
ES6	53	49	3

The distribution of SNPs in the genome of evolved populations would be an interesting feature to look at, particularly those genes that showed the highest number of SNPs. Therefore, the genes with most SNPs were ranked and the result is summarized in Table 4.2. Two regulator genes, Sputcn32_1639 and Sputcn32_2580, showed the most SNPs, reaching 17 SNPs. However, the pattern the SNPs emerged was totally different. The SNP in Sputcn32_1639, encoding a DNA-binding response regulator, was only observed in EC populations and they were scattered, i.e. these SNPs were distributed across the 6 parallel EC populations rather than appear only in select EC populations. No SNPs in Sputcn32_1639 was found in ES populations, suggesting that this gene may be important for growth under salt stress. On the contrary, Sputcn32_2580, encoding a Sigma-54 interaction regulator, also found 17 total SNPs but they exist in every parallel population in both ES and EC. Similar situations were observed in gene Sputcn32_1478, encoding the cytochrome OmcA, with SNPs only found in EC populations, and genes Sputcn32_1084, Sputcn32_0771, and Sputcn32_3803, encoding aspartate aminotransferase, phosphodiesterase, and histidine kinase, respectively, with SNPs detected in all EC and ES populations.

There were a number of genes with SNPs mainly detected in ES populations and therefore may indicate their potential role in the improved salt stress tolerance in ES lines. One gene is Sputcn32_3078, encoding a histidine kinase. Among the 10 SNPs detected in this gene, 9 were scattered in ES populations and only 1 was found in EC populations. A similar result was also seen in gene Sputcn32_2835, encoding a NusA elongation factor, with 7 out of the 8 SNPs scattered in ES populations and only one in EC lines. Both genes were involved in regulation of gene expression.

Table 4. 2 Ranking of genes with most SNPs detected

Gene	No. total SNP	No. SNP in EC	No. SNP in ES	Annotation
Sputcn32_1639	17	17	0	DNA-binding response regulator
Sputcn32_2580	17	8	9	Sigma 54 interaction regulator
Sputcn32_1084	12	6	6	Aspartate aminotransferase
Sputcn32_0771	13	7	6	Phosphodiesterase
Sputcn32_3803	11	6	5	Hypothetical
Sputcn32_0350	11	8	3	Histidine kinase
Sputcn32_3078	10	1	9	Histidine kinase
Sputcn32_0016	10	6	4	Potassium transporter
Sputcn32_2835	8	1	7	NusA elongation factor
Sputcn32_1478	7	7	0	OmcA/MtrC
Upstream of Sputcn32_2747	6	6	0	Upstream of RecA

4.5 Discussion

Salinity is one of the most important environmental factors determining microbial growth and function (Nan Yan Petra Marschner, 2015; Wood, 2015). Salt stress as a result of high salinity is frequently observed in various contamination sites. With increasing recognition of potential application of environmental microbiology for pollution treatment, bioremediation and bioenergy, understanding the effect of long term salt stress on the growth and function of environmentally important microorganism is indispensable for boosting the performance and longevity of the desired process. High salinity can impose stress on bacteria through means such as osmosis, ionic strength, and also in the particular types of ions that may exceed the normal needs from the organism. Although there has been ample literature about microbial response to salt stress(Burg and Ferraris, 2008; Csonka, 1989; Sleator and Hill, 2002), very limited reports are available regarding long term salt stress effect and whether similar mechanisms were involved in short term and long term salt stress response, especially in environmental microorganisms. Therefore, in this study, we use the strategy of

experimental evolution to explore the fitness change under control and salt stress conditions of an important environmental strain, *Shewanella putrefaciens* CN-32; more importantly, to investigate the mechanisms contributing to such fitness changes.

One thousand generations of propagation under control or salt stress conditions led to significant phenotypic changes in *Shewanella putrefaciens* CN-32 populations and their salt tolerance. Not surprisingly, after consistently propagated in mild salt stress condition, ES populations showed overall significant fitness gain under salt stress compared to EC populations and An, reflected by the much higher growth rate and peak biomass. In fact, although the growth rate of ES decreased when the salinity of media increase in M1TC, M1TS1, and M1TS2 media, the peak biomass of ES populations remained at similar level, suggesting that the ES populations are more effective in converting resources in the media to biomass under salt stress. The EC populations and An showed decrease both in growth rate and peak biomass with the increased salinity. The fact that the EC lines showed higher biomass than An under salt stress is likely due to the basal level of salt (150mM sodium ion) in the M1EC media. It is worth noting that there is great variance in growth rate and peak biomass among the 6 parallel populations in both EC and ES group. Such variance decrease with increasing salinity, indicating that stress conditions can restrict the resource utilization, with less options of biological processes.

The fitness gain under salt stress was obtained at the cost of significant decrease in motility, and potentially with other tradeoffs not yet tested. All evolved populations were much less motile compared to An as revealed in motility test, under both control and salt stress conditions. Similar results were observed in another experimental

evolution study on *Desulfovibrio vulgaris* hildenborough (Zhou et al., 2013) in that two colonies isolated from one ES and one EC population also showed decreased motility compared to An under control or salt stress conditions. In this study, the motility test was conducted using the population instead of a particular colony, therefore may better represent the overall motility of each population. Nonetheless, decreased motility was a response frequently observed in microbes facing stresses. Previous studies showed that the expression of genes involved in flagella synthesis were significantly down-regulated under stress. From the perspective of surviving strategy, resource re-allocation is necessary when microbes are exposed to stress conditions. Flagella synthesis is a costly process in terms of energy and material. Flagella powered motion is also a high energy consuming process. The synthesis and functioning of flagella is very cost-ineffective, which is especially true when the bacteria is cultured in a closed system in which the stress factor (salinity) is evenly distributed, i.e. the advantage of motility to avoid harsh environment no longer exist.

Metabolite profiling has emerged as an important strategy to investigate microbial physiology under stress conditions. Similar to transcriptome analysis, metabolome change is swift and can be more specific to particular stress conditions (Jozefczuk et al., 2010). Besides, in salinity stress conditions, metabolite analysis is also important because it allows for direct investigation on many of the compatible solutes the organism uptake or synthesize, which are directly involved in salt stress tolerance. DCA analysis based on the 32 identified metabolites in An and evolved populations under M1TC and M1TS1 provided an overall scheme of the metabolite profile, clearly showing the significant impact of salinity stress level in the culture media and the

treatment level during experimental evolution on shaping the metabolite composition. The change in metabolite profile in EC and ES populations from An indicated a significant change of metabolism and response toward salt stress during the course of evolution.

The protective role of compatible solutes during salt stress has long been recognized, but detailed studies under the context of long time scale and evolution are rare. Different from the 'salt-in' strategy, accumulation of compatible solutes is a more common strategy among halo-tolerant bacteria (Roberts, 2005). The 'salt-in' strategy involves import of inorganic ions, particularly potassium or sodium, up to molar concentration level. Halophiles using this method have evolved their special set of enzymes and structural proteins that function only under such high ionic strength (Galinski, 1995). Compatible solutes, on the other hand, protect cellular process through means such as maintaining proper turgor pressure and level of electrolytes. More importantly, many of these molecules can protect macro bio-molecules, such as proteins and DNA, under conditions that lead to osmotic stress, such as high salinity and desiccation (Csonka, 1989). Some of the compatible solutes are more commonly seen during osmotic stress in various bacteria, such as glutamate, while others may be preferred only in certain phylogenetic groups of bacteria. In this study, several known compatible solutes were identified in the metabolome and interestingly, different patterns were observed. For example, the most commonly observed osmolyte glutamate showed increase in An, EC, and ES under salt stress, which was not surprising, as glutamate accumulation, along with uptake of K^+ and efflux of Na^+, were documented as early responses to salt stress in many microbes, including *Shewanella* (Fu et al.,

2014; Galinski, 1995; McLaggan et al., 1994). However, the extent of glutamate accumulation varied, with ES lines showed the least increase, suggesting that glutamate may not play as important role in ES lines compared to An or EC lines when facing salt stress and that ES lines may use other osmolytes to ensure cell growth and propagation. Since glutamate plays critical role both in biological processes and in serving as the basal material for numerous biosynthesis pathways, it is possible that ES populations did not rely as heavily on glutamate for salt stress resistance.

Compared with glutamate, it was more likely that proline and ectoine may play more important role in salt stress response in ES populations. Proline and ectoine are two osmolytes long recognized. Both compounds increased in An, EC, and ES populations when facing salt stress but the magnitude is very different. The increase in ES populations was much higher compared to An and EC, indicating not only that these two compatible solutes may play critical role in maintaining cell function under salt stress in *Shewanella putrefaciens* CN-32, but also that the high level of proline and ectoine may be the strategy that the ES lines developed during the long term salt stress they have been exposed to. The protective role of proline under salt stress is documented in various prokaryotes (Brill et al., 2011; Csonka and Hanson, 1991; Kempf and Bremer, 1998), with the recognition that it can help stabilize protein and promote correct folding of protein under conditions that are not favored (Perez-Arellano et al., 2010a; Perez-Arellano et al., 2010b). However, direct evidence of proline accumulation under salt stress in *Shewanella* is lacking, although previous studies on time-course transcriptome response of *Shewanella algae* reported significant and sustained upregulation of glutamate-5-semialdehyde dehydrogenase and glutamate 5-

kinase (Fu et al., 2014). Enhanced expression of the operon involved in proline synthesis and uptake across An and the selected EC, and ES populations was consistent with the metabolite result, suggesting proline accumulation is a shared strategy in CN-32. However, it is puzzling as how ES populations can reach a proline pool around 3 times of An or EC under the same condition. No significant difference is observed on the expression level of the proline uptake/synthesis operon between the An and the ES population, therefore it is highly unlikely that the different level of proline is due to regulation at transcription level, or at least not through regulation of this particular operon. As previously reported, proline synthesis is often self-regulated via a negative feedback mechanism, typically by binding of proline to the glutamate kinase (Perez-Arellano et al., 2010a). It could either be that the ES populations were evolved to circumvent such negative feedback or that the level of proline in ES lines under salt stress is still not high enough to trigger the negative feedback.

The role of ectoine and its immediately related compound, such as hydroxyectoine and Nγ-acetyldiaminobutyric acid (NADA) for providing bacteria salt tolerance has been well documented, especially in various halophilic bacteria (Galinski et al., 1985). Bacteria capable of synthesis and accumulation of ectoine are more advantageous when competing with counterparts that cannot synthesize ectoine under osmotic stresss conditions (Pflughoeft et al., 2003). Ectoine are reported to protect cell under thermal stress by stabilizing proteins and change DNA conformation to avoid being cleaved by endonuclease (Canovas et al., 1999; Malin et al., 1999). The synthesis of ectoine is realized via the *ectABC* genes in various halophilic bacteria and *Bacillus* species(Kuhlmann and Bremer, 2002; Louis and Galinski, 1997). However, *de novo*

synthesis of ectoine in *Shewanella* has not been reported. Protein sequence comparison by BLAST suggested low likelihood of *ectA* or ectC homologues in *Shewanella*. However, BLAST result suggested that there is likely an *ectB* homologue may be present (e.g. SO_1276, with an *ectB* domain). However, SO_1276 is arranged in the operon SO_1274-SO_1276, annotated as *puuBCE* for degradation of putrescine. Nonetheless, our metabolite data suggested that CN-32 can synthesize ectoine under salt stress conditions. It is also possible that *Shewanella* may use different machinery for ectoine synthesis.

Various mutations were discovered across the evolved populations, which were expected from the 1 thousand generation evolutionary course. The fact that EC populations showed two times higher SNPs than ES populations suggest that the effect of salt stress may impose a selection effect, which may have led to wiping out of mutations that lead to immediate negative fitness effect among the population. Among genes that show the most SNPs, Sputcn32_1639 showed 17 mutations in EC populations, but none in ES populations, suggesting that this gene may play important role in salt tolerance response. Sputcn32_1639 encodes a transcription regulator protein belonging to a two-component system, with a REC signal receiving domain and HTH DNA binding domain. Gene Sputcn32_3078 and Sputcn32_2835 showed 9 and 8 SNPs, respectively, in ES populations but only 1 in EC populations, indicating that these mutations may actually contributing to salt tolerance in ES populations. Sputcn32_3078 encodes osmosensitive potassium channel signal transduction histidine kinase KdpD, belonging to the potassium transport two-component system. Sputcn32_2835 encodes NusA family transcription elongation/termination/anti-termination factor, which is

involved in the elongation and termination stage during transcription. Increased *nusA* expression has been reported in *Shewanella oneidensis* MR-1 under cold stress conditions (Gao et al., 2006c). More recently, the role of NusA in DNA repair has been recognized, including recruitment of translesion synthesis DNA polymerase and transcription coupled repair(Cohen et al., 2009). Therefore, it is possible that the mutations observed in *nusA* can change the RNAP binding capability of NusA, altering the extension and/or termination process during transcription. It is also possible that these mutations can promote the DNA damage repair function of NusA, thereby enhancing the salt tolerance of the ES populations.

How to maintain proper osmotic pressure is one of the fundamental processes in bacterial growth. In this study we showed the influence of 1 thousand generation of propagation under control or salt stress led to distinctive phenotypical and molecular level changes of *Shewanella putrefaciens* CN-32. Unique metabolome profiles formed based on culture condition and evolution condition. Two compatible solutes proline and ectoine showed much higher level of increase in the ES populations under salt stress condition, suggesting the importance of these osmolytes during long term salt stress conditions. The unique SNPs detected in the evolved populations provided important candidates for further elucidating their roles in salt stress tolerance. In conclusion, the overall phenotypical differences observed in the evolved populations, especially the enhanced salt tolerance in ES populations, reflects the fundamental changes in the metabolism, regulation, and genome DNA sequence during the course of evolution.

Chapter 5: Enhanced performance of *Shewanella* based bioanodes with incorporation of PVP-Os redox polymer

5.1 Abstract

Microbial Fuel Cells (MFCs) have great potential for both pollution treatment and as an environmental friendly sustainable energy source. However, the current generation and power output of concurrent MFCs are generally low. Proper engineering of bioanode is critical for boosting MFC performance. Redox polymers were known to enhance electron communication between enzymes and electrodes in various biofuel cells, but their application is MFCs is rare. In this study, the potential application of several strains of *Shewanella* as bioanode with the incorporation of PVP-Os redox polymer was evaluated using 3-electrode system with potentionstat. The result showed that among the several strains of *Shewanella*, *S. putrefaciens* W3-18-1 was the superior bioanode catalyst in terms of current generation and the maximum current density of 14.17μA/cm² was produced. PVP-Os coated electrodes showed significant increase of current density among all strains tested, varying from 2.4 fold to 6.6 fold. The effect of PVP-Os loading on current generation was evaluated in the range of 9.33 μg to 111.96 ug. The result showed that the polymer loading had no significant effect on current generation in the range tested, likely due to the nature of the electron transfer in redox polymers. Several different bacterial/PVP-Os incorporation methods were compared, including coating glassy carbon electrodes with PVP-Os and inject bacteria in bulk media; coating PVP-Os on electrode surface and then put a layer of bacteria cell on top of the PVP-Os layer; and coat the electrode surface with a mixture of PVP-Os and bacterial cell. The results showed that direct coating of PVP-Os on electrode surface

and inject bacteria into bulk media was the best in terms of current generation. Lastly, a layer by layer method of incorporation of bacteria and PVP-Os was applied using gold electrode, which showed 70% increase in maximum current density, suggesting a more efficient electron transfer network in this setup. However, increasing the bacteria/PVP-Os layer number does not further boost the current generation. This study provides useful insights into the boosting effect of the PVP-Os polymer for *Shewanella* based bioanodes, shedding important hints regarding the application of redox polymers on MFC systems.

Keywords: *Shewanella*; microibal fuel cell; bioanode; redox polymer; PVP-Os; amperometric curve; cyclic voltammetry;

5.2 Introduction

In the past few decades, biofuel cells have emerged as a promising strategy for sustainable energy, waste water treatment, and sensors for monitoring environmental changes (Ellen Dannys, 2015; Shantaram et al., 2005). Based on the actual catalyst in the system, the numerous types of biofuel cells can be divided into enzymatic biofuel cells (EBFCs) and Microbial biofuel cells (MFCs) (Davis and Higson, 2007; Du et al., 2007; Rimboud et al., 2014). In EBFCs, a chosen enzyme (or series of enzymes) is employed in the system to catalyze the electrochemical reaction, producing electricity (Willner et al., 2009). Whereas in MFCs, live microbial cells of a pure culture or mixed culture are used instead of enzymes (Du et al., 2007). Biofuel cell performance is typically evaluated by several parameters, such as power output, cell potential, current generation and stability. The anode performance is critical for the overall functioning of EBFCs or MFCs. Because of the high turnover rate and specificity of the enzymes, EBFCs generally have higher power density output and do not require a semi-permeable membrane to separate the anode from the cathode (Ramanavicius et al., 2008). However, the advantage of using live microbial cells as the anode catalyst lies in that they can produce the enzymes needed to fully oxidize the substrate, thereby capturing all of the potential electrons. In addition, microbe based bioanodes can provide better stability due to the greater resilience of live cells to environmental fluctuations, which is important for mid-term or long term in-situ environmental applications (Quek et al., 2015).

Low efficiency of electron communication between the microbes and an electrode's surface has been regarded as one of the key issues limiting current

generation in bioanodes. Currently, there are two major mechanisms that have been widely recognized for this process, direct electron transfer (DET) and mediated electron transfer (MET). In DET, electrons released from substrate oxidation are directly transported from the microbes to electrode, while a mediator is used to shuttle the electron to electrode in MET (Schroder, 2007). Several strategies have been developed to facilitate the electron transport between bacteria and the electrode, such as adding freely diffusing mediators in the buffer system (Park and Zeikus, 2000), modification of electrode surface with redox polymers (Hasan et al., 2013), and modification of electrode surface with conductive materials such as carbon nanotubes and conductive polymers (Hasan et al., 2013; Hung-Yin Tsaia, 2009).

The advantage of redox polymers lies in the fact that their redox potentials can be modified by design of the polymer, which allows one to obtain desired potential on the electrode. In addition, the electron transfer in redox polymers is highly efficient, leading to higher current or power density. The polymers can also form a network with crosslinkers to immobilize microbial cells (Coman et al., 2009). To date, several redox polymers and microbes have been applied in various MFCs. Osmium based polymers were the most frequently used redox polymers and have been investigated in various bacteria, such as *Bacillus subtilis* (Coman et al., 2009), *Pseudonomas fluorescen* (Timur et al., 2007)s, and *Shewanella oneidensis* (Patil et al., 2012). It has been reported that osmium based polymers could improve the current density and power density of MFCs up to 2355mW/m^2 in some cases (Yuan et al., 2016). However, a detailed and systematic study of factors that affect bioanode systems with Osmium based redox polymer is lacking.

In addition to the redox polymer, the type of bacteria is another key component in MFC as they harness the electrons from substrate and pass them onto electrodes. However, electron transfer from a live cell to the electrode is more complicated compared to those in an enzymatic redox reaction, since the electrons released via substrate oxidation needs to make their way across the cell's membrane to the electrode surface. In most bacteria, this is a difficult process as they do not have the machinery for DET. As a result, mediators are typically needed to shuttle the electrons to the electrode (MET) (Liu and Logan, 2004). Some bacteria can produce mediators themselves, while others need supplemented mediators for the cell to function in an MFC. The dissimilatory metal reducing bacteria *Shewanella* are unique because they possess both DET and MET mechanisms, which are very rare in microorganisms. For DET, these microbes produce numerous multi-heme outer membrane cytochromes and conductive pili to pass electron directly to electrode (Kouzuma et al., 2015). For MET, they are known to produce mediators such as flavins to shuttle electrons (Newton et al., 2009). Because of these, members of *Shewanella* are regarded as exo-electrogen and have been used as model organisms for mechanism study and MFC applications (Bretschger et al., 2007; Fredrickson et al., 2008; Qian et al., 2009; Wu et al., 2014).

In this study, we systematically studied the performance of *Shewanella* based bioanodes using an Osmium based -Osredox polymer poly[(vinylpyridine)Os(bipyridyl)$_2$Cl]$^{2+/3+}$ (PVP-Os). The effect of *Shewanella* strain, polymer loading and polymer/bacteria incorporation methods were studied.

5.3 Materials and Methods

All bacterial culture, experimental setup, electrochemical cell tests and electrochemical analysis were performed in Dr. David Schmidtke's lab in the Biomedical Device Department, University of Texas at Dallas. Reagents used in this experiment were purchased from Sigma Aldridge and Fisher Scientific and used without further purification. The PVP-Os polymer used in this paper was provided by our collaborator Dr. Glathofer's group in Department of Biochemistry at the University of Oklahoma.

5.3.1 Bacterial strains and culture condition

The four *Shewanella* strains, namely *Shewanella putrefaciens* CN-32 and W3-18-1, *Shewanella oneidensis* MR-1, and *Shewanella loihica* PV-4, were lab stocks provided by Dr. Jizhong Zhou in University of Oklahoma. The bacteria were revived from frozen stock in Luria Broth (LB) overnight and then inoculated into 200 ml of LB medium with shaking at 200 rpm at room temperature. The bacterial cells were collected by centrifuge at 4500 rpm for 10 minutes after the optical density reached OD_{600} 0.6~0.8. The cells were then washed twice in M1 buffer (1.5g/l Ammonium Chloride, 0.01g/L Potassium Chloride, 0.0952g/L Magnesium Chloride, 0.022g/L Calcium Chloride, 0.6g/L Sodium Phosphate Monobasic, 17.316g/L Sodium PIPES, vitamin solution and trace minerals solution), centrifuged again, and finally resuspended into 8ml of M1 buffer before injecting into the electrochemical cell.

5.3.2 Electrochemical cell setup

The electrochemical cells used in this study were 5-neck bottles (ACE Hardware). The electrodes were connected to a CH Instrument potentionstat (Model 1010C) using the 3 electrode setup (one working electrode (Glassy Carbon Electrode, GCE, CH Instruments), one reference electrode (Standard Calomel Electrode, CH Instruments), and one platinum counter electrode (CH Instruments). Each bottle allows for testing of two working electrodes simultaneously. Each electrochemical cell was filled with 150 ml of M1 defined medium and flushed with medical grade nitrogen gas for 15 minutes after the cell was assembled. Then, an equal volume of resuspended bacterial cell solution was introduced either by direct injection into each chamber, or by coating onto the electrode surface. After the appropriate electrochemical potential was applied, 8 ml of a 1 M Sodium Lactate stock solution was injected into the medium for a final lactate concentration of 50 mM.

5.3.3 Glassy Carbon Electrode preparation

The working electrodes used were either glassy carbon electrodes (GCE) with a working area of 0.07 cm^2, or gold electrodes (GE) with a working area of 0.031 cm^2 (CH Instruments). GCEs were serially polished with 1 μm, 0.3 μm and 0.05 μm alumina polishing solutions (Buehler Inc.), sterilized with ethanol, cleaned with sterile water and allowed to dry. Stock solution of PVP-Os was prepared at a concentration of 10 mg/ml. To investigate the effect of bacterial strain type and the effect of polymer loading, the PVP-Os solutions were mixed with poly(ethylene glycol) 400 diglycidyl ether crosslinker solution at a volume ratio of 14:1. Designated amounts of the as-

prepared PVP-Os-crosslinker solution were then dropped onto the surface of the GCE and allowed to dry and crosslink overnight before putting in the electrochemical cell for testing.

5.3.4 Gold Electrode preparation

GEs were also polished serially with 1um, 0.3um diamond paste (Buehler Inc.) and finally in 0.05 um alumina polishing reagent. A layer-by-layer technique based on electrostatic interaction among the positively charged PVP-Os and the negatively charged 11-mercatoundecanoic acid (MUA) or poly-glutamic acid (PGA) was used for immobilizing PVP-Os/bacteria onto the electrode surface. Preparation of the bacterial culture was conducted as previously described, except that the final bacterial suspension was adjusted to OD_{600} of 0.45. The PVP-Os/bacteria mixture was prepared by mixing 10 mg/ml PVP-Os with an equal volume of the bacterial suspension. Briefly, the polished GEs were first immersed in 5 mM 11-Mercaptoundecanoic acid (MUA) solution for 20 minutes to create a negatively charged surface as the basis for building multiple polymer layers. After brief washing, the GEs were added into 5 mg/ml PVP-Os/bacteria solution for 10 minutes, washed and immersed into 2.58mg/ml PGA solution for 10 minutes. This PVP-Os/PGA coating process is repeated to accumulate desired number of PVP-Os layers onto the electrode surface.

5.3.5 Electrochemical analysis

Cyclic voltammetry (CV) and amperometric curves were conducted to characterize the working electrodes. CVs were conducted before and after injection of bacteria cells. All

working electrodes were poised at 0.4V vs. a Saturated Calomel Electrode (SCE) during amperometric test. CVs were also taken immediately after amperometric test at a scan rate of 10 mv unless noted otherwise. All cells were purged with medical grade nitrogen throughout the experiments. No stirring was performed throughout all electrochemical measurements.

5.4 Results

5.4.1 Comparison of current generation among four Shewanella strains.

Shown in Fig. 5.1 is a schematic of the electrochemical cell set up for testing the effect of different *Shewanella* strains and coating GCE with PVP-Os on current generation. The chemical structure of the PVP-Os polymer is also illustrated. In this method, 3 µl of the crosslinked PVP-Os was coated on top of GCE and allowed to dry to form a layer of PVP-Os coating on top of the electrode. This electrode was then put into the electrochemical cell containing M1 bulk medium. Different bacteria strain was injected into the medium. After poising started and injection of electron donor (lactate), electrons were transferred from the bacteria cells onto the surface of electrode during respiration, and electricity was produced. This method will be referred to as the Suspension Method (SM) hereafter.

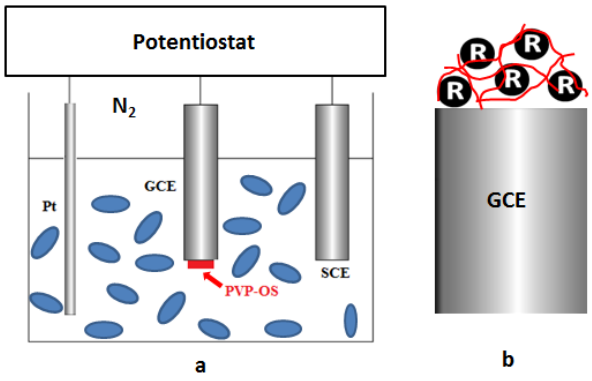

Fig. 5. 1 Schematic of *Shewanella* bioanodes with redox polymer PVP-Os(a, overall schematic of the electrochemical cell setup; b, enlarged schematic of the GCE surface modified with a layer of PVP-Os, red lines represent the backbone of the polymer, R in black circles represent redox centers, blue oval represent bacterial cell.

To determine how different *Shewanella* strains affect the amount of current produced, we tested 4 different strains: Fig. 5.2 shows the representative amperometric curves for each of the four strains obtained with bare GCEs and GCEs coated with a crosslinked PVP-Os redox polymer film. Shortly after injection of lactate, the current at both the PVP-Os coated and bare GCEs gradually increased, reached a maximum and then decreased for all four strains. As hypothesized, the current generated by all four bacteria cultures was significantly higher on the PVP-Os coated GCEs than on bare electrodes. For three of the *Shewanella* strains the maximum current density was reached earlier on the bare electrode compared to the PVP-Os coated electrodes, while with the W3-18-1 strain the maximum current densities were reached at about the same time (Table 1). Different rate of biofilm formation for the different strains at the redox polymer coated electrode might help explain the quite different response times.

Table 5. 1 Typical incubation time for the four strains to reach maximum current density (hour)

strain	Bare GCE	PVP-Os coated GCE
S. putrefaciens W3-18-1	30	25
S. oneidensis MR-1	18	28
S. loihica PV-4	7	35
S. putrefaciens CN-32	40	80

Fig. 5.3 shows the average maximum current densities measured with the PVP-Os coated GCEs and bare GCEs. For bare GCEs, the maximum current densities were fairly low, ranging from 1.59μA/cm^2 for CN-32 to 3.97μA/cm^2 for W3-18-1. In contrast, the maximum current density response for the PVP-Os coated GCEs ranged from 8.1 to 14.2μA/cm^2, which was 2 – 3.6 times greater than the bare GCEs. The increased current response with the PVP-Os coated GCEs for all four strains were statistically significant ($p<0.01$). In fact, all strains showed at least two-fold increase in maximum current density for PVP-Os coated GCEs, indicating that the PVP-Os coated electrode surface might be more favorable for *Shewanella* to pass electrons under the tested conditions. The results also showed that strain W3-18-1 was a more favorable bioanode candidate for generating anodic current. Because of this, strain W3-18-1 was chosen for all the remaining experiments.

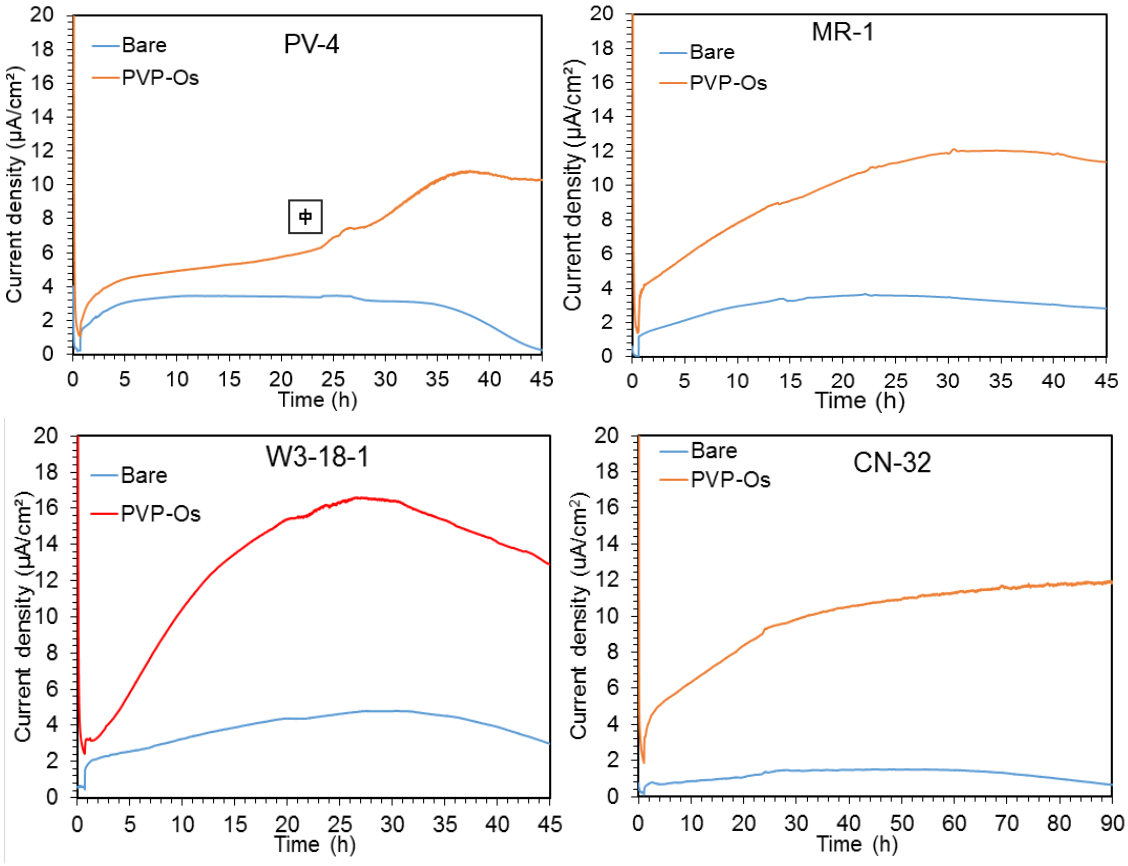

Fig. 5. 2 Representative amperometric curve of the four Shewanella strains.

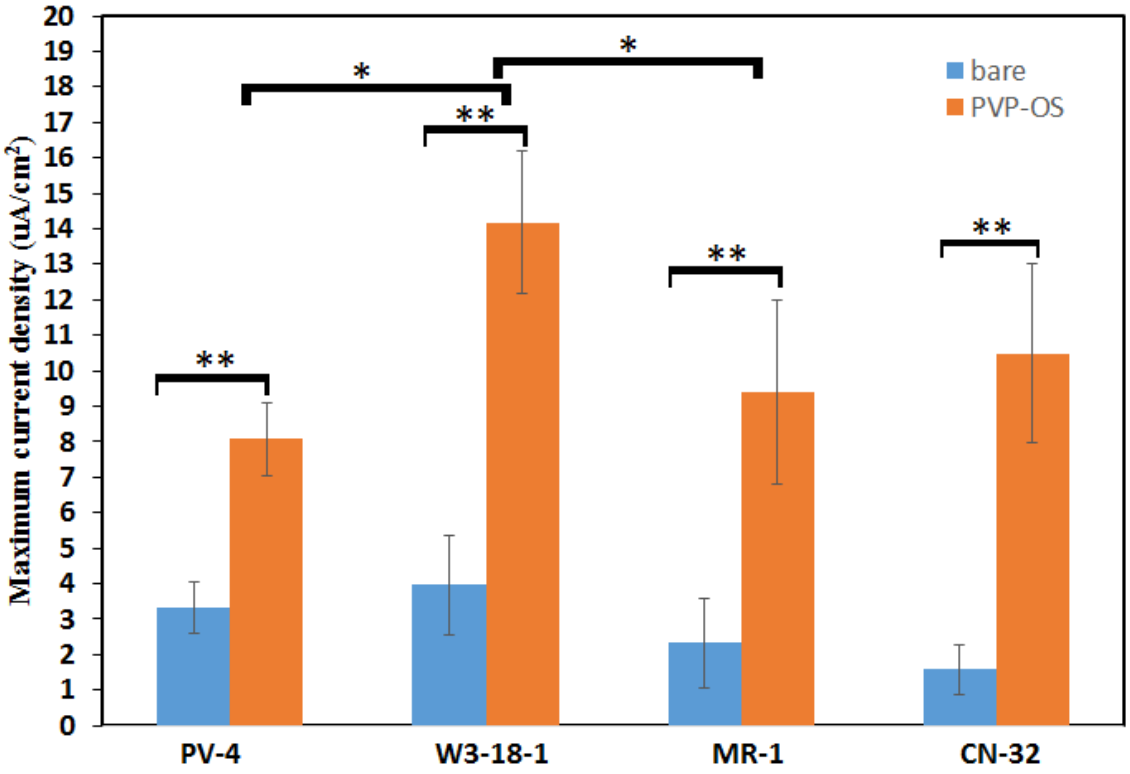

Fig. 5. 3 Maximum current density of four Shewanella strains with bare GCE or PVP-Os coated GCEs (* $p<0.05$; ** $p<0.01$) Maximum current density of four *Shewanella* strains with bare GCE or PVP-Os coated GCEs (* $p<0.05$; ** $p<0.01$)

The representative CV curves of each strain on bare GCEs or PVP-Os coated GCEs were shown in Fig. 5.4. In fact, all strains showed similar pattern of current generation and CV curves. The CV curves of these strains on bare electrode showed a typical asymmetric peaking pattern emerged at potentials of around -0.34 V and -0.07 V, which were similar to previous reports. However, the CV curves of PVP-Os coated electrodes did not show much change. The redox potentials remained the same, only peak current showed slight decrease after incubation.

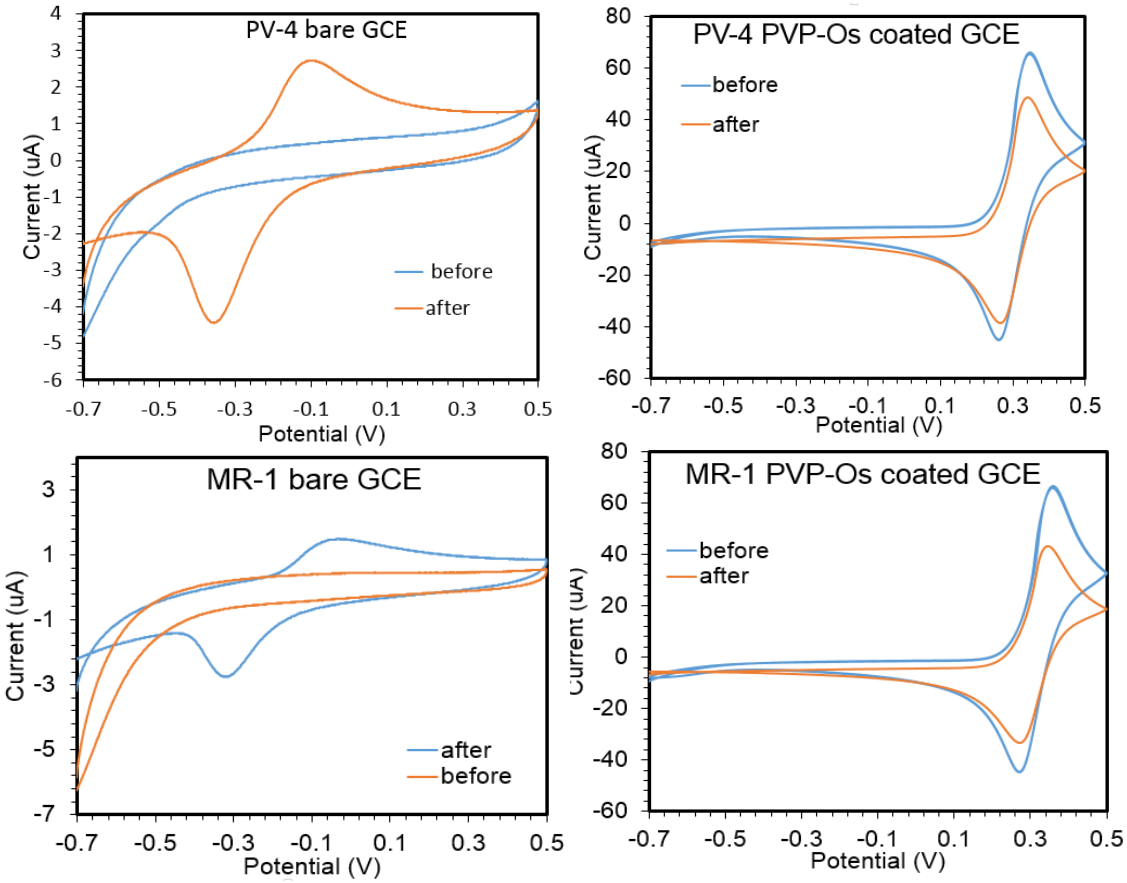
PV-4 bare GCE
Current (uA)
Potential (V)
before
after
PV-4 PVP-Os coated GCE
Current (uA)
Potential (V)
before
after
MR-1 bare GCE
Current (uA)
Potential (V)
after
before
MR-1 PVP-Os coated GCE
Current (uA)
Potential (V)
before
after

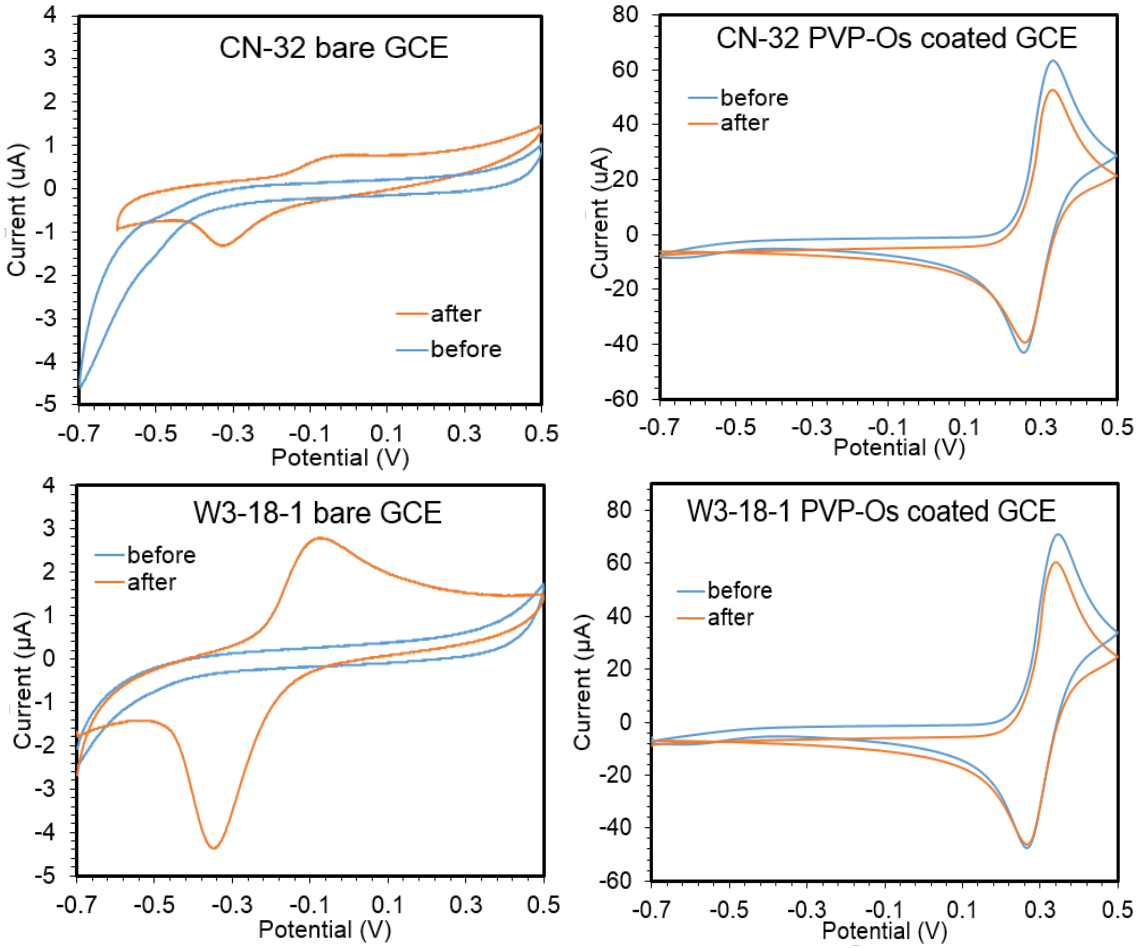

Fig. 5. 4 Representative CV curves of the four *Shewanella* strains on bare GCE or PVP-Os coated

5.4.2 Effect of Polymer loading on current generation of W3-18-1

Because of the fact that PVP-Os coating can efficiently boost maximum current generation, it is valuable to ask whether changing the loading (i.e. the mass) of PVP-Os on the electrode surface will affect current generation. To test this, we prepared GCEs modified with different amount of PVP-Os and the performances were evaluated in W3-18-1. In this experiment, the four loading levels tested were tested 9.33µg, 27.99µg, 55.98µg, and 111.96µg. The maximum current densities were summarized in Fig. 5.5. To our surprise, the result showed that there was no statistically significant difference among the 4 loading levels, although the mean maximum current density of 27.99µg

loading was higher than the other loadings. The CV results showed that there is a significant boost of peak current when polymer loading increased from 9.33µg to 27.99µg, with the peak current increasing from ~20µA to ~65 µA. However, the peak current stayed at similar level when the loading was further increased to 55.98 or 111.96µg. Besides, the increase of peak current of 27.99µg loading did not translate into statistically significant increase in maximum current density from bioanode compared with 9.33µg loading, although the mean value was higher.

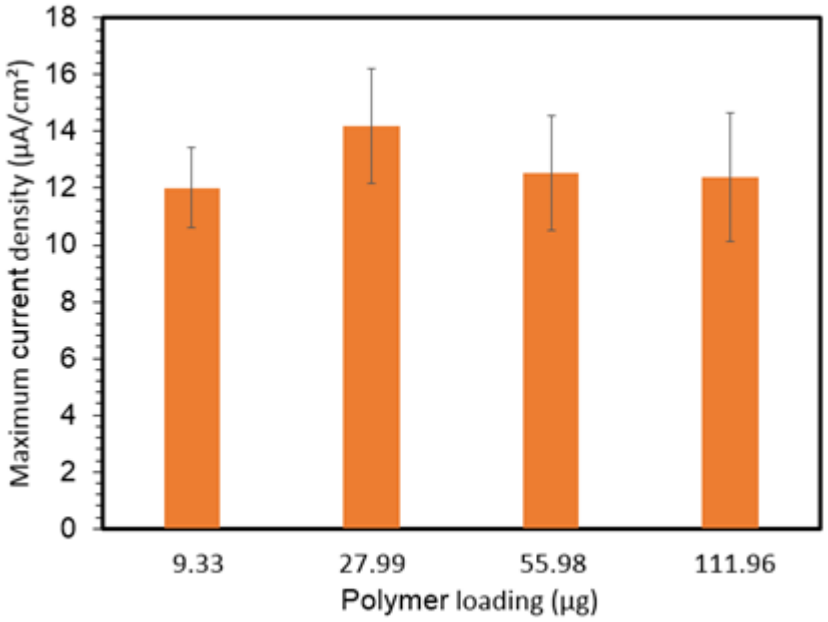

Fig. 5. 5 Effect of polymer loading on current production of W3-18-1

5.4.3 Effect of bacteria/polymer incorporation on bioanode performance

How bacteria cell is incorporated onto electrode surface may significantly affect the anode performance. Therefore, we also evaluated two different methods to introduce W3-18-1 onto GCE with PVP-Os. Fig. 5.6 illustrates the setup of the two different methods. In the Lay-Over Method (LOM), 2 µl of concentrated bacterial suspension was deposited on top of a GCE with a pre-dried PVP-Os layer and allowed to dry for 20

minutes. In the Mix and Cast Method (MCM) the 2 µl bacteria solution was first well-mixed with 3 µl of PVP-Os solution, and then 5µl mixture was coated a clean bare GCE. For both methods, growth of bacteria in the bulk medium was minimal as the liquid remained clear by the time the amperometric test was complete. The result indicated that the LOM produced significantly higher maximum current density (6.74 ± 1.38µA/cm^2) than MCM (2.13 ± 0.87µA/cm^2). However, both values were significantly lower compared with the SM (14.18µA/cm^2), in which bacteria were injected into the bulk media rather than coated on the surface. As shown in Fig. 5.7, the CVs of the two methods also differed greatly. The CV pattern of the LOM was very similar to SM before and after incubation, with redox potentials remained the same and only minor decrease in peak current after incubation. For electrodes prepared by MCM, the CV before incubation showed a major redox pair typical of PVP-Os, but the magnitude of peak current was about 10 times lower than LOM even though the amount of PVP-Os coated was the same. A minor redox pair was also observed at -0.1V/0V. After incubation, the PVP-Os redox pair decreased, while a new peak appeared at ~ -0.3V.

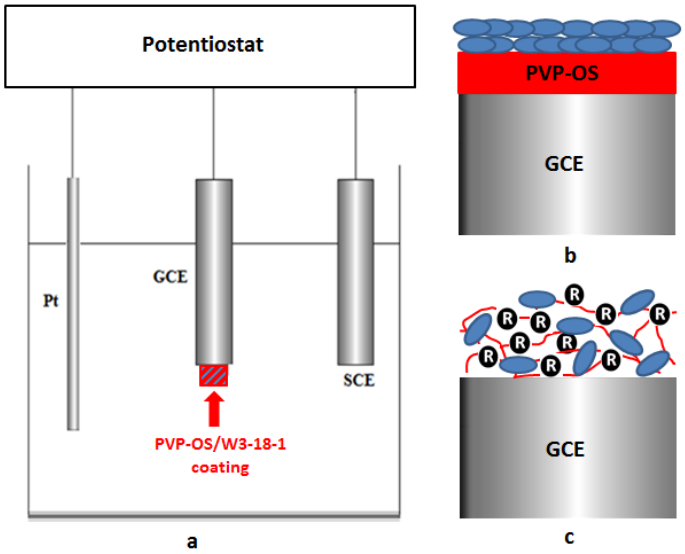

Fig. 5. 6 Schematic of LOM and MCM (a, the overall electrochemical cell set up. No bacteria is introduced into the bulk media; b, enlarged schematic of GCE modified by LOM, in which the GCE is first coated with PVP-Os, allowed to dry, and then coated with W3-18-1 suspension; c enlarged schematic of GCE modified by MCM, in which the W3-18-1 cells were first mixed with PVP-Os and then the mixture is cast onto GCE and allowed to dry. The blue ovals represent W3-18-1 cells)

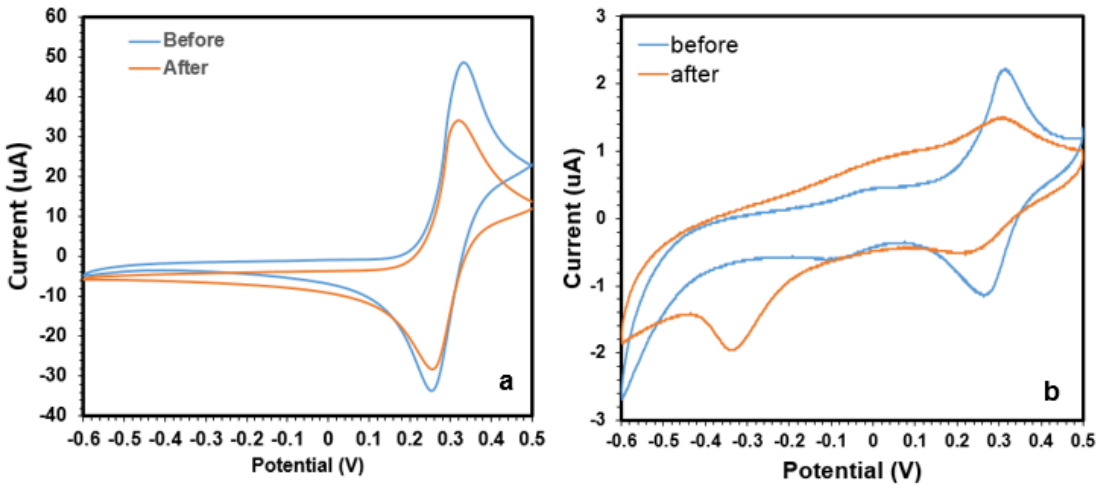

Fig. 5. 7 CV curves before and after incubation for LO method (left) or MCM method (right)

5.4.4 Performance of GE based W3-18-1 bioanode using LBL method

Gold electrodes (GEs) were widely used in biosensors and EBFCs because of their biocompatibility. However, for MFC applications, GEs were reported to interact

poorly with *Shewanella* (Kane et al., 2013). In this study, we tried to see if modifying the surface of GEs using the Layer by Layer (LBL) method by MUA and PVP-Os will enhance the anode current generation, as illustrated in Fig. 5.8. In this method, bacteria cells were mixed with PVP-Os before coated onto GE. The effect of the number of PVP-Os/W3-18-1 layer on current generation performance was also evaluated. As shown in Fig. 5.9, the maximum current density of these gold electrodes using the LBL method was significantly higher than GCEs, reaching 24μA/cm², which was a ~71% increase compared to the highest value obtained in SM method. Besides, our result also showed that the number of PVP-Os/W3-18-1 layers did not affect the maximum current density, with 1, 3, 5, or 7 layers showing non-statistically significant difference. A typical amperometric curve of these electrodes was shown in Fig. 5.10 (c). Noticeably, these electrodes took much longer duration (more than 72 hours) to reach maximum current density compared with GCEs with bacteria in suspension.

The representative CV curves and amperometric curve of the GEs coated with LBL method before and after incubation were shown in Fig. 5.10 (3 PVP-Os layers, with or without W3-18-1). In the abiotic control, where no bacteria were introduced, current generation was negligible (10^{-10}A level). The redox potentials did not change after incubation, with only minor decrease in peak current. In contrast, when W3-18-1 was incorporated, current slowly increased in the first 2 days, gradually increased in days 3 and 4, increased rapidly after 120 hours and reached peak at ~24μA/cm² and fell back. Interestingly, the CV curve showed significant changes after incubation. One major oxidative peak remained at the potential of 0.27V, but the peak current increased from 0.3μA before incubation to 0.73μA during the first cycle and 0.54μA in the

second cycle. The original reductive peak at ~0.25V shifted to ~0.1V. Besides, a strong reductive peak emerged at -0.36V. A minor oxidative peak can be observed at ~0.2V. The changes in the redox peaks indicated a shift of surface electrochemistry property, possibly due to the growth and functioning of bacteria.

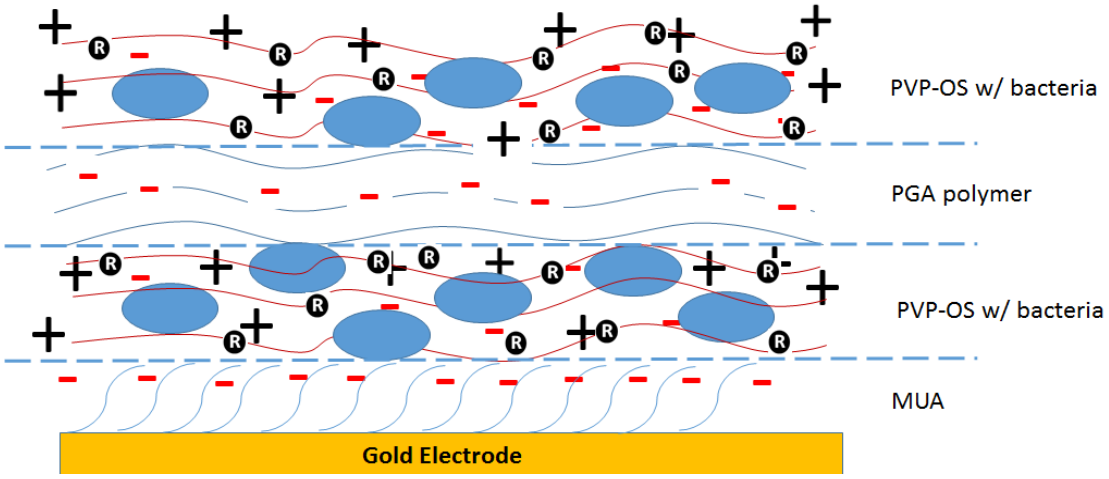

Fig. 5. 8 Schematic for incorporation of W3-18-1 onto GE via LBL method. Blue ovals represent W3-18-1 cells. MUA forms the basal level and provides a negatively charged surface. The positively charged PVP-Os binds to bacteria cell and MUA via electrostatic interaction. The negatively charged PGA polymer is introduced in between PVP-OS/W3-18-1 layers for introducing more positively charged layers. No bacteria cells were supplied in the bulk media.

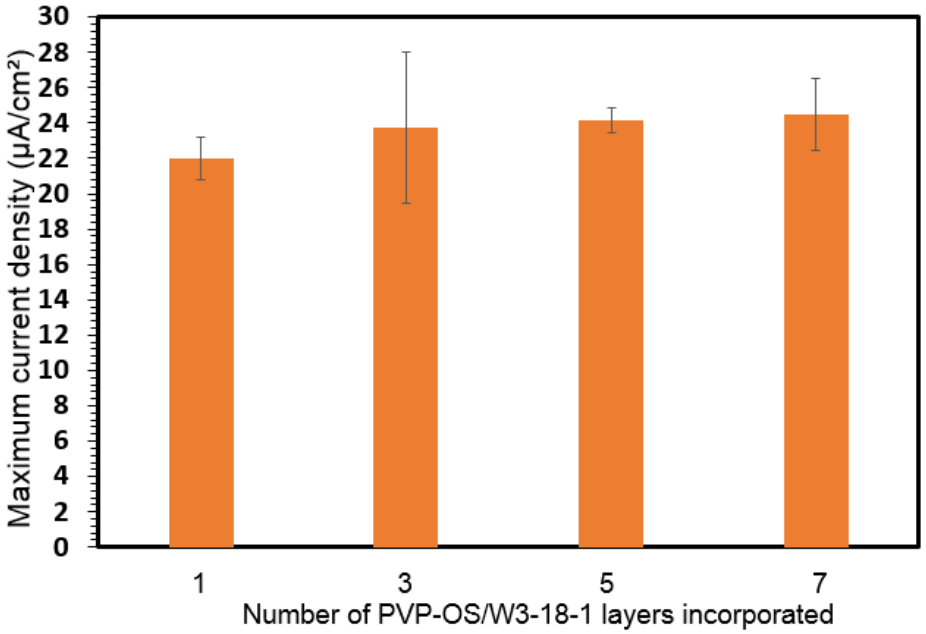

Fig. 5. 9 Maximum current density of gold electrodes with W3-18-1 incorporated via layer by layer method.

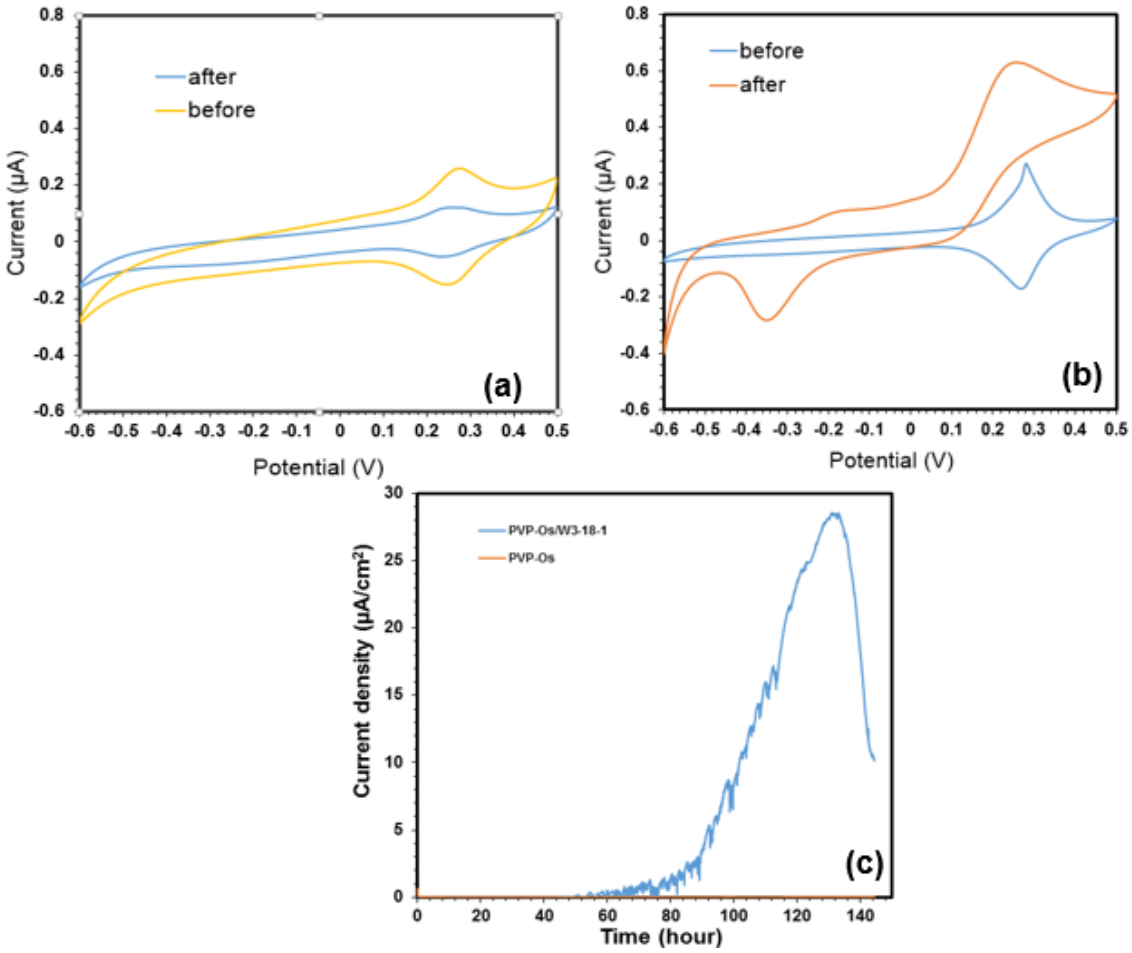

Fig. 5. 10 Amperometric (c) and CV curves before and after incubation for GE with PVP-Os (a) or GE with PVP-Os/W3-18-1 (b)

5.6 Discussion

Bacteria in the *Shewanella* genus are among the very few microbes that can transport electrons across the cell membrane and to extracellular electron acceptors during respiration, including solid materials such as metal oxides and electrode. The potential of using *Shewanella* as bioanode for current generation in MFCs has been widely investigated (Biffinger et al., 2011; Patil et al., 2012; Wu et al., 2013) . Various methods have been developed to facilitate electron transfer, in order to improve current production and power output. In this study, we focused on investigating the effect of

modifying electrode surface with redox polymer PVP-Os for *Shewanella* based bioanodes. Strain W3-18-1 showed the highest maximum current density among the four strains with unmodified GCEs, which was in consistence with previous observations (Bretschger et al., 2010). The result showed that the current generation was significantly improved upon modification with PVP-Os polymer. For PVP-Os coated GCEs, strain W3-18-1 again showed the best performance. The maximum peak current density (14.18μA/cm^2) reported in our study may be lower than some of the previous publications using a slightly different redox polymer (Patil et al., 2012). However, a critical factor that may have contributed to the difference other than the type of polymer used in experiment is the actual surface, which is a critical parameter when calculating current density. The serial polishing of electrodes in 1um, 0.3 μm and 0.05 μm polishing reagent in this study not only resulted in a fine and smooth surface but also ensured complete removal of any previously coated materials, increasing the reproducibility of the experiment. In contrast, polishing GCEs with coarse material such as emery paper would lead to significantly increased surface area. Our calculation may better reflect the true current density by minimizing the potential area difference compared to polishing with coarse material. In the future, we can potentially boost the current density by switching electrode type or use other methods to create larger surface area.

CV is an important technique to capture the electrochemistry behavior of the electrode surface, thereby providing useful information for interpreting the redox process occurred. The ~-0.34V to ~-0.07V asymmetrical redox peaking pattern from our bare GCEs after incubation indicated irreversible electron transfer, which was

typical indication of functioning outer membrane cytochromes of *Shewanella* strains for direct electron transfer from the cells to the electrode (Kim et al., 1999). For PVP-Os coated electrodes, however, such redox peak pair was not observed. Despite the fact that current production was several folds higher in GCEs coated with PVP-Os, the peak potentials virtually remained unchanged before and after incubation for all the strains tested. The redox pair with potentials of around 0.27V and 0.33V was typical for the PVP-Os used in this study. This result was surprising as it indicated the electrochemistry property of the coated electrode surface might have remained the same despite incubation with bacteria and significant current generation. It was possible that bacteria cells were less prone to grow directly onto the PVP-Os surface despite more efficient electron transfer due to presence of the PVP-Os polymer. Rather, the cells might use their MET machineries such as secretion of flavins in the presence of PVP-Os. To substantiate this, microscopic imaging of the electrode surface area would be a necessary next step.

Regarding the effect of polymer loading on current generation, although at first it seemed logical to deduce that with more redox polymers, more redox centers would be provided to mediate electron transfer, thereby facilitating current generation from bacteria, our data suggested that in the loading range we tested (9.33μg to 111.96ug), the effect of polymer loading on current generation was minimal. No statistically significant difference was found in terms of current generation among the four PVP-Os polymer loadings. This result was not unexpected, as similar observations were reported in EBFCs using similar redox polymers (Merchant et al., 2009). The thickness of the polymer film might be an important factor contributing to the result. Maintain the cross

section surface areas of the films at similar level resulted in thicker films for higher polymer loadings. As the film thickness increased, not all the additional redox centers were electrochemically accessible. In fact, it has been suggested that only redox centers within a certain thickness actually contributed to electron transfer in EBFCs (Merchant et al., 2009). The data generated was consistent with previous observations. Increased loading of redox polymer alone did not lead to improvement on current generation in MFCs, likely due to the fundamental mechanism of electron transfer in redox polymers.

The maximum current density from electrodes prepared by LOM or MCM was significantly less than those by SM, although the PVP-Os loading on these electrodes were the same. This result reflected the importance of how bacteria were incorporated into the electrode in the MFC system. The reason that the MCM electrodes showed much lower current generation might be that the mixing of a dense bacteria solution with PVP-Os solution resulted in disruption of the electron communication among redox centers because of the numerous bacterial cells that were relatively larger in size (~1μm in length). Such disruption could lead to a less efficient electron transfer network, causing an overall low current density. When the bacteria were coated as a layer on top of the dried PVP-Os layer (LOM), the segregation would no longer occur; the redox centers of PVP-Os would form a well-connected network and result in better current generation than LOM. Another likely reason is the actual number of bacteria cells that are alive and functioning may differ greatly in these methods. The 20 minute drying process for either LOM or MCM might be harmful for the bacterial cells due to cell death. The dead bacterial cells were still incorporated onto the electrode surface and would hinder electron transfer between redox centers or between redox center and other

live bacteria. In contrast, the SM setup allows live bacteria to actively move toward the more attractive site, the vicinity of the poised electrode surface. Such selective effect resulted in the accumulation of live and functioning bacterial cell close to the electrode surface, leading to higher current generation. Besides, *Shewanella* were known to secret free diffusing flavins that function as mediators for electron transfer (Brutinel and Gralnick, 2012). The bacteria cells injected into the chamber (SM) but not grown on the electrode surface can indirectly contribute to electron transfer through mediator secretion.

GEs were frequently used in EBFCs and biosensors for incorporating enzymes with redox polymer and other materials (Dong and Li, 1997; Xiao et al., 2000; Zhao et al., 1996). Previous study on probiotics also used PVP based polymer to coat the bacteria to protect them from the harmful conditions so that more viable bacteria could reach the ideal site (R. Vidhyalakshmi, 2009). However, using this strategy to incorporate live bacterial cells onto gold electrode surface is unprecedented to the best of our knowledge. In this study, we successfully incorporated live *Shewanella putrefactions* W3-18-1 cells onto GE surface with LBL method. The previously reported incompatibility of GEs with exoelectrogenic W3-18-1 was circumvented with the LBL surface modification strategy, resulting in significant increase in bioanode performance compared to GCE. The maximum current density produced from the LBL method with GE was significantly higher compared to a previous publication in which a *Shewanella* strain was engineered to facilitate its binding to GEs(Kane et al., 2013), as well as another study that used self-assembled monolayer to modify GE surface (Crittenden et al., 2006). Due to the principle and procedure of the LBL method, the

GEs prepared by LBL had much lower PVP-Os loading compared with the GCEs in this study, which was also reflected by significant lower peak current from the CV curves. The amount of bacteria incorporated was also expected to be much lower than those incorporated into GCE in the LOM and MCM test due to the nature of the LBL protocol, which might explain the much longer time needed for these electrodes to produce significant current and resembles the lag phase of bacterial growth. Despite these, the maximum current density is 70% higher; indicating the electron transfer network in these GEs is more efficient than those in the GCEs. The mechanisms for the unique CV peaks emerged after incubation in these GEs were not clear and currently under investigation.

5.7 *Conclusions and future work*

In this study, systematic experiments were conducted to evaluate the potential application of *Shewanella* based bioanodes with the incorporation of redox polymer PVP-Os. Four *Shewanella* strains MR-1, PV-4, CN-32 and W3-18-1 were compared and the result indicated that strain W3-18-1 was a superior candidate for bioanode application. Incorporation of PVP-Os resulted in 3 fold to 9 fold increase in maximum current density, suggesting that GCEs with PVP-Os modified surface was more favorable for *Shewanella* to respire. The effect of polymer loading was minimal, as bioanode performance did not show significant change within the range of 9.33 μg to 111.96 μg PVP-Os. Comparison of different methods for bioanode fabrication showed that injection of bacteria into bulk medium was better than introducing bacteria directly onto the GCE surface. However, the bacteria could be incorporated onto the electrode

surface using GEs and LBL method and the bioanodes showed ~71% increase in maximum current density, reaching 24μA/cm^2.

Our results showed that there is great potential to improve the performance of bioanodes and potentially MFCs using exoelectrogenic bacteria with incorporation of redox polymers. Rather than the redox polymer loading or the number of bacteria cells introduced onto the electrode surface, proper method of polymer and bacteria incorporation may be more important in determining the performance of bioanodes. The electron shuttling from bacteria to the electrode might be very different among different methods, as reflected by cyclic voltammetry. With incorporation of PVP-Os, GEs could incorporate electrode respiring bacteria and produced superior current density.

In the future, it is worthwhile to test the performance with different types of redox polymers or conductive polymers, such as ferrocene based polymer family. Incorporation of carbon nanotubes can potentially further enhance bioanode performance based on current reports in EBFCs. Optimization of cathode performance is a necessary next step as cathode performance is usually what limits the overall performance of MFCs. Overall, the integration of choice of electrode material, the configuration of the electrode, electrode surface modification, choice of anode/cathode catalyst, and proper MFC design is needed for constructing high-performance MFCs as sustainable energy source and/or for pollution treatment.

Chapter 6: Summary and Output

With increasing recognition of the great potential of Environmental Microbiology applications, such as bioremediation, bioenergy, and for industrial production of valuable compounds, there has been growing interest in understanding and engineering of various environmental microorganisms. Despite the great potential, the desired function and efficiency was usually too low for real-life application. In order to improve the performance of interested function, insights into the physiology, genetics, stress response at molecular level, with combination of genetic manipulation and engineering is indispensable.

This thesis investigated the eco-physiology of bacteria in the *Shewanella* genus, a versatile group of bacteria that can not only be used for removal of several toxic heavy metals, numerous organic pollutants, but also for current generation in MFCs and for industrial production of valuable compounds such as Omega-3. The thesis focused on stress response at molecular level, and using engineering to explore for industrial applications and boost performance in environmental applications. In chapter2, we reported inactivation of the *hemH1* gene in *Shewanella loihica* PV-4 led to production of very high level of PPIX, a compound with useful application in various fields, especially in PDT for cancer treatment, drug deliver and imaging, etc. The yield of PPIX production is hundreds of times higher than other counterpart bacteria strains. A patent was published for this finding. There is great potential for industrial production of PPIX based on this patent.

The PPIX overproduction is due to existence of two ferrochelatase encoding genes in PV-4. In fact, many other *Shewanella* strains harbor two ferrochelatase homologues

genes in their genome, a phenomenon not observed in other bacteria genera. Moreover, similar redundancy was found in other genes in the heme synthesis pathway in various *Shewanella* strain. The apparent functional redundancy of possessing two genes encoding enzymes with the same function triggered our interest in understanding the expression and regulation of these paralogues. Therefore, in chapter 3, analysis was conducted for the redundancy of heme synthesis genes in *Shewannela*, with focus on the two *hemH* paralogues, with the questions whether the two paralogous genes have similar expression pattern, regulated by similar machinery, or that despite functional similarity, these two genes actually have different roles in this organism. It was confirmed that both genes encode functioning ferrochelatase, Temporal expression monitoring revealed that these two genes showed expression pattern that are very different from each other. These results suggested that *hemH1* is playing the dominant role as ferrochelatase. But in the incident of disruption in *hemH1*, expression of *hemH2* gene is turned on to produce ferrochelatase to meet the cellular need for heme.

Such different expression pattern led to investigation on the transcriptional regulation of the two paralogues. Using 5'-RACE, the transcriptional start site of both genes were identified and their promoter region was inferred. DNA sequence alignment showed that there are highly conserved regions in the upstream DNA of both genes among *Shewanella*, with *hemH1* likely regulated by OxyR and RpoD, and *hemH2* regulated by RpoE2. Such regulatory effect was supported by enhanced expression of *hemH1* and *hemH2* with OxyR and RpoE2 expressed *in-trans*, respectively. Moreover, the complementation of *ΔhemH1* strain with *rpoE2* can also revert the PPIX accumulation, again supporting the regulation of RpoE2 on *hemH2*.

Since both OxyR and RpoE2 are regulatory proteins involved in oxidative stress response, the effect of oxidative stress on expression of the two *hemH* paralogues and cellular phenotype was investigated via addition of hydrogen peroxide or using light exposure. As expected, addition of hydrogen peroxide induced the expression of *hemH1*, *hemH2*, and *rpoE2* in the parental strain. Light exposure had no effect on the parental strain, but induced significant expression of *rpoE2* and *hemH2* in the *ΔhemH1*strain, and reverted the PPIX accumulation phenotype. Based on our understanding of the regulation mechanism, it is likely that the trival level of PPIX accumulated in the *ΔhemH1* strain led to production of ROS when exposed to light. The ROS generated triggered oxidative stress response, leading to induction in *rpoE2*, which in turn, drives up expression of *hemH2*, preventing further accumulation of PPIX. Based on these findings, a model for the heme homeostasis in *Shewanella* was proposed.

In chapter 4, the effect of long term salt stress on a versatile *Shewanella* CN-32 strain was investigated with the strategy of experimental evolution. The one thousand generation of evolution under control or salt stress conditions led to significant fitness improvement, as reflected by the better growth rate and peak biomass compared to the ancestor. However, such gain in fitness is at the cost of decreased motility and other potential tradeoffs. The metabolome, transcriptome, and genome sequence of the evolved populations were analyzed for understanding the mechanism contributing to the fitness gain. It was found that the metabolite profile is determined by the salinity of the culture media, as well as the evolutionary condition based on DCA analysis. Several interesting patterns of particular metabolites and known osmolytes were found.

Glutamate increased for all population when exposed to salt stress but the level decrease in the order of An>EC>ES. Proline and ectoine also increased among all populations when cultured under high salinity. However, the level of proline and ectoine in ES populations were about 3 folds of An and EC populations under salt stress, suggesting the importance of these two compatible solutes in salt stress response in ES lines. Transcriptome analysis support the accumulation of proline, as all populations tested showed significant up-regulation in the proline uptake/synthesis operon. Other gene expression changes, such as down-regulation of flagella related genes, various regulator genes, membrane porin genes, and some biosynthetic genes, all showed varied level of change in expression, but each population appear to be very different in the transcriptome profile, suggesting the variation of the regulation in the evolved populations, which corresponds to the variance of growth characteristics among the parallel cell lines. Evaluation of mutation after 1 thousand generation revealed varied level of Single Nucleotide Polymorphisms (SNPs) in the evolved cell lines, with EC lines showing much higher number of SNPs than ES lines. The number of SNPs is positively correlated to mutations in the DNA replication/mismatch repair genes. The cell lines with most SNPs also showed lowest growth rate, suggesting the higher mutation rate due to mutation in DNA replication and mismatch repair negatives affected the fitness of these cell lines, at least in the current stage of adaptation. Genes with most SNPs detected were analyzed and potentially important mutation/genes were sorted, revealing potentially important mutations that may contribute to improved salt tolerance in ES populations.

Because of their capability of transferring electrons to extracellular electron acceptors and electrodes, the potential application of *Shewanella* in MFCs has long been investigated. Various factors, such as medium, carbon source, electrode materials, electrode surface modification, MFC configuration, etc., can affect the overall performance of MFCs. The electron transfer facilitating property of redox polymers has long been recognized in many EBFC applications, but their use in MFCs is not as common. In chapter 5, we investigated the current generation of *Shewanella* based anodes using 3-electrode system with incorporation of a well-known redox polymer PVP-Os. The effects of strains, polymer loading, and different anode chamber setup were tested. Cyclic Voltammetry was employed to study the electro chemical behavior of the electrode surface for all electrodes. Our result showed that among the four *Shewanella* strains tested, *Shewanella putrefaciens* CN-32 showed the best current generation, higher than *Shewanella oneidensis* MR-1, *Shewanella loihica* PV-4, and *Shewanella putrefaciens* CN-32, both on unmodified bare GCEs and PVP-Os modified GCEs, with maximum current density reaching 14.17uA/cm^2. Modification of GCE surface with PVP-Os led to significant improvement in current generation for all four strains, with different folds of increase, suggesting the redox polymers facilitated the electron shuttling between the electrode surface and *Shewanella* strains tested. CV analysis of these electrode revealed very similar patterns when the bacteria is cultured with bare electrode compared to previous published results, showing a pair of asymmetrical redox peaks that are indicative of outer membrane cytochromes. The electrodes with PVP-Os layer, however, did not show such peaks after incubation. Rather, the redox peaks potentials are typical PVP-Os behavior and remained the same

before and after incubation, with only slight decrease in peak current. This different CV behavior after incubation suggested that the mechanism involved in electron shuttling on bare electrode is very different from those modified with PVP-Os and that the bacteria cells may not preferably grow onto PVP-Os modified electrodes. Further analysis by varying the loading of PVP-Os on GCE showed that 9.66μg of PVP-Os modification showed similar level of current generation boost than other polymer loadings such as 27.99ug, 55.98ug, and 111.27ug, likely due to the reported effect of polymer layer thickness on their electron shuttling property. Then the current generation of different bacteria incorporation method LOM and MCM was compared with that of previously tested SM. The result showed that the current generation of LOM and MCM were much lower than SM. Investigating the underlying mechanism with CV result suggested the MCM method peak current is much smaller than LOM, possibly due to blockage of electron shuttling between the redox polymers from inactive bacterial cells. Since the bacteria were passively incorporated onto the electrode surface in LOM and MCM, not all bacteria were alive and actively respiring after the incorporation procedure. In SM, the bacteria suspended in the media can actively swim toward the electrode surface in SM, such selective effect can accumulate live and actively respiring bacteria cell onto the electrode surface, resulting in higher current generation. In the last setup, we used GEs that were widely used in biosensors and the LBL method to incorporate bacteria/PVP-Os composite onto the GEs. Although previously it has been reported that the GEs were poorly compatible with exoelectrogenesis bacteria such as *Shewanella*, in our case the modification of GE surface with PVP-Os via the LBL method showed significant enhancement of bioanode performance, leading to 71%

increase in maximum current density, reaching 24uA/cm^2, although longer time period is needed to reach such current density. Because of the dipping and cleaning procedure of the LBL method, the actual amount of PVP-Os and bacteria cell incorporated onto the GE surface is much less than other methods with the GCEs, which is supported by CV result showing the peak current of less than 1uA. Therefore, the bacteria/polymer incorporation method, rather than the amount of polymer and bacteria, is more critical for boosting bioanode performance.

In summary, bacteria in the genus of *Shewanella* are versatile microbes with great potential for production of valuable compounds, as well as bioremediation and bioenergy applications. Their flexibility to thrive in a wide gradient of various environmental conditions, broad spectrum of electron acceptors, and their relatively easy genetic manipulation, make them ideal model organisms for both research purposes and industrial applications. This thesis focused on investigating the physiology, with emphasis on stress response and regulation, of various strains in the *Shewanella* genus for their potential industrial and environmental applications. A high yield PPIX producing mutant strain of *Shewanella loihica* PV-4 was identified and published as a patent. It is shown that the PPIX accumulation is as a result of the functioning of two ferrochelatase encoding genes, each with its own expression pattern and regulation. In depth study on regulation led to the establishment of the underlying link between expressional regulation, heme homeostatsis, light exposure response, and oxidative stress response. The long term salt stress effect on phenotype and the molecular level mechanistic study was conducted using *Shewanella putrefaciens* CN-32. The performance of *Shewanella* based bioanode was improved with engineering

involving incorporation of redox polymer PVP-Os and different incorporation methods. These studies demonstrate the merit of this organism for their real life applications, especially that PPIX production as a new area of potential industrial application, while providing valuable insights into the long term stress response mechanism, the regulation, the environmental implication of the apparent genetic redundancy of this unique environmental organism. The electrode engineering for bioanodes provides new clues for improving bioanode performance and has great potential to be further expanded into full MFC in the future.

Statement for including previously published contents in dissertation as original author

This is to acknowledge that the following contents of my dissertation, including figures 2.1 to 2.3, and figures 2.5 to 2.8 in Chapter 2, as well as all the figures and majority of the texts in chapter 3, were published previously in Applied and Environmental Microbiology, in which I am the co-first author, with the following article information, "Differential Regulation of the Two Ferrochelatase Paralogues in *Shewanella loihica* PV-4 in Response to Environmental Stresses", Applied and Environmental Microbiology, Volume 82, Number 17, pages 5077-5087, 2016.

References

Ahmad, S.W.T. (2013). Use of Pseudomonas spp. for the bioremediation of environmental pollutants: a review. Environ Monit Assess *185*, 8147-8155.

Allison, R.R., Downie, G.H., Cuenca, R., Hu, X.H., Childs, C.J.H., and Sibata, C.H. (2004). Photosensitizers in clinical PDT. Photodiagn Photodyn *1*, 27-42.

Amiri-Jami, M., and Griffiths, M.W. (2010). Recombinant production of omega-3 fatty acids in Escherichia coli using a gene cluster isolated from Shewanella baltica MAC1. J Appl Microbiol *109*, 1897-1905.

Anzaldi, L.L., and Skaar, E.P. (2010). Overcoming the heme paradox: heme toxicity and tolerance in bacterial pathogens. Infect Immun *78*, 4977-4989.

Baba Uqab, S.M., Ruqeya Nazir (2016). Review on Bioremediation of Pesticides. Journal of Bioremediation & Biodegradation *7*.

Balan, V. (2014). Current challenges in commercially producing biofuels from lignocellulosic biomass. ISRN biotechnology *2014*, 463074.

Bali, S., Lawrence, A.D., Lobo, S.A., Saraiva, L.M., Golding, B.T., Palmer, D.J., Howard, M.J., Ferguson, S.J., and Warren, M.J. (2011). Molecular hijacking of siroheme for the synthesis of heme and d(1) heme. P Natl Acad Sci USA *108*, 18260-18265.

Baran, R., Bowen, B.P., Price, M.N., Arkin, A.P., Deutschbauer, A.M., and Northen, T.R. (2013). Metabolic Footprinting of Mutant Libraries to Map Metabolite Utilization to Genotype. Acs Chem Biol *8*, 189-199.

Barrick, J.E., and Lenski, R.E. (2013). Genome dynamics during experimental evolution. Nat Rev Genet *14*, 827-839.

Bashyam, M.D., and Hasnain, S.E. (2004). The extracytoplasmic function sigma factors: role in bacterial pathogenesis. Infect Genet Evol *4*, 301-308.

Basoglu, H., Bilgin, M.D., and Demir, M.M. (2016). Protoporphyrin IX-loaded magnetoliposomes as a potential drug delivery system for photodynamic therapy: Fabrication, characterization and in vitro study. Photodiagn Photodyn *13*, 81-90.

Baumann, P., Baumann, L., Lai, C.Y., Roubakhsh, D., Moran, N.A., and Clark, M.A. (1995). Genetics, Physiology, and Evolutionary Relationships of the Genus Buchnera - Intracellular Symbionts of Aphids. Annu Rev Microbiol *49*, 55-94.

Baysse, C., Matthijs, S., Pattery, T., and Cornelis, P. (2001). Impact of mutations in hemA and hemH genes on pyoverdine production by Pseudomonas fluorescens ATCC17400. Fems Microbiol Lett *205*, 57-63.

Belchik, S.M., Kennedy, D.W., Dohnalkova, A.C., Wang, Y.M., Sevinc, P.C., Wu, H., Lin, Y.H., Lu, H.P., Fredrickson, J.K., and Shi, L. (2011). Extracellular Reduction of Hexavalent Chromium by Cytochromes MtrC and OmcA of Shewanella oneidensis MR-1. Appl Environ Microb *77*, 4035-4041.

Berrier, C., Coulombe, A., Szabo, I., Zoratti, M., and Ghazi, A. (1992). Gadolinium Ion Inhibits Loss of Metabolites Induced by Osmotic Shock and Large Stretch-Activated Channels in Bacteria. Eur J Biochem *206*, 559-565.

Biffinger, J.C., Fitzgerald, L.A., Ray, R., Little, B.J., Lizewski, S.E., Petersen, E.R., Ringeisen, B.R., Sanders, W.C., Sheehan, P.E., Pietron, J.J., *et al.* (2011). The utility of Shewanella japonica for microbial fuel cells. Bioresource Technol *102*, 290-297.

Blount, Z.D., Barrick, J.E., Davidson, C.J., and Lenski, R.E. (2012). Genomic analysis of a key innovation in an experimental Escherichia coli population. Nature *489*, 513-518.

Bouhenni, R., Gehrke, A., and Saffarini, D. (2005). Identification of genes involved in cytochrome c biogenesis in Shewanella oneidensis, using a modified mariner transposon. Appl Environ Microb *71*, 4935-4937.

Boukhalfa, H., Icopini, G.A., Reilly, S.D., and Neu, M.P. (2007). Plutonium(IV) reduction by the metal-reducing bacteria Geobacter metallireducens GS15 and Shewanella oneidensis MR1. Appl Environ Microb *73*, 5897-5903.

Bouwer, E.J., and McCarty, P.L. (1983). Transformations of 1- and 2-carbon halogenated aliphatic organic compounds under methanogenic conditions. Appl Environ Microbiol *45*, 1286-1294.

Bouwer, E.J., Rittmann, B.E., and McCarty, P.L. (1981). Anaerobic degradation of halogenated 1- and 2-carbon organic compounds. Environ Sci Technol *15*, 596-599.

Bowman, J.P., McCammon, S.A., Nichols, D.S., Skerratt, J.H., Rea, S.M., Nichols, P.D., and McMeekin, T.A. (1997). Shewanella gelidimarina sp. nov. and Shewanella frigidimarina sp. nov., novel Antarctic species with the ability to produce eicosapentaenoic acid (20:5 omega 3) and grow anaerobically by dissimilatory Fe(III) reduction. Int J Syst Bacteriol *47*, 1040-1047.

Bretschger, O., Cheung, A.C.M., Mansfeld, F., and Nealson, K.H. (2010). Comparative Microbial Fuel Cell Evaluations of Shewanella spp. Electroanal *22*, 883-894.

Bretschger, O., Obraztsova, A., Sturm, C.A., Chang, I.S., Gorby, Y.A., Reed, S.B., Culley, D.E., Reardon, C.L., Barua, S., Romine, M.F., *et al.* (2007). Current production and metal oxide reduction by Shewanella oneidensis MR-1 wild type and mutants. Appl Environ Microb *73*, 7003-7012.

Brill, J., Hoffmann, T., Bleisteiner, M., and Bremer, E. (2011). Osmotically Controlled Synthesis of the Compatible Solute Proline Is Critical for Cellular Defense of Bacillus subtilis against High Osmolarity. J Bacteriol *193*, 5335-5346.

Brutinel, E.D., and Gralnick, J.A. (2012). Shuttling happens: soluble flavin mediators of extracellular electron transfer in Shewanella. Applied microbiology and biotechnology *93*, 41-48.

Buettner, G.R., and Oberley, L.W. (1979). Superoxide Formation by Protoporphyrin as Seen by Spin Trapping. Febs Lett *98*, 18-20.

Burg, M.B., and Ferraris, J.D. (2008). Intracellular organic osmolytes: Function and regulation. J Biol Chem *283*, 7309-7313.

Canovas, D., Borges, N., Vargas, C., Ventosa, A., Nieto, J.J., and Santos, H. (1999). Role of N gamma-acetyldiaminobutyrate as an enzyme stabilizer and an intermediate in the biosynthesis of hydroxyectoine. Appl Environ Microb *65*, 3774-3779.

Carpentier, W., Sandra, K., De Smet, I., Brige, A., De Smet, L., and Van Beeumen, J. (2003). Microbial reduction and precipitation of vanadium by Shewanella oneidensis. Appl Environ Microb *69*, 3636-3639.

Chastanet, A., Fert, J., and Msadek, T. (2003). Comparative genomics reveal novel heat shock regulatory mechanisms in Staphylococcus aureus and other Gram-positive bacteria. Mol Microbiol *47*, 1061-1073.

China, E.P.A. (2002). Water and wastewater monitoring methods, 4th ed. Chinese Environmental Science Publishing House, 266-274.

Cohen, S.E., Godoy, V.G., and Walker, G.C. (2009). Transcriptional Modulator NusA Interacts with Translesion DNA Polymerases in Escherichia coli. J Bacteriol *191*, 665-672.

Coman, V., Gustavsson, T., Finkelsteinas, A., von Wachenfeldt, C., Hagerhall, C., and Gorton, L. (2009). Electrical Wiring of Live, Metabolically Enhanced Bacillus subtilis Cells with Flexible Osmium-Redox Polymers. J Am Chem Soc *131*, 16171-16176.

Cox GS, B.C., Whitten DG. (1982). Photooxidation and singlet oxygen sensitization by protoporphyrin IX and its photooxidation products. Photochem. Photobiol *36*, 401-407.

Crittenden, S.R., Sund, C.J., and Sumner, J.J. (2006). Mediating electron transfer from bacteria to a gold electrode via a self-assembled monolayer. Langmuir *22*, 9473-9476.

Csonka, L.N. (1989). Physiological and Genetic Responses of Bacteria to Osmotic-Stress. Microbiol Rev *53*, 121-147.

Csonka, L.N., and Hanson, A.D. (1991). Prokaryotic osmoregulation: genetics and physiology. Annu Rev Microbiol *45*, 569-606.

Dai, J., Wei, H., Tian, C., Damron, F.H., Zhou, J., and Qiu, D. (2015). An extracytoplasmic function sigma factor-dependent periplasmic glutathione peroxidase is involved in oxidative stress response of Shewanella oneidensis. Bmc Microbiol *15*, 34.

Dailey, F.E., McGraw, J.E., Jensen, B.J., Bishop, S.S., Lokken, J.P., Dorff, K.J., Ripley, M.P., and Munro, J.B. (2016). The Microbiota of Freshwater Fish and Freshwater Niches Contain Omega-3 Fatty Acid-Producing Shewanella Species. Appl Environ Microb *82*, 218-231.

Dailey, H.A., Finnegan, M.G., and Johnson, M.K. (1994). Human Ferrochelatase Is an Iron-Sulfur Protein. Biochemistry-Us *33*, 403-407.

Dailey, H.A., Gerdes, S., Dailey, T.A., Burch, J.S., and Phillips, J.D. (2015). Noncanonical coproporphyrin-dependent bacterial heme biosynthesis pathway that does not use protoporphyrin. P Natl Acad Sci USA *112*, 2210-2215.

Davis, F., and Higson, S.P.J. (2007). Biofuel cells - Recent advances and applications. Biosens Bioelectron *22*, 1224-1235.

Diez, B., Russo, R.C., Teijo, M.J., Hajos, S., Batlle, A., and Fukuda, H. (2009). Ros Production by Endogenously Generated Protoporphyrin Ix in Murine Leukemia Cells. Cell Mol Biol *55*, 15-19.

Diplock, E.E., Alhadrami, H.A., and Paton, G.I. (2010). Application of Microbial Bioreporters in Environmental Microbiology and Bioremediation. Adv Biochem Eng Biot *118*, 189-209.

Dong, S.J., and Li, J.H. (1997). Self-assembled monolayers of thiols on gold electrodes for bioelectrochemistry and biosensors. Bioelectroch Bioener *42*, 7-13.

Dong, X., Wei, C., Liu, T.J., Lv, F., and Qian, Z.Y. (2016). Real-Time Fluorescence Tracking of Protoporphyrin Incorporated Thermosensitive Hydrogel and Its Drug Release in Vivo. Acs Appl Mater Inter *8*, 5104-5113.

Du, Z.W., Li, H.R., and Gu, T.Y. (2007). A state of the art review on microbial fuel cells: A promising technology for wastewater treatment and bioenergy. Biotechnol Adv *25*, 464-482.

Elizabeth S. Heidrich, Stephen R. Edwards, Jan Dolfing, Sarah E. Cotterill, Thomas P. Curtis (2014). Performance of a pilot scale microbial electrolysis cell fed on domestic wastewater at ambient temperatures for a 12 month period. Bioresource Technol *173*, 87-95.

Ellen Dannys, T.G., Andrew Wettlaufer, Chandra Mouli R Madhurnathakam and Ali Elkamel (2015). Wastewater Treatment with Microbial Fuel Cells: A Design and Feasibility Study for Scale-up in Microbreweries. Journal of Bioprocessing & Biotechniques *6*.

Fang, J., Tsukigawa, K., Liao, L., Yin, H.Z., Eguchi, K., and Maeda, H. (2016). Styrene-maleic acid-copolymer conjugated zinc protoporphyrin as a candidate drug for tumor-targeted therapy and imaging. J Drug Target *24*, 399-407.

Fapetu, S., Keshavarz, T., Clements, M., and Kyazze, G. (2016). Contribution of direct electron transfer mechanisms to overall electron transfer in microbial fuel cells utilising Shewanella oneidensis as biocatalyst. Biotechnol Lett *38*, 1465-1473.

Farrenkopf, A.M., Dollhopf, M.E., NiChadhain, S., Luther, G.W., and Nealson, K.H. (1997). Reduction of iodate in seawater during Arabian Sea shipboard incubations and in laboratory cultures of the marine bacterium Shewanella putrefaciens strain MR-4. Mar Chem *57*, 347-354.

Foti, M., Medici, R., and Ruijssenaars, H.J. (2013). Biological production of monoethanolamine by engineered Pseudomonas putida S12. J Biotechnol *167*, 344-349.

Franks, A.E., and Nevin, K.P. (2010). Microbial Fuel Cells, A Current Review. Energies *3*, 899-919.

Fredrickson, J.K., Romine, M.F., Beliaev, A.S., Auchtung, J.M., Driscoll, M.E., Gardner, T.S., Nealson, K.H., Osterman, A.L., Pinchuk, G., Reed, J.L., *et al.* (2008). Towards environmental systems biology of Shewanella. Nat Rev Microbiol *6*, 592-603.

Fu, X., Wang, D., Yin, X., Du, P., and Kan, B. (2014). Time course transcriptome changes in Shewanella algae in response to salt stress. PloS one *9*, e96001.

G. Sidney Cox, Christiane Bobillier, and Whitten, D.G. (1982). PHOTOOXIDATION AND SINGLET OXYGEN SENSITIZATION BY PROTOPORPHYRIN IX AND ITS PHOTOOXIDATION PRODUCTS. Photochem Photobiol *36*, 401-407.

Galinski, E.A. (1995). Osmoadaptation in bacteria. Advances in microbial physiology *37*, 272-328.

Galinski, E.A., Pfeiffer, H.P., and Truper, H.G. (1985). 1,4,5,6-Tetrahydro-2-Methyl-4-Pyrimidinecarboxylic Acid - a Novel Cyclic Amino-Acid from Halophilic Phototrophic Bacteria of the Genus Ectothiorhodospira. Eur J Biochem *149*, 135-139.

Gao, H., Obraztova, A., Stewart, N., Popa, R., Fredrickson, J.K., Tiedje, J.M., Nealson, K.H., and Zhou, J. (2006). Shewanella loihica sp. nov., isolated from iron-rich microbial mats in the Pacific Ocean. Int J Syst Evol Microbiol *56*, 1911-1916.

Gao, H.C., Yang, Z.M.K., Wu, L.Y., Thompson, D.K., and Zhou, J.Z. (2006c). Global transcriptome analysis of the cold shock response of Shewanella oneidensis MR-1 and mutational analysis of its classical cold shock proteins. J Bacteriol *188*, 4560-4569.

Gorby, Y.A., Yanina, S., McLean, J.S., Rosso, K.M., Moyles, D., Dohnalkova, A., Beveridge, T.J., Chang, I.S., Kim, B.H., Kim, K.S., *et al.* (2006). Electrically

conductive bacterial nanowires produced by Shewanella oneidensis strain MR-1 and other microorganisms. P Natl Acad Sci USA *103*, 11358-11363.

Hamblin, M.R., and Hasan, T. (2004). Photodynamic therapy: a new antimicrobial approach to infectious disease? Photoch Photobio Sci *3*, 436-450.

Hanai, T., Atsumi, S., and Liao, J.C. (2007). Engineered synthetic pathway for isopropanol production in Escherichia coli. Appl Environ Microb *73*, 7814-7818.

Hansson, M.D., Karlberg, T., Rahardja, M.A., Al-Karadaghi, S., and Hansson, M. (2007). Amino acid residues His183 and Glu264 in Bacillus subtilis ferrochelatase direct and facilitate the insertion of metal ion into protoporphyrin IX. Biochemistry-Us *46*, 87-94.

Hasan, K., Patil, S.A., Gorecki, K., Leech, D., Hagerhall, C., and Gorton, L. (2013). Electrochemical communication between heterotrophically grown Rhodobacter capsulatus with electrodes mediated by an osmium redox polymer. Bioelectrochemistry *93*, 30-36.

Hau, H.H., Gilbert, A., Coursolle, D., and Gralnick, J.A. (2008). Mechanism and Consequences of Anaerobic Respiration of Cobalt by Shewanella oneidensis Strain MR-1. Appl Environ Microb *74*, 6880-6886.

Hau, H.H., and Gralnick, J.A. (2007). Ecology and biotechnology of the genus Shewanella. Annu Rev Microbiol *61*, 237-258.

He, Z., Gentry, T.J., Schadt, C.W., Wu, L., Liebich, J., Chong, S.C., Huang, Z., Wu, W., Gu, B., Jardine, P., *et al.* (2007). GeoChip: a comprehensive microarray for investigating biogeochemical, ecological and environmental processes. Isme J *1*, 67-77.

Heidelberg, J.F., Paulsen, I.T., Nelson, K.E., Gaidos, E.J., Nelson, W.C., Read, T.D., Eisen, J.A., Seshadri, R., Ward, N., Methe, B., *et al.* (2002). Genome sequence of the dissimilatory metal ion-reducing bacterium Shewanella oneidensis. Nat Biotechnol *20*, 1118-1123.

Hjelm, M., Hilbert, L.R., Moller, P., and Gram, L. (2002). Comparison of adhesion of the food spoilage bacterium Shewanella putrefaciens to stainless steel and silver surfaces. J Appl Microbiol *92*, 903-911.

Holt, H.M., Gahrn-Hansen, B., and Bruun, B. (2005). Shewanella algae and Shewanella putrefaciens: clinical and microbiological characteristics. Clinical microbiology and infection : the official publication of the European Society of Clinical Microbiology and Infectious Diseases *11*, 347-352.

Huang, J., Sun, B., and Zhang, X. (2010). Shewanella xiamenensis sp. nov., isolated from coastal sea sediment. Int J Syst Evol Microbiol *60*, 1585-1589.

Huang, J.H., Elzinga, E.J., Brechbuchl, Y., Voegelin, A., and Kretzschmar, R. (2011). Impacts of Shewanella putrefaciens Strain CN-32 Cells and Extracellular Polymeric Substances on the Sorption of As(V) and As(III) on Fe(III)-(Hydr)oxides. Environ Sci Technol *45*, 2804-2810.

Hung-Yin Tsaia, , Chen-Chang Wub, Chi-Yuan Leec, Eric Pierre Shiha (2009). Microbial fuel cell performance of multiwall carbon nanotubes on carbon cloth as electrodes. J Power Sources *194*.

Hurt, R.A., Qiu, X.Y., Wu, L.Y., Roh, Y., Palumbo, A.V., Tiedje, J.M., and Zhou, J.H. (2001). Simultaneous recovery of RNA and DNA from soils and sediments. Appl Environ Microb *67*, 4495-4503.

Iolascon, A., De Falco, L., and Beaumont, C. (2009). Molecular basis of inherited microcytic anemia due to defects in iron acquisition or heme synthesis. Haematol-Hematol J *94*, 395-408.

Jeong, Y.S., Song, S.K., Lee, S.J., and Hur, B.K. (2006). The growth and EPA synthesis of Shewanella oneidensis MR-1 and expectation of EPA biosynthetic pathway. Biotechnol Bioproc E *11*, 127-133.

JOHN BASSEL, P.H., ROBERT MORTIMER, AND ALAN J. BEARDEN (1975). Mutant of the Yeast Saccharomycopsis lipolytica that
Accumulates and Excretes Protoporphyrin IX. J Bacteriol *123*, 118-122.

Jorge, A.B., and Hazael, R. (2016). Use of Shewanella oneidensis for Energy Conversion in Microbial Fuel Cells. Macromol Chem Phys *217*, 1431-1438.

Joshi, V.K., and Tamhane, D.V. (1974). Fermentative Production of L-Sorbose from D-Sorbitol by Acetobacter-Suboxydans (Vinegar Isolate). Indian J Exp Biol *12*, 422-424.

Jozefczuk, S., Klie, S., Catchpole, G., Szymanski, J., Cuadros-Inostroza, A., Steinhauser, D., Selbig, J., and Willmitzer, L. (2010). Metabolomic and transcriptomic stress response of Escherichia coli. Molecular systems biology *6*, 364.

Kane, A.L., Bond, D.R., and Gralnick, J.A. (2013). Electrochemical Analysis of Shewanella oneidensis Engineered To Bind Gold Electrodes. Acs Synth Biol *2*, 93-101.

Karlberg, T., Lecerof, D., Gora, M., Silvegren, G., Labbe-Bois, R., Hansson, M., and Al-Karadaghi, S. (2002). Metal binding to Saccharomyces cerevisiae ferrochelatase. Biochemistry-Us *41*, 13499-13506.

Kawecki, T.J., Lenski, R.E., Ebert, D., Hollis, B., Olivieri, I., and Whitlock, M.C. (2012). Experimental evolution. Trends Ecol Evol *27*, 547-560.

Kazmierczak, M.J., Wiedmann, M., and Boor, K.J. (2005). Alternative sigma factors and their roles in bacterial virulence. Microbiol Mol Biol R *69*, 527-+.

Kempf, B., and Bremer, E. (1998). Uptake and synthesis of compatible solutes as microbial stress responses to high-osmolality environments. Arch Microbiol *170*, 319-330.

Kim, B.H., Ikeda, T., Park, H.S., Kim, H.J., Hyun, M.S., Kano, K., Takagi, K., and Tatsumi, H. (1999). Electrochemical activity of an Fe(III)-reducing bacterium, Shewanella putrefaciens IR-1, in the presence of alternative electron acceptors. Biotechnol Tech *13*, 475-478.

Kimoto, H., Kurisaki, J., Tsuji, N.M., Ohmomo, S., and Okamoto, T. (1999). Lactococci as probiotic strains: adhesion to human enterocyte-like Caco-2 cells and tolerance to low pH and bile. Lett Appl Microbiol *29*, 313-316.

King, K.C., Brockhurst, M.A., Vasieva, O., Paterson, S., Betts, A., Ford, S.A., Frost, C.L., Horsburgh, M.J., Haldenby, S., and Hurst, G.D. (2016). Rapid evolution of microbe-mediated protection against pathogens in a worm host. Isme J *10*, 1915-1924.

Kirkbride, K.P., Yap, S.M., App, B., Andrews, S., Pigou, P.E., Klass, G., Dinan, A.C., and Peddie, F.L. (1992). Microbial-Degradation of Petroleum-Hydrocarbons - Implications for Arson Residue Analysis. J Forensic Sci *37*, 1585-1599.

Klonowska, A., Heulin, T., and Vermeglio, A. (2005). Selenite and tellurite reduction by Shewanella oneidensis. Appl Environ Microb *71*, 5607-5609.

Konstantinidis, K.T., Serres, M.H., Romine, M.F., Rodrigues, J.L.M., Auchtung, J., Mccue, L.A., Lipton, M.S., Obraztsova, A., Giometti, C.S., Nealson, K.H., *et al.* (2009). Comparative systems biology across an evolutionary gradient within the Shewanella genus. P Natl Acad Sci USA *106*, 15909-15914.

Kouzuma, A., Kasai, T., Hirose, A., and Watanabe, K. (2015). Catabolic and regulatory systems in Shewanella oneidensis MR-1 involved in electricity generation in microbial fuel cells. Frontiers in microbiology *6*.

Kuhlmann, A.U., and Bremer, E. (2002). Osmotically regulated synthesis of the compatible solute ectoine in Bacillus pasteurii and related Bacillus spp. Appl Environ Microb *68*, 772-783.

Kumar.A, B.B.S., Joshi.V.D, Dhewa.T (2011). Review on Bioremediation of Polluted Environment. INTERNATIONAL JOURNAL OF ENVIRONMENTAL SCIENCES *1*, 1079-1089.

Leahy, J.G., and Colwell, R.R. (1990). Microbial degradation of hydrocarbons in the environment. Microbiol Rev *54*, 305-315.

Lee, S.J., Jeong, Y.S., Kim, D.U., Se, J.W., and Hur, B.K. (2006). Eicosapentaenoic acid (EPA) biosynthetic gene cluster of Shewanella oneidensis MR-1: Cloning, heterologous expression, and effects of temperature and glucose on the production of EPA in Escherichia coli. Biotechnol Bioproc E *11*, 510-515.

Lin, Y., and Tanaka, S. (2006). Ethanol fermentation from biomass resources: current state and prospects. Applied microbiology and biotechnology *69*, 627-642.

Liu, H., and Logan, B. (2004). Electricity generation using an air-cathode single chamber microbial fuel cell (MFC) in the absence of a proton exchange membrane. Abstr Pap Am Chem S *228*, U622-U622.

Lloyd, J.R., Yong, P., and Macaskie, L.E. (2000). Biological reduction and removal of Np(V) by two microorganisms. Environ Sci Technol *34*, 1297-1301.

Logan, B.E., and Regan, J.M. (2006). Microbial fuel cells--challenges and applications. Environ Sci Technol *40*, 5172-5180.

Louis, P., and Galinski, E.A. (1997). Characterization of genes for the biosynthesis of the compatible solute ectoine from Marinococcus halophilus and osmoregulated expression in Escherichia coli. Microbiol-Uk *143*, 1141-1149.

Luan, F.B., Liu, Y., Griffin, A.M., Gorski, C.A., and Burgos, W.D. (2015). Iron(III)-Bearing Clay Minerals Enhance Bioreduction of Nitrobenzene by Shewanella putrefaciens CN32. Environ Sci Technol *49*, 1418-1426.

Macdonell, M.T., and Colwell, R.R. (1985). Phylogeny of the Vibrionaceae, and Recommendation for 2 New Genera, Listonella and Shewanella. Syst Appl Microbiol *6*, 171-182.

Maisch, T., Bosl, C., Szeimies, R.M., Love, B., and Abels, C. (2007). Determination of the antibacterial efficacy of a new porphyrin-based photosensitizer against MRSA ex vivo. Photoch Photobio Sci *6*, 545-551.

Malin, G., Iakobashvili, R., and Lapidot, A. (1999). Effect of tetrahydropyrimidine derivatives on protein nucleic acids interaction - Type II restriction endonucleases as a model system. J Biol Chem *274*, 6920-6929.

Manchester, K.L. (1995). Louis Pasteur (1822-1895)--chance and the prepared mind. Trends in biotechnology *13*, 511-515.

McGovern, P.E., Zhang, J., Tang, J., Zhang, Z., Hall, G.R., Moreau, R.A., Nunez, A., Butrym, E.D., Richards, M.P., Wang, C.S., *et al.* (2004). Fermented beverages of pre- and proto-historic China. Proc Natl Acad Sci U S A *101*, 17593-17598.

McLaggan, D., Naprstek, J., Buurman, E.T., and Epstein, W. (1994). Interdependence of K+ and glutamate accumulation during osmotic adaptation of Escherichia coli. J Biol Chem *269*, 1911-1917.

Meinecke, L., Alawady, A., Schroda, M., Willows, R., Kobayashi, M.C., Niyogi, K.K., Grimm, B., and Beck, C.F. (2010). Chlorophyll-deficient mutants of Chlamydomonas reinhardtii that accumulate magnesium protoporphyrin IX. Plant Mol Biol *72*, 643-658.

Mendoza-Vargas, A., Olvera, L., Olvera, M., Grande, R., Vega-Alvarado, L., Taboada, B., Jimenez-Jacinto, V., Salgado, H., Juarez, K., Contreras-Moreira, B., *et al.* (2009). Genome-wide identification of transcription start sites, promoters and transcription factor binding sites in E. coli. PloS one *4*, e7526.

Merchant, S.A., Tran, T.O., Meredith, M.T., Cline, T.C., Glatzhofer, D.T., and Schmidtke, D.W. (2009). High-Sensitivity Amperometric Biosensors Based on Ferrocene-Modified Linear Poly(ethylenimine). Langmuir *25*, 7736-7742.

Michel, V., Lehoux, I., Depret, G., Anglade, P., Labadie, J., and Hebraud, M. (1997). The cold shock response of the psychrotrophic bacterium Pseudomonas fragi involves four low-molecular-mass nucleic acid binding proteins. J Bacteriol *179*, 7331-7342.

Miyamoto, K., Nakahigashi, K., Nishimura, K., and Inokuchi, H. (1991). Isolation and Characterization of Visible Light-Sensitive Mutants of Escherichia-Coli K12. J Mol Biol *219*, 393-398.

Miyamoto, K., Nishimura, K., Masuda, T., Tsuji, H., and Inokuchi, H. (1992). Accumulation of Protoporphyrin-Ix in Light-Sensitive Mutants of Escherichia-Coli. Febs Lett *310*, 246-248.

Moore, M.R. (1998). The biochemistry of heme synthesis in porphyria and in the porphyrinurias. Clin Dermatol *16*, 203-223.

Mustafa Balat, H.B. (2009). Recent trends in global production and utilization of bio-ethanol fuel. Appl Energ *86*, 2273-2282.

Nakahigashi, K., Nishimura, K., Miyamoto, K., and Inokuchi, H. (1991). Photosensitivity of a Protoporphyrin-Accumulating, Light-Sensitive Mutant (Visa) of Escherichia-Coli K-12. P Natl Acad Sci USA *88*, 10520-10524.

Nan Yan Petra Marschner, W.C., Changqing Zuo, Wei Qin (2015). Influence of salinity and water content on soil microorganisms. International Soil and Water Conservation Research *3*, 316-323.

Newton, G.J., Mori, S., Nakamura, R., Hashimoto, K., and Watanabe, K. (2009). Analyses of Current-Generating Mechanisms of Shewanella loihica PV-4 and Shewanella oneidensis MR-1 in Microbial Fuel Cells. Appl Environ Microb *75*, 7674-7681.

Obornik, M., and Green, B.R. (2005). Mosaic origin of the heme biosynthesis pathway in photosynthetic eukaryotes. Mol Biol Evol *22*, 2343-2353.

Panek, H., and O'Brian, M.R. (2002). A whole genome view of prokaryotic haem biosynthesis. Microbiol-Sgm *148*, 2273-2282.

Park, D.H., and Zeikus, J.G. (2000). Electricity generation in microbial fuel cells using neutral red as an electronophore. Applied and environmental microbiology *66*, 1292-1297.

Patil, S.A., Hasan, K., Leech, D., Hagerhall, C., and Gorton, L. (2012). Improved microbial electrocatalysis with osmium polymer modified electrodes. Chem Commun *48*, 10183-10185.

Perez-Arellano, I., Carmona-Alvarez, F., Gallego, J., and Cervera, J. (2010a). Molecular Mechanisms Modulating Glutamate Kinase Activity. Identification of the Proline Feedback Inhibitor Binding Site. J Mol Biol *404*, 890-901.

Perez-Arellano, I., Carmona-Alvarez, F., Martinez, A.I., Rodriguez-Diaz, J., and Cervera, J. (2010b). Pyrroline-5-carboxylate synthase and proline biosynthesis: From Osmotolerance to rare metabolic disease. Protein Sci *19*, 372-382.

Pflughoeft, K.J., Kierek, K., and Watnick, P.I. (2003). Role of ectoine in Vibrio cholerae osmoadaptation. Appl Environ Microb *69*, 5919-5927.

Picardal, F.W., Arnold, R.G., Couch, H., Little, A.M., and Smith, M.E. (1993). Involvement of Cytochromes in the Anaerobic Biotransformation of Tetrachloromethane by Shewanella-Putrefaciens 200. Appl Environ Microb *59*, 3763-3770.

Pinchuk, G.E., Geydebrekht, O.V., Hill, E.A., Reed, J.L., Konopka, A.E., Beliaev, A.S., and Fredrickson, J.K. (2011). Pyruvate and Lactate Metabolism by Shewanella oneidensis MR-1 under Fermentation, Oxygen Limitation, and Fumarate Respiration Conditions. Appl Environ Microb *77*, 8234-8240.

Qian, F., Baum, M., Gu, Q., and Morse, D.E. (2009). A 1.5 mu L microbial fuel cell for on-chip bioelectricity generation. Lab Chip *9*, 3076-3081.

Qiu, D., Damron, F.H., Mima, T., Schweizer, H.P., and Yu, H.D. (2008). PBAD-based shuttle vectors for functional analysis of toxic and highly regulated genes in Pseudomonas and Burkholderia spp. and other bacteria. Appl Environ Microbiol *74*, 7422-7426.

Quek, S.B., Cheng, L., and Cord-Ruwisch, R. (2015). Microbial fuel cell biosensor for rapid assessment of assimilable organic carbon under marine conditions. Water research *77*, 64-71.

R. Vidhyalakshmi, R.B.a.R.S.S. (2009). Encapsulation "The Future of Probiotics"-A Review. Advances in Biological Research *3*, 96-103.

Ramanavicius, A., Kausaite, A., and Ramanaviciene, A. (2008). Enzymatic biofuel cell based on anode and cathode powered by ethanol. Biosens Bioelectron *24*, 767-772.

Reid, G.A., and Gordon, E.H. (1999). Phylogeny of marine and freshwater Shewanella: reclassification of Shewanella putrefaciens NCIMB 400 as Shewanella frigidimarina. Int J Syst Bacteriol *49 Pt 1*, 189-191.

Rimboud, M., Pocaznoi, D., Erable, B., and Bergel, A. (2014). Electroanalysis of microbial anodes for bioelectrochemical systems: basics, progress and perspectives. Phys Chem Chem Phys *16*, 16349-16366.

Roberts, M.F. (2005). Organic compatible solutes of halotolerant and halophilic microorganisms. Saline systems *1*, 5.

Saiki, R.K., Gelfand, D.H., Stoffel, S., Scharf, S.J., Higuchi, R., Horn, G.T., Mullis, K.B., and Erlich, H.A. (1988). Primer-directed enzymatic amplification of DNA with a thermostable DNA polymerase. Science *239*, 487-491.

Sassa, S. (2006). Modern diagnosis and management of the porphyrias. Brit J Haematol *135*, 281-292.

Schroder, U. (2007). Anodic electron transfer mechanisms in microbial fuel cells and their energy efficiency. Phys Chem Chem Phys *9*, 2619-2629.

Senderovich, Y., and Halpern, M. (2013). The protective role of endogenous bacterial communities in chironomid egg masses and larvae. Isme J *7*, 2147-2158.

Shantaram, A., Beyenal, H., Raajan, R., Veluchamy, A., and Lewandowski, Z. (2005). Wireless sensors powered by microbial fuel cells. Environ Sci Technol *39*, 5037-5042.

Sharma, K.K., and Kalawat, U. (2010). Emerging infections: shewanella - a series of five cases. Journal of laboratory physicians *2*, 61-65.

Sheng, L., and Fein, J.B. (2014). Uranium Reduction by Shewanella oneidensis MR-1 as a Function of NaHCO3 Concentration: Surface Complexation Control of Reduction Kinetics. Environ Sci Technol *48*, 3768-3775.

Shi, L.A., Richardson, D.J., Wang, Z.M., Kerisit, S.N., Rosso, K.M., Zachara, J.M., and Fredrickson, J.K. (2009). The roles of outer membrane cytochromes of Shewanella and Geobacter in extracellular electron transfer. Env Microbiol Rep *1*, 220-227.

Sleator, R.D., and Hill, C. (2002). Bacterial osmoadaptation: the role of osmolytes in bacterial stress and virulence. Fems Microbiol Rev *26*, 49-71.

Solaiman, D.K.Y., Ashby, R.D., and Foglia, T.A. (2001). Production of polyhydroxyalkanoates from intact triacylglycerols by genetically engineered Pseudomonas. Applied microbiology and biotechnology *56*, 664-669.

Sun, J.Z., Kingori, G.P., Si, R.W., Zhai, D.D., Liao, Z.H., Sun, D.Z., Zheng, T., and Yong, Y.C. (2015). Microbial fuel cell-based biosensors for environmental monitoring: a review. Water Sci Technol *71*, 801-809.

Tenaillon, O., Barrick, J.E., Ribeck, N., Deatherage, D.E., Blanchard, J.L., Dasgupta, A., Wu, G.C., Wielgoss, S., Cruveiller, S., Medigue, C., *et al.* (2016). Tempo and mode of genome evolution in a 50,000-generation experiment. Nature *536*, 165-170.

Thakker, C., San, K.Y., and Bennett, G.N. (2013). Production of succinic acid by engineered E. coli strains using soybean carbohydrates as feedstock under aerobic fermentation conditions. Bioresource Technol *130*, 398-405.

Thomas, P.E., Ryan, D., and Levin, W. (1976). An improved staining procedure for the detection of the peroxidase activity of cytochrome P-450 on sodium dodecyl sulfate polyacrylamide gels. Anal Biochem *75*, 168-176.

Timur, S., Anik, U., Odaci, D., and Gorton, L. (2007). Development of a microbial biosensor based on carbon nanotube (CNT) modified electrodes. Electrochem Commun *9*, 1810-1815.

Toffin, L., Bidault, A., Pignet, P., Tindall, B.J., Slobodkin, A., Kato, C., and Prieur, D. (2004). Shewanella profunda sp. nov., isolated from deep marine sediment of the Nankai Trough. Int J Syst Evol Microbiol *54*, 1943-1949.

Tu, Q., Yu, H., He, Z., Deng, Y., Wu, L., Van Nostrand, J.D., Zhou, A., Voordeckers, J., Lee, Y.J., Qin, Y., *et al.* (2014). GeoChip 4: a functional gene-array-based high-throughput environmental technology for microbial community analysis. Molecular ecology resources *14*, 914-928.

Wan, X.F., Verberkmoes, N.C., McCue, L.A., Stanek, D., Connelly, H., Hauser, L.J., Wu, L., Liu, X., Yan, T., Leaphart, A., *et al.* (2004). Transcriptomic and proteomic characterization of the Fur modulon in the metal-reducing bacterium Shewanella oneidensis. J Bacteriol *186*, 8385-8400.

Wang, F., Xiao, X., Ou, H.Y., Gai, Y.B., and Wang, F.P. (2009). Role and Regulation of Fatty Acid Biosynthesis in the Response of Shewanella piezotolerans WP3 to Different Temperatures and Pressures. J Bacteriol *191*, 2574-2584.

Wasi, S., Tabrez, S., and Ahmad, M. (2013). Use of Pseudomonas spp. for the bioremediation of environmental pollutants: a review. Environ Monit Assess *185*, 8147-8155.

Weber, T., Charusanti, P., Musiol-Kroll, E.M., Jiang, X.L., Tong, Y.J., Kim, H.U., and Lee, S.Y. (2015). Metabolic engineering of antibiotic factories: new tools for antibiotic production in actinomycetes. Trends in biotechnology *33*, 15-26.

Wen, M., Bond-Watts, B.B., and Chang, M.C.Y. (2013). Production of advanced biofuels in engineered E. coli. Curr Opin Chem Biol *17*, 472-479.

Wiatrowski, H.A., Ward, P.M., and Barkay, T. (2006). Novel reduction of mercury(II) by mercury-sensitive dissimilatory metal reducing bacteria. Environ Sci Technol *40*, 6690-6696.

Wielinga, B., Mizuba, M.M., Hansel, C.M., and Fendorf, S. (2001). Iron promoted reduction of chromate by dissimilatory iron-deducing bacteria. Environ Sci Technol *35*, 522-527.

Wildung, R.E., Gorby, Y.A., Krupka, K.M., Hess, N.J., Li, S.W., Plymale, A.E., McKinley, J.P., and Fredrickson, J.K. (2000). Effect of electron donor and solution chemistry on products of dissimilatory reduction of technetium by Shewanella putrefaciens. Appl Environ Microb *66*, 2451-2460.

Willner, I., Yan, Y.M., Willner, B., and Tel-Vered, R. (2009). Integrated Enzyme-Based Biofuel Cells-A Review. Fuel Cells *9*, 7-24.

Won, S.H., Lee, B.H., Lee, H.S., and Jo, J. (2001). An Ochrobactrum anthropi gene conferring paraquat resistance to the heterologous host Escherichia coli. Biochem Biophys Res Commun *285*, 885-890.

Wong, A., Rodrigue, N., and Kassen, R. (2012). Genomics of adaptation during experimental evolution of the opportunistic pathogen Pseudomonas aeruginosa. Plos Genet *8*, e1002928.

Wood, J.M. (2015). Bacterial responses to osmotic challenges. J Gen Physiol *145*, 381-388.

Wu, D., Xing, D.F., Mei, X.X., Liu, B.F., Guo, C.H., and Ren, N.Q. (2013). Electricity generation by Shewanella sp HN-41 in microbial fuel cells. Int J Hydrogen Energ *38*, 15568-15573.

Wu, L., Wang, J., Tang, P., Chen, H., and Gao, H. (2011). Genetic and molecular characterization of flagellar assembly in Shewanella oneidensis. PloS one *6*, e21479.

Wu, W.G., Yang, F., Liu, X., and Bai, L.L. (2014). Influence of substrate on electricity generation of Shewanella loihica PV-4 in microbial fuel cells. Microb Cell Fact *13*.

Xiao, Y., Ju, H.X., and Chen, H.Y. (2000). Direct electrochemistry of horseradish peroxidase immobilized on a colloid/cysteamine-modified gold electrode. Anal Biochem *278*, 22-28.

Yang, H.J., Sasarman, A., Inokuchi, H., and Adler, J. (1996). Non-iron porphyrins cause tumbling to blue light by an Escherichia coli mutant defective in hemG. P Natl Acad Sci USA *93*, 2459-2463.

Yazawa, K., Araki, K., Okazaki, N., Watanabe, K., Ishikawa, C., Inoue, A., Numao, N., and Kondo, K. (1988). Production of eicosapentaenoic acid by marine bacteria. Journal of biochemistry *103*, 5-7.

Ye, X.T., Honda, K., Sakai, T., Okano, K., Omasa, T., Hirota, R., Kuroda, A., and Ohtake, H. (2012). Synthetic metabolic engineering-a novel, simple technology for designing a chimeric metabolic pathway. Microb Cell Fact *11*.

Yilmaz, E.I. (2003). Metal tolerance and biosorption capacity of Bacillus circulans strain EB1. Res Microbiol *154*, 409-415.

Yin, J., and Gao, H. (2011). Stress responses of shewanella. International journal of microbiology *2011*, 863623.

Yoon, S., Sanford, R.A., and Loffler, F.E. (2015). Nitrite Control over Dissimilatory Nitrate/Nitrite Reduction Pathways in Shewanella loihica Strain PV-4. Appl Environ Microb *81*, 3510-3517.

Yoon, S.H., Hwan Do, J., Lee, S.Y., and Nam Chang, H. (2000). Production of poly-gamma-glutamic acid by fed-batch culture of Bacillus licheniformis. Biotechnol Lett *22*, 585-588.

Yuan, Y., Shin, H., Kang, C., and Kim, S. (2016). Wiring microbial biofilms to the electrode by osmium redox polymer for the performance enhancement of microbial fuel cells. Bioelectrochemistry *108*, 8-12.

Yura, T., Nagai, H., and Mori, H. (1993). Regulation of the Heat-Shock Response in Bacteria. Annu Rev Microbiol *47*, 321-350.

Zhang, J.Z. (2012). Genetic Redundancies and Their Evolutionary Maintenance. Adv Exp Med Biol *751*, 279-300.

Zhao, J.G., ODaly, J.P., Henkens, R.W., Stonehuerner, J., and Crumbliss, A.L. (1996). A xanthine oxidase colloidal gold enzyme electrode for amperometric biosensor applications. Biosens Bioelectron *11*, 493-502.

Zhao, J.S., Manno, D., Beaulieu, C., Paquet, L., and Hawari, J. (2005). Shewanella sediminis sp nov., a novel Na+-requiring and hexahydro-1,3,5-trinitro-1,3,5-trinitro-degrading bacterium from marine sediment. Int J Syst Evol Micr *55*, 1511-1520.

Zhou, A., Baidoo, E., He, Z., Mukhopadhyay, A., Baumohl, J.K., Benke, P., Joachimiak, M.P., Xie, M., Song, R., Arkin, A.P., *et al.* (2013). Characterization of NaCl tolerance in Desulfovibrio vulgaris Hildenborough through experimental evolution. Isme J *7*, 1790-1802.

Zhou, A., Hillesland, K.L., He, Z., Schackwitz, W., Tu, Q., Zane, G.M., Ma, Q., Qu, Y., Stahl, D.A., Wall, J.D., *et al.* (2015). Rapid selective sweep of pre-existing polymorphisms and slow fixation of new mutations in experimental evolution of Desulfovibrio vulgaris. Isme J *9*, 2360-2372.

Zverlov, V.V., Berezina, O., Velikodvorskaya, G.A., and Schwarz, W.H. (2006). Bacterial acetone and butanol production by industrial fermentation in the Soviet Union: use of hydrolyzed agricultural waste for biorefinery. Applied microbiology and biotechnology *71*, 587-597.